Advanced Petroleum-Based Fuels—Diesel Emissions Control Project (APBF-DEC)

2,000-Hour Performance of a NO_x Adsorber Catalyst and Diesel Particle Filter System for a Medium-Duty, Pick-Up Truck Diesel Engine Platform

Final Report

March 2007

Sponsored by:
The U.S. Department of Energy
American Chemistry Council
American Petroleum Institute
California Air Resources Board
Engine Manufacturers Association
Manufacturers of Emission Controls Association
South Coast Air Quality Management District

U.S. Department of Energy
Energy Efficiency and Renewable Energy
Bringing you a prosperous future where energy is clean, abundant, reliable, and affordable

The test program and subsequent data analysis represent a collaborative effort of a technical working group consisting of representatives from the government and industry organizations listed on the front cover of this report. The work group prepared this report using methods believed to be consistent with accepted practice. All results and observations are based on information available using technologies that were state-of-the-art at the time of this effort. To the extent that additional information becomes available, or factors on which analyses are based change, the findings could subsequently be affected.

Executive Summary

The Advanced Petroleum-Based Fuels—Diesel Emission Control (APBF-DEC) Program was a government/industry collaboration seeking the optimal combinations of low-sulfur diesel fuels, lubricants, diesel engines, and emission control systems (ECSs) to meet projected emission standards for the 2004 to 2010 time period. APBF-DEC consisted of five projects that used a systems approach to enhance the collective knowledge base on engines, diesel fuels, lubricants, and emission control technologies. The five test projects evaluated include:

- Selective catalytic reduction/diesel particle filter (DPF) technologies
- Nitrogen oxides adsorber catalyst (NAC)/DPF technologies for passenger cars, light-duty trucks/sport-utility vehicles (SUVs), and heavy-duty applications (three projects on different engine/vehicle platforms)
- Lubricant formulations that may affect the performance and durability of advanced diesel ECSs.

The National Renewable Energy Laboratory provided technical leadership for the APBF-DEC program, which was sponsored and conducted by a broad collaboration of government and industry organizations including: the U.S. Department of Energy, the American Chemistry Council, the American Petroleum Institute, the Engine Manufacturers Association, the Manufacturers of Emission Controls Association, the California Air Resources Board, and the South Coast Air Quality Management District.

This report presents the results of a 2,000-hour test of an ECS consisting of a NAC in combination with a DPF, advanced fuels, and advanced engine controls in an SUV/pick-up truck vehicle platform. The 2,000-hour aging of this system represents approximately 100,000 miles of on-road use, which approaches the 120,000-mile useful life emission standard.

Introduction

The previously completed Diesel Emission Control – Sulfur Effects (DECSE) project (National Renewable Energy Laboratory 2002) quantified the impact of diesel fuel sulfur on the performance and short-term durability of individual diesel emission control devices, including diesel oxidation catalysts, lean-nitrogen oxides (NO_x) catalysts, NACs, and DPFs. This project evaluated the performance of an entire system consisting of NAC technology in combination with DPFs, advanced fuels, and advanced engine controls.

Project Overview

The goal of this project was to demonstrate the ability of a NAC and DPF ECS to meet Tier 2–Bin 5 standards with Federal Test Procedure (FTP) transient test limits of 0.07 g/mi NO_x and 0.01 g/mi particulate matter (PM) in an SUV/pick-up truck vehicle platform without producing unreasonably high emissions during other modes of operation. Additionally, hydrocarbon and carbon monoxide (CO) emissions standards had to be met while minimizing impacts on fuel economy.

The testing was performed for 2,000 hours with evaluations performed before and after desulfurizations that were performed every 100 hours. The majority of the testing was performed with 15-ppm sulfur fuel developed for the DECSE program. Additionally, an 8-ppm sulfur fuel was evaluated. Unregulated emissions tests were performed; however, these results will be presented in a separate report that incorporates findings from other APBF-DEC projects.

Objectives

The objectives of this project:

1. Demonstrate the emissions potential of advanced fuels, engines, and ECSs for meeting federal Tier 2–Bin 5 emissions standards
2. Evaluate the effect of fuel sulfur level on emissions and fuel economy, ECS performance, and catalyst degradation.

The 2004-2009 federal standards are as follows: PM of 0.01 g/mi, NO_x of 0.07 g/mi, and non-methane hydrocarbons (NMHC) of 0.09 g/mi. These standards are to be met when testing over the FTP-75 test cycle at a full, useful life of 120,000 miles.

Research Questions

To achieve the project objectives, a series of study questions were developed to guide the experimental design and data analysis. They are organized into five categories: initial performance; aging and desulfurization; sulfur mass balance; fuel effects on regulated emissions; and unregulated emissions.

Initial Performance

These questions addressed the performance of the ECS during the initial 300-hours of aging, focusing on the initial impact of the ECS on regulated emissions and fuel economy, and the impact of sulfur on a fresh ECS.

Q1.1 Can the system meet the 2004-2009 regulated emissions levels for NO_x, NMHC, and PM?

Q1.2 What is the impact on other regulated emissions [total hydrocarbons (THC) and CO] and fuel economy?

Q1.3 How does system performance change during the early life (under 300-hours) of the system?

Q1.4 Are there similar patterns for various transient, duty cycles [Cold- and Hot-Start Urban Dynamometer Driving Schedule, US06 (part of the Supplemental FTP), Highway Fuel Economy Test]?

Aging and Desulfurization

This area addressed the impact of 2,000-hours of aging and sulfur accumulation on ECS performance, and the effectiveness of periodic desulfurizations for restoring NO_x reduction performance. The long-term impact on regulated emissions and fuel economy was also investigated.

Q2.1 How do NO_x emissions change as the system ages? Specifically, how do the maximum (pre-desulfurization), minimum (post-desulfurization), and average NO_x levels change?

Q2.2 Is the increase in NO_x emissions between consecutive desulfurizations constant over time?

Q2.3 How effective is desulfurization at restoring the initial NO_x reduction performance of the system (initially and over time)?

Q2.4 Does the performance of the system stabilize within the first 2,000 hours? If so, at what point does this occur?

Q2.5 Are there temporal trends with respect to other regulated emissions or fuel economy?

Sulfur Mass Balance

Understanding the mechanisms by which sulfur from the fuel and lubricants interact with the ECS is important for designing an effective and durable system. A mass balance approach is used to gain insight on this issue.

Q3.1 How much sulfur is emitted during the desulfurization process?

Q3.2 How does the amount of sulfur emitted during the aging cycle compare to the amount emitted during the desulfurization process? Do these rates change over time?

Q3.3 What happens to the differences between these amounts?

Fuel Effects on Regulated Emissions

Two different varieties of low-sulfur diesel fuels (15 ppm) were tested. This area considered whether the fuels have direct impacts on regulated emissions or fuel economy.

Q4.1 Are there differences in emissions from DECSE and British Petroleum (BP) fuels?

Q4.2 If such differences exist, are they consistent over time?

Unregulated Emissions

Periodic tests were performed to determine whether a fresh or aging ECS impacts emissions of unregulated gases and PM. The emissions of interest included selected hydrocarbon species, soluble organic fraction/sulfate, metals, nitroxy-alkanes, and polycyclic-aromatic hydrocarbons/nitro-polycyclic-aromatic hydrocarbon.

Q5.1 Which unregulated toxic (or potentially toxic) compounds are present in tailpipe emissions?

Q5.2 How do the levels compare to engine-out emissions?

Q5.3 How do unregulated emissions change with time?

Methods

The project was divided into two tasks: Task A and Task B. Task A involved the setup of the test cell with an engine and emissions measurement systems; measurement of baseline (engine-out) emissions and fuel consumption; configuration and installation of the ECSs; and development of regeneration and desulfurization strategies as needed. The test vehicle was a 2002 Chevrolet Silverado 2500 Series pick-up truck equipped with a Duramax 6.6L engine and ZF six-speed manual transmission. The engine/vehicle combination met the California medium-duty emission requirements for 2002. Two different ECS configurations were designed in Task A. In Task B, one of the two systems was aged for 2,000 hours, and periodically evaluated for regulated and unregulated emissions using selected low-sulfur fuels (15 ppm). The ECS tested in Task B consisted of NACs, oxidation catalysts, and a catalyzed DPF configured as shown in Figure ES-1. The system included a diesel fuel burner used for thermal management and supplemental fuel injectors for control of the regeneration reductant.

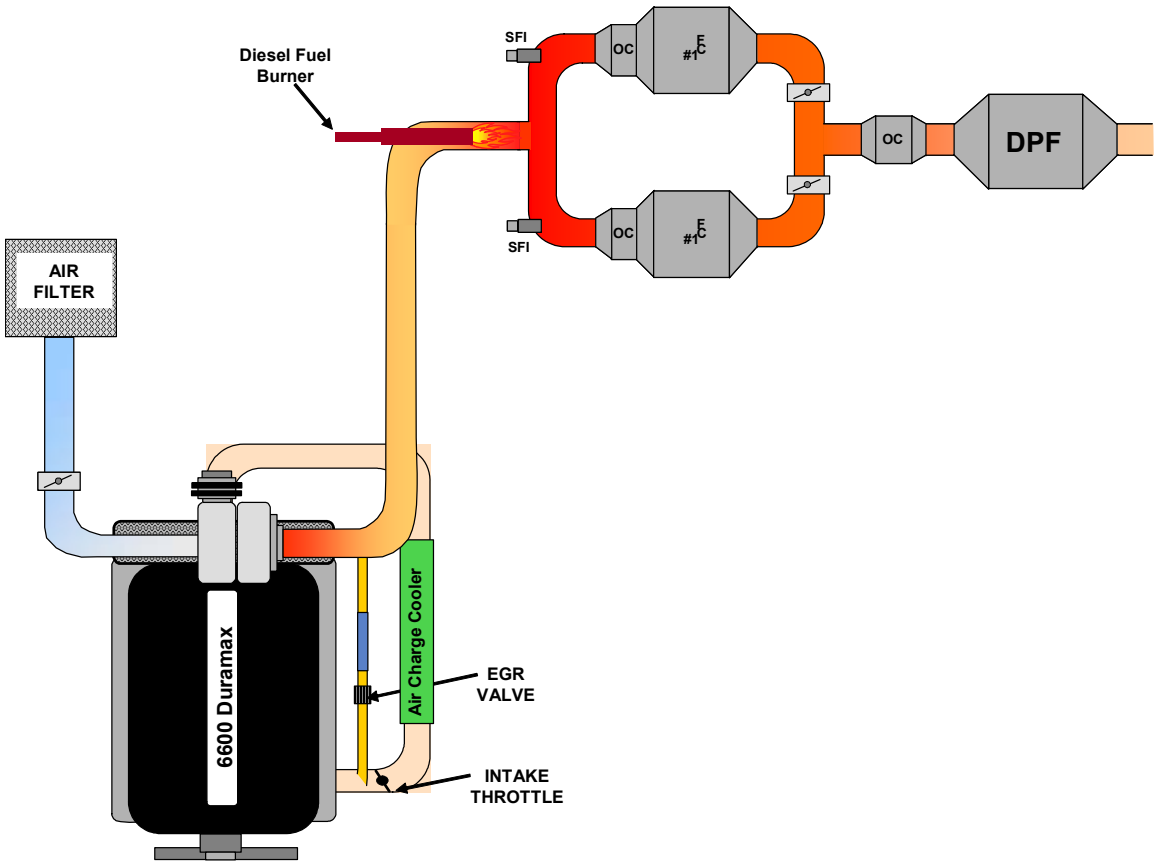

Figure ES-1. Schematic of tested ECS

Findings and Conclusions

The following is a summary of the significant conclusions from the study. Further details are provided in Section 4 of the report.

Initial Performance

- During the first 200 hours of testing, tailpipe emissions of NO_x averaged 0.095 g/mi (+/- 0.026 g/mi with 95% confidence) using the FTP composite test cycle. Although higher than the regulated emissions limit of 0.07 g/mi, the estimated NO_x emissions were 97.8% lower than engine-out emissions without EGR and 95.5% lower than engine-out emissions with EGR. Figure ES-2 presents the NO_x emissions and reduction efficiency results during the first 300 hours of testing.
- The ECS reductions in NO_x (97.8%), CO (87.2%), and PM (91.6%) emissions were statistically significant, as was the reduction in fuel economy (18.7%). The 16.7% decrease in NMHC emissions (from 0.198 to 0.165 g/mi) was also statistically significant. Initial tailpipe emissions of CO and PM were below the regulated limits; however, the engine-out

and tailpipe emissions of NMHC were above the Tier 2–Bin 5 limit of 0.09 g/mi. These test results are shown in Figure ES-3.

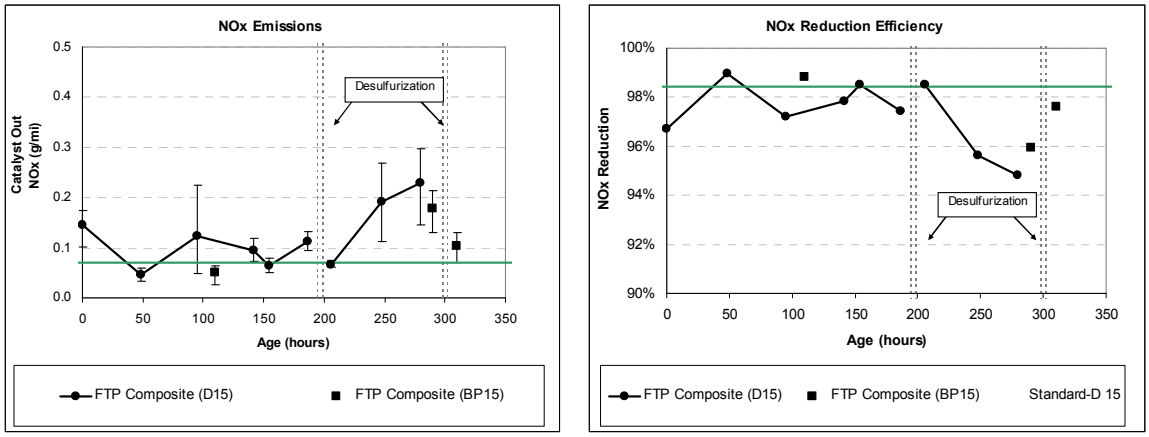

Figure ES-2. NO_x composite FTP emissions and reduction efficiency during the first 300 hours of aging (Error bars indicate the range of individual test results.)

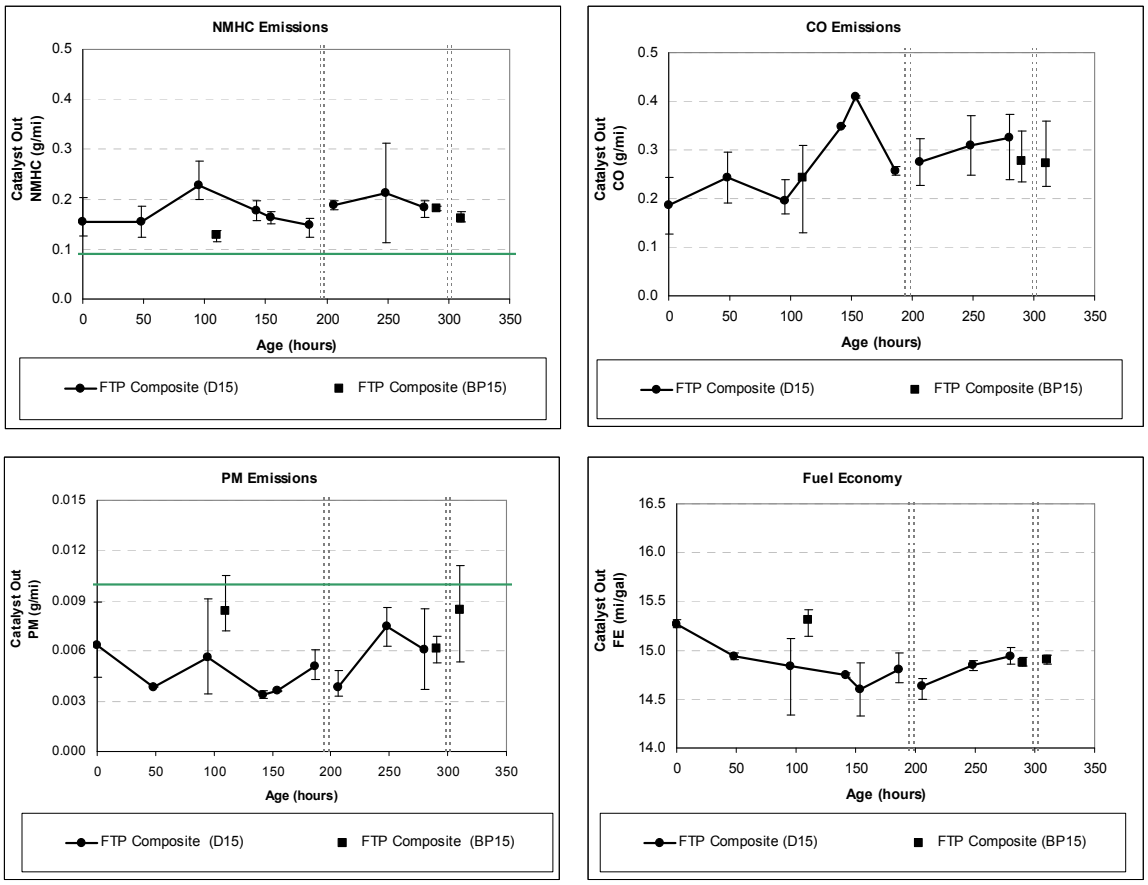

Figure ES-3. Composite FTP emissions of NMHC, CO, and PM, and fuel economy during the first 300 hours of aging

Aging and Desulfurization

- The loss in NO_x reduction efficiency of the catalysts between consecutive desulfurization events increased slightly from 4% to 6% throughout the 2,000-hour test. However, the desulfurization process was effective at restoring catalyst performance. The desulfurization process produced an improvement in NO_x reduction efficiency that changed from 3% at the beginning of the test to 6% at end of the 2,000-hour test.
- Although there was a decrease in NO_x reduction efficiency during the early aging periods, Figure ES-4 illustrates that the increase in NO_x emissions—or decrease in NO_x reduction efficiency—was not statistically significant after approximately 850 hours of testing.

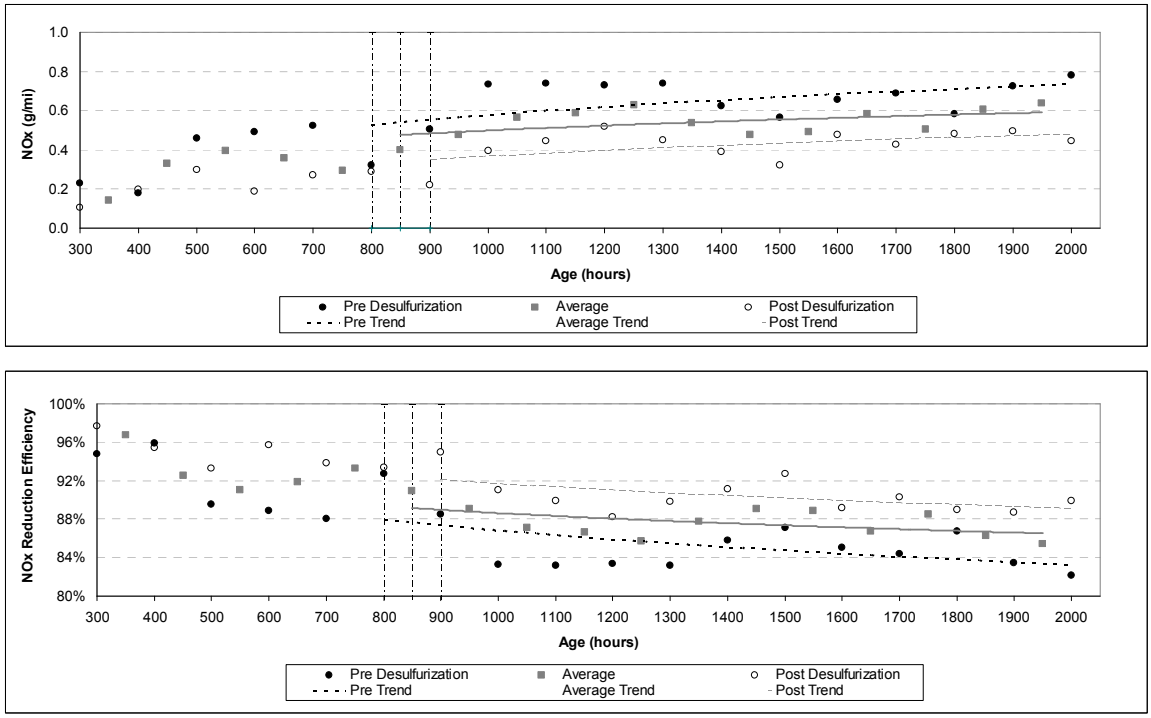

Figure ES-4. Statistical trends in FTP composite NO_x emissions and NO_x conversion at pre-desulfurization, post-desulfurization, and midpoint between desulfurizations are not statistically significant after 800, 900, and 850 hours, respectively

- There were statistically significant increases in NMHC and CO emissions, and fuel consumption during the 2,000-hour test; but there was no significant change in PM emissions. Table ES-1 compares the initial estimated engine-out regulated emissions and fuel economy (with and without EGR) with the estimated tailpipe emissions at 1,950 hours—midway between the last two desulfurization events. The system achieved emissions reduction efficiencies of 85.9% for NOx, 69.3% for CO, and 91.8% for PM. Fuel economy decreased by 16%; and NMHC emissions increased by 87.6%, this was partially due to the use of the diesel fuel burner and use of the diesel fuel as a reductant for catalyst regeneration.

Table ES-1. Average Engine-Out and Estimated 1,950-Hour Average Tailpipe Composite FTP Regulated Emissions and Fuel Economy—with 95% Confidence Intervals

Emission Parameter	Unit	Engine Out			Tailpipe Average (1,950 Hours) w/ EGR			Regulated Emission Standard[3]
		EGR	Average[1]	95% Confidence Interval	Average[2]	95% Confidence Interval	Percent Reduction	
NO_X	g/mi	Without	4.38	(4.34, 4.42)	0.616	(0.558, 0.675)	85.9%	0.07
		With	2.12	-[4]			70.9%	
NMHC	g/mi	Without	0.20	(0.19, 0.207)	0.372	(0.349, 0.395)	-87.6%	0.09
		With	no data	-			-	
THC	g/mi	Without	0.20	(0.194, 0.213)	0.730	(0.695, 0.764)	-257.8%	N/A
		With	0.26	-			-176.2%	
CO	g/mi	Without	2.02	(1.85, 2.18)	0.620	(0.571, 0.669)	69.3%	4.2
		With	4.43	-			86.0%	
PM	g/mi	Without	0.07	(0.056, 0.074)	0.005	(0.005, 0.006)	91.8%	0.01
		With	0.15	-			96.3%	
Fuel Economy	mi/gal	Without	18.40	(18.2, 18.6)	15.453	(15.312, 15.594)	16.0%	N/A
		With	17.95	-			13.9%	

[1] Engine-out average without EGR is based on 6 tests; engine-out average with EGR is based on 1 test.
[2] Estimates based on the regression model derived from measurements taken between 350 and 1,950 hours.
[3] Tier 2-Bin 5 full useful life
[4] Confidence intervals cannot be determined based on a single test; however, the values are generally consistent with the average engine-out results obtained during testing with the ECS.
N/A = Not applicable

- A comparison of measured sulfur emissions, with the amount of sulfur contained in the fuel and lubricant, demonstrated that nearly all of the sulfur accumulated on the catalysts was effectively removed during the desulfurization process.

Fuel Effects on Regulated Emissions

- There were no consistent significant differences in the emissions from tests conducted with the DECSE and BP fuels.

Unregulated Emissions

- Unregulated emissions results are presented in a separate report.

Future Work

The results of this work have identified a number of areas worthy of additional study. These include further evaluation of the NAC desulfurization process analyzing both deterioration mechanisms and the composition of the liberated sulfur compounds, and the evaluation of other fuel formulations on the performance of emission control devices (e.g., the impact of biodiesel blends on NACs and DPFs). One specific area of research is related to the impact of biodiesel blends on DPF regeneration temperature.

Table of Contents

List of Tables

List of Figures

Acronyms and Abbreviations

APBF-DEC	Advanced Petroleum-Based Fuels - Diesel Emission(s) Control
API	American Petroleum Institute
APP	accelerator pedal position
ASTM	American Society for Testing and Materials
BP	British Petroleum
C	degrees centigrade (Celsius)
CARB	California Air Resources Board
CC	continuing calibration
CDPF	coated [catalyzed] diesel particle filter
CO	carbon monoxide
CO_2	carbon dioxide
CR-DPF	continuously regenerating diesel particle filter
CRC	Coordinating Research Council
CVS	constant volume sampling [system]
DCM	dichloromethane
DECSE	Diesel Emission Control–Sulfur Effects
DFI	direct filter injection
DOC	diesel oxidation catalyst
DPF	diesel particle filter
ECS	emission control system
EGR	exhaust gas recirculation
EMS	engine management system
EPA	U.S. Environmental Protection Agency
ERIC	Emissions Reduction Integration Controller
FID	flame ionization detector
FTIR	Fourier transform infrared
FTP	Federal Test Procedure (engine cycle)
GC	Gas chromatography or chromatograph
GM	General Motors
g/mi	gram/mile
H_2S	hydrogen sulfide
HFET	Highway Fuel Economy Test
hp	horsepower
ICAL	initial calibration
IS	internal standard
Lambda (λ)	calculated ratio of amount of air available for combustion to the amount of air required for combustion to be stoichiometric.
LCS	laboratory control sample
LCSD	laboratory control sample duplicate
MAF	mass airflow
MECA	Manufacturers of Emission Controls Association
MS	mass spectrometry

MY	model year
N_2	nitrogen
NAC	nitrogen oxides adsorber catalyst
ng	nanogram
NMHC	nonmethane hydrocarbons
NO	nitrogen oxide
NO_2	nitrogen dioxide
NO_x	oxides of nitrogen
NPAH	nitro-polycyclic-aromatic hydrocarbon
O_2	oxygen
ORNL	Oak Ridge National Laboratory
PAH	polycyclic-aromatic hydrocarbons
PM	particulate matter
ppm	parts per million
PUF	polyurethane foam
QC	quality control
RRF	relative response factor
RPM/rpm	revolutions per minute
RSD	relative standard deviation
S1	cold-start strategy 1
S2	cold-start strategy 2
S3	cold-start strategy 3
SFI	supplemental [exhaust] fuel injection
SO_2	sulfur dioxide
SO_4	sulfate
SOF	soluble organic fraction
SUV	sport-utility vehicle
SwRI	Southwest Research Institute (San Antonio, Texas)
THC	total hydrocarbon
TIGF	Teflon-impregnated glass fiber [filter]
TWC	three-way conversion [catalyst]
UDDS	Urban Dynamometer Driving Schedule
US06	part of the Supplemental Federal Test Procedure
VOF	volatile organic fraction

Section 1: Introduction

1.1 Advanced Petroleum-Based Fuels—Diesel Emission Control Program

Advanced Petroleum-Based Fuels—Diesel Emission Control (APBF-DEC) is a government/industry project to identify and evaluate:

- The optimal combinations of low-sulfur diesel fuels, lubricants, diesel engines, and emission control systems (ECS) to meet projected emission standards for the 2004 to 2010 time period
- Properties of fuels and vehicle systems that could lead to even lower emissions beyond 2010.

The National Renewable Energy Laboratory provided technical leadership to this project, which was funded and directed by federal and state government agencies, trade associations, and private industry. The primary sponsors are the U.S. Department of Energy, the American Chemistry Council, the American Petroleum Institute (API), the Engine Manufacturers Association, the Manufacturers of Emission Controls Association (MECA), the California Air Resources Board (CARB), and the South Coast Air Quality Management District. The U.S. Environmental Protection Agency (EPA) is providing technical assistance. Additional technical support is being provided by the National Petrochemical and Refiners Association. Representatives from these and other agencies, associations, national laboratories, and private sector companies serve on the 20-member APBF-DEC Steering Committee and its working groups.

A systems approach is being used to simultaneously investigate how fuels, lubricants, engines, and ECSs can enable clean and efficient transportation systems. APBF-DEC Program consists of five individual projects to evaluate how sulfur and other compounds impact the performance and durability of advanced diesel ECSs. The projects are summarized in Table 1.

Table 1. APBF-DEC Project Summary

Technology	Platform	Test Vehicle/Engine	Subcontractor
NO_x Adsorber Catalysts and Diesel Particle Filters	Light-duty	1.9L TDI Audi A4	FEV Engine Technology, Inc.
	SUV/light truck	Chevrolet Silverado Isuzu/GM Duramax	Southwest Research Institute
	Heavy-duty	Cummins ISX (engine only)	Ricardo, Inc.
Urea Selective Catalytic Reduction and Diesel Particle Filters	Heavy-duty	Caterpillar C12	Southwest Research Institute
Lubricants	Medium-duty	International T444E (Phase 1)	Automotive Testing Laboratories (Phase 1)
		Cummins ISB (Phase 2)	Analytical Engineering, Inc. (Phase 2)

This report summarizes the results from the APBF-DEC project that studied nitrogen oxides adsorber catalysts (NACs) and diesel particle filters (DPFs) for sport-utility vehicles (SUV)/light trucks.

1.2 Background

The previously completed Diesel Emission Control – Sulfur Effects (DECSE) Project (National Renewable Energy Laboratory 2002) quantified the impact of diesel fuel sulfur on the performance and short-term durability of diesel emission control devices [diesel oxidation catalysts (DOCs)], lean-nitrogen oxides (NO_x) catalysts, NACs, and DPFs. Because some of these new technologies have demonstrated sensitivity to fuel-borne sulfur, considerable research was conducted, and regulations limiting the permissible levels of sulfur in diesel fuel were promulgated. Beginning in October 2006, on-highway diesel fuel will be subject to a maximum sulfur content of 15 ppm.

This project aimed to demonstrate the potential of NAC technology in combination with DPFs, advanced fuels, and advanced engine controls to achieve stringent emission levels while maintaining high fuel economy. To meet stringent Tier 2 light-duty emissions standards, tailpipe emissions for NO_x must be below 0.2 g/mi while particulate matter (PM) emissions levels must be below 0.02 g/mi. Goals of this project were to meet Tier 2 – Bin 5 with limits of 0.07 g/mi NO_x and 0.01 g/mi PM. The goal was to achieve these emissions levels on the Federal Test Procedure (FTP) transient test cycle without producing high emissions during other modes of operation.

Additionally, hydrocarbon and carbon monoxide (CO) emissions standards had to be met. Minimizing fuel economy impacts while meeting emissions requirements was also an important aspect of the project. The base fuel for the project was the 0.6-ppm sulfur DECSE base fuel. Additionally, the 8- and 15-ppm sulfur fuels were evaluated, with the majority of testing performed using the 15-ppm sulfur fuel.

It is anticipated that, in order for light-duty vehicles to meet these low emission levels, active ECSs will be required. NACs in conjunction with DPFs and other engine and combustion strategies (e.g., exhaust gas recirculation or EGR, and high-pressure fuel injection) are seen as possible approaches to meet these goals. One of the key issues with these systems is their long-term tolerance to fuel-borne sulfur. For these reasons, this project was planned within APBF-DEC to look specifically at fuel sulfur effects on catalyst durability and emissions in an SUV/pick-up truck vehicle platform.

1.3 NO_x Adsorber Catalyst/Diesel Particle Filter Technologies

The following sections present brief discussions of the factors that are known to affect the performance of NACs and DPFs, respectively.

1.3.1 Principle of Operation of NO_x Adsorber Catalysts

A NAC is a flow-through exhaust emissions control device, which has the potential to significantly lower NO_x, hydrocarbon, and CO emissions present in diesel engine exhaust. Because it contains high levels of precious metals, it is also effective in oxidizing the soluble organic fraction (SOF) of diesel PM and other unregulated diesel emissions.

A NO_x adsorber is a storage device for NO_x. During typical diesel engine operation, NO_x in the lean exhaust gas is stored as a base metal nitrate. Before the NO_x adsorbent becomes fully saturated, it must be regenerated. Regeneration is accomplished periodically by producing a fuel-rich exhaust. Under rich conditions, the stored NO_x is released from the adsorbent and simultaneously reduced to nitrogen—and/or nitrous oxide or ammonia—over precious metal sites. Numerous approaches to achieving the fuel-rich exhaust conditions for NAC regeneration are being researched, including in-cylinder fuel injection and in-pipe fuel injection, among others.

A NAC consists of two principal components: a NO_x adsorbent and a three-way conversion (TWC) catalyst. The NO_x adsorbent is typically an alkali or alkaline earth carbonate. These carbonates are capable of chemically interacting with NO_2 and O_2 present in typical diesel engine exhaust, resulting in the formation of an alkali or alkaline earth nitrate. Platinum in the TWC catalyst is responsible for the oxidation of nitrogen oxide (NO) to nitrogen dioxide (NO_2) facilitating the adsorption process. Periodically, NO_x stored by the adsorbent is released and reduced to nitrogen. This process requires a fuel-rich exhaust gas composition and a TWC catalyst. These catalysts are typically based on combinations of platinum, palladium, and rhodium and are capable of using reductants (CO, hydrogen, and hydrocarbon) present in rich engine exhaust to selectively reduce NO_x to nitrogen. TWC catalysts have been utilized for more than 20 years to perform these same reactions in the exhaust of stoichiometric gasoline engines.

An engine management system (EMS) is critically involved in the operation of a NO_x adsorber system. The EMS must determine when the NO_x adsorbent is approaching saturation and then trigger the change in engine operation resulting in the rich condition required for release and reduction of the stored NO_x. The timing, duration, and stoichiometry of the rich pulse are also critical. If it is too long and/or too rich, hydrocarbon and CO can break through the adsorber resulting in poor control of these pollutants, as well as introducing an unnecessary increase in fuel economy penalty.

It is well known that sulfur compounds in diesel fuel are combusted in the engine, resulting in the release of sulfur dioxide (SO_2). In a NO_x adsorber, this SO_2 undergoes reactions, which are completely analogous to those of NO_x, resulting in the formation of alkali and alkaline earth sulfates. Unlike their corresponding nitrates, these sulfates are extremely stable. It has been shown repeatedly in the literature that the decomposition of these sulfates requires a combination of rich condition and temperatures in excess of 600^oC. As a result, SO_2 in the exhaust effectively poisons the NO_x adsorption sites, and special procedures to desulfurize the adsorber must be applied. Although the chemical processes for removal of NO_x and sulfur are similar, the removal of sulfur requires higher temperatures and longer duration. As such, *desulfurization* is the term commonly used to describe sulfur removal, while *regeneration* refers to removal and reduction of NO_x.

1.3.2 Principle of Operation of Diesel Particle Filters

The DPF system consists of a filter positioned in the exhaust stream designed to collect much of the particle emissions while allowing the exhaust gases to pass through the system. Because the volume of PM generated by a diesel engine is sufficient to fill up and plug a reasonably sized DPF over time, some means of disposing of this trapped PM must be provided. The most promising means of disposal is to burn or oxidize the PM in the filter, thus regenerating or cleansing the filter. Under some conditions, precious metals in the DPF can oxidize sulfur compounds—such as SO_2 and sulfite to sulfuric acid—increasing the PM emissions.

The two types of DPFs evaluated in the DECSE program were the catalyzed diesel particle filter (CDPF) and the continuously regenerating diesel particle filter (CR-DPF). The CR-DPF accomplishes filter regeneration by continuously generating NO_2 from emitted NO over an oxidation catalyst placed upstream of the filter. It has been established that NO_2 is an effective low-temperature oxidizing agent for diesel PM. The CDPF affects the filter regeneration by using a catalyst coating on the filter element to promote the oxidation/combustion of the collected PM using available oxygen in the diesel exhaust. A third DPF technology utilizes a fuel-borne catalyst to promote oxidation of the PM.

A complete DPF system consists of the filter and the means to facilitate the regeneration. The EMS can play a key role in facilitating regeneration at appropriate intervals.

1.4 Project Scope, Goals, and Objectives

The objectives of this project were to:

1. Demonstrate the emissions potential of advanced fuels, engines, and ECSs for meeting federal Tier 2-Bin 5 emissions standards

2. Evaluate the effect of fuel sulfur level on emissions and fuel economy, ECS performance, and catalyst degradation.

The 2004-2009 federal standards are as follows:

- PM of 0.01 g/mi
- NO_x of 0.07 g/mi
- Non-methane hydrocarbons (NMHC) of 0.09 g/mi.

These standards are to be met when testing over the FTP-75 test cycle at a full useful life of 120,000 miles.

The project was divided into two tasks: Task A and Task B. Task A involved the setup of the test cell with an engine and emissions measurement systems, measurement of baseline (engine-out) emissions and fuel consumption, configuration and installation of the ECSs, and development of regeneration and desulfurization strategies as needed. Two different

configurations were designed in Task A. In Task B, one of the two systems was aged for 2,000 hours and periodically evaluated for regulated and unregulated emissions using selected low-sulfur fuels (15 ppm). The 2,000-hour aging of this system represent approximately 100,000 miles of on-road use, which approaches the 120,000-mile useful life emission standard.

The experimental design and analysis of test data from Task B was guided by a series of study questions organized into five topic areas: initial performance; durability and desulfurization; sulfur mass balance; fuel effects on regulated emissions; and unregulated emissions.

1.4.1 Initial Performance

These questions address the performance of the ECS during the initial 300 hours of aging, focusing on the initial impact of the ECS on regulated emissions and fuel economy, and the impact of sulfur on a fresh ECS.

Q1.1 Can the system meet the 2007-2010 regulated emissions levels for NO_x, NMHC, and PM?

Q1.2 What is the impact on other regulated emissions [total hydrocarbon (THC), CO, PM, and NMHC] and fuel economy?

Q1.3 How does system performance change during the early life (under 300 hours) of the system?

Q1.4 Are there similar patterns for various transient duty cycles [Cold- and Hot-Start Urban Dynamometer Driving Schedule (UDDS), US06 (part of the Supplemental Federal Test Procedure), Highway Fuel Economy Test (HFET)]?

1.4.2 Durability and Desulfurization

This area addresses the impact of 2,000 hours of aging and sulfur accumulation on ECS performance and the effectiveness of periodic desulfurizations for restoring NO_x reduction performance. Long-term impact on regulated emissions and fuel economy are also investigated.

Q2.1 How do NO_x emissions change as the system ages? Specifically, how do the maximum (pre-desulfurization), minimum (post-desulfurization), and average NO_x levels change?

Q2.2 Is the increase in NO_x emissions between consecutive desulfurizations constant over time?

Q2.3 How effective is desulfurization at restoring the initial NO_x reduction performance of the system (initially and over time)?

Q2.4 Does the performance of the system stabilize within the first 2,000 hours? If so, at what point does this occur?

Q2.5 Are there temporal trends with respect to other regulated emissions or fuel economy?

1.4.3 Sulfur Mass Balance

Understanding the mechanisms by which sulfur from the fuel and lubricants interacts with the ECS is important for designing an effective and durable system. A mass balance approach is used to gain insight on this issue.

Q3.1 How much sulfur is emitted during the desulfurization process?

Q3.2 How does the amount of sulfur emitted during the aging cycle compare to the amount emitted during desulfurization process? Do these rates change over time?

Q3.3 What happens to the differences between these amounts?

1.4.4 Fuel Effects on Regulated Emissions

Two different ultra-low-sulfur diesel fuels (15 ppm) were tested. This area considers whether the fuels have direct impacts on regulated emissions or fuel economy.

Q4.1 Are there differences in emissions from DECSE and BP fuels?

Q4.2 If such differences exist, are they consistent over time?

1.4.5 Unregulated Emissions

Periodic tests were performed to determine whether a fresh or aged ECS impacts emissions of unregulated gases and PM. The emissions of interest include selected hydrocarbon species, SOF/sulfate metals, nitroxy-alkanes, and polycyclic-aromatic hydrocarbons (PAH)/nitropolycyclic-aromatic hydrocarbon (NPAH).

Q5.1 Which unregulated toxic (or potentially toxic) compounds are present in tailpipe emissions?

Q5.2 How do the levels compare to engine-out emissions?

Q5.3 How do unregulated emissions change with time?

The answers to these questions and associated discussions are included in a separate report focusing on unregulated emissions across all of the ABPF-DEC platforms.

Section 2: Technical Approach

The following section details the technical approach for this project. This includes a discussion of the experimental design, which includes the platform engine selection, emissions control system selection, and fuel and lubricant selection. In addition the section also covers experimental procedure, including laboratory testing setup, ECS configuration, test procedures, aging cycle development, oil analysis, emissions sampling and analysis, data handling, and statistical analysis.

2.1 Experimental Design

The original plan for this project was to develop two different ECSs, conduct limited testing on both systems for up to 300 hours, and then, select one system for durability testing up to 2,000 hours. Selections of the engine and ECSs are discussed in Sections 2.1.1 and 2.1.2, respectively. Section 2.1.3 describes the fuels and lubricants used in this study.

Emissions measurements on regulated gases and PM were made every 100 hours while operating over four different transient test cycles using DECSE 15-ppm sulfur fuel. Unregulated emissions in the form of metals, PAH, NPAH, and selected gases were measured at four different time points using the BP15 fuel. Section 2.1.4 contains a complete list of emissions parameters measured during this study. Finally, Section 2.1.5 presents a test matrix showing the combinations of test conditions encountered and measurements performed.

2.1.1 Engine Selection

At project inception (August 2001), no common-rail diesel engines sized appropriately for a typical SUV (3 to 5L) were commercially available nor offered by any of the program participants. Therefore a reasonable surrogate engine selected by the APBF-DEC program steering committee for use in this program was a model year (MY) 2002 Isuzu Duramax. This 6.6 liter, V8 engine came equipped with a common-rail fuel injection system; a high-pressure EGR system incorporating a vacuum-actuated EGR valve and intake throttle; four-valve-per-cylinder heads; pilot injection; and met the 2002 California medium-duty emission regulations when equipped with an oxidation catalyst. A development fleet vehicle (2500 series Chevrolet Silverado, shown in Figure 1) equipped with this engine was supplied by General Motors (GM). This vehicle came equipped with a ZF six-speed manual transmission. Two additional loose engines were supplied by Isuzu Motors America. The engine specifications are shown in Table 2, while the engine itself is shown in Figure 2. A photograph of the underbody of the vehicle, identifying the turbocharger exhaust downpipe and oxidation catalyst locations, is shown in Figure 3.

Figure 1. Development fleet vehicle supplied by GM equipped with Duramax 6.6L engine

Table 2. Engine Specifications for MY 2002 Duramax

Rated Speed (rpm)	3000
Rated Power (hp)	300 ± 12
Engine Displacement (liters)	6.6
Fuel Rate at Rated Speed and Power (lb/hr)	120
Fuel Temp. at Rated Speed and Power (°F)	Min: 100 Max: 106
Rated Torque Speed (rpm)	1800
Rated Torque (lb-ft)	520 ± 20
Fuel Rate at Rated Torque Speed and Torque (lb/hr)	62
Governed Speed (rpm)	3250 governed, 3400 ± 25 no load
Low Idle (rpm)	680 ± 25
Cranking Speed (rpm)	135-180
Water Outlet Temperature (°F)	187-192
Pressure Drop across Intercooler (in. H_2O)	53 ± 1
Air Temperature after Intercooler (°F)	min. 116 max. 124
Engine Oil Rating	*15W40*
Engine Coolant Type	50% water + 50% DEX-COOL glycol
Intake Restriction - Max (in. H_2O)	2
Exhaust Restriction - Max (w/converter) (in. Hg)	12
Intake Restriction Location @Vehicle Adaptor (in. H_2O)	4.5 ± 0.5
Exhaust Restriction Location @Center of Turbo (in. Hg)	10.5 ± 0.5
Exhaust Pipe Diameter (inches)	3
Exhaust Flow at Rated Power (kg/min)	22.8
Exhaust Temperature Maximum at Rated Power (°C)	575

Figure 2. Isuzu Duramax 6.6L engine

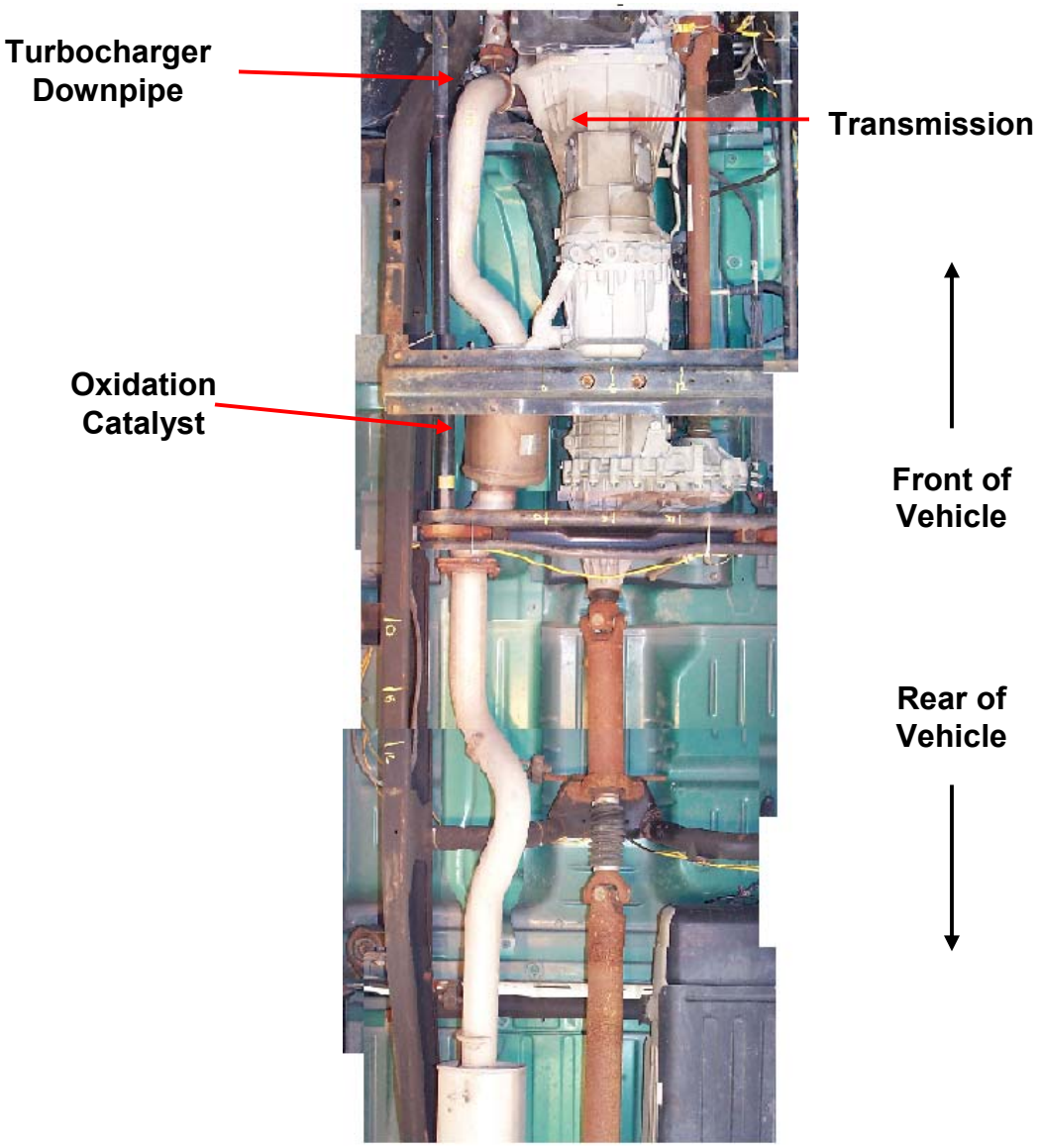

Figure 3. Vehicle underbody showing stock exhaust system

2.1.2 Emission Control Systems (A and B)

Two different ECS configurations were initially planned to provide two different approaches to meet the program goals. System A was a single, in-line NAC/DPF combination, which was expected to have the lowest overall system cost and physical size. However, the ability of this configuration to meet the ambitious program emission goals was in question. System B was a more complex, physically larger, dual-leg NAC system that was expected to increase the overall NO_x reduction efficiency of the system and reduce the fuel economy penalty. Schematics of the two different proposed systems are shown in Section 2.2.1.

Baseline vehicle emission and exhaust temperature data for the selected driving cycles were generated using the selected engine/vehicle, and provided to the MECA supplier in order to appropriately size the NAC and DPF for meeting the program emission goals. In addition to the NACs and DPF, the Southwest Research Institute (SwRI) also requested some highly loaded oxidation catalysts (pre-NAC and pre-DPF) to assist in breaking down the selected reductant (diesel fuel) and help minimize hydrocarbon breakthrough during regeneration. A selective catalytic reduction system using an ammonia-based reductant was evaluated under a different project with the APBF-DEC activity.

Diesel fuel was selected as the reductant to allow commonality between the engine fuel and ECS system reductant. In addition, it was felt that use of diesel fuel as the reductant was more realistic than laboratory-provided reductants, such as pure CO, hydrogen, or individual hydrocarbons.

Over the course of the program two different generations of components were supplied. Both generations of components consisted of oxidation catalysts, NACs, and DPFs.

The first-generation System B consisted of two pre-NAC oxidation catalysts, each 14.4-cm in diameter and 7.6-cm length (2.5L total volume). These catalysts were each followed by a NAC 24.1-cm in diameter and 15.2cm in length (14L total volume). The two legs of the exhaust were then combined into a single pipe—which was followed by a single oxidation catalyst 14.4-cm in diameter and 7.6-cm long (2.5L); and a DPF 26.7-cm in diameter and 30.5-cm long (17L)—for a total ECS system volume of 36 liters.

Second-generation components were provided in order to more appropriately size the oxidation catalysts and DPF for the system, and to provide more thermally durable NACs. The second-generation System B consisted of two pre-NAC oxidation catalysts 24.1-cm in diameter and 7.6-cm length (7L total volume) installed immediately upstream of the new, more thermally durable NACs with the same dimensions as the first-generation system (24.1-cm diameter x 51.2-cm length, 14L total volume). The two exhaust legs were combined after the NACs—followed by an oxidation catalyst 24.3-cm in diameter and 7.6-cm in length (3.5L volume); and a DPF 22.9-cm in diameter and 30.5-cm in length (12.5L volume)—for a total ECS system volume of approximately 37 liters.

The final System B configuration included in-exhaust fuel injection upstream of each NAC to provide reductant for regeneration of the NACs and also a single in-exhaust injector upstream of the rear oxidation catalyst/DPF combination to provide fuel to ensure regeneration of the DPF. The two injectors upstream of the NACs were of a type using a frequency valve/poppet valve/air-assist combination, while the third injector was an air-assisted, pintle-type fuel injector.

To provide the necessary heat to the system and assist in achieving overall reducing conditions required for efficient NAC regeneration, a diesel fuel burner was developed and included as part of the overall ECS system. This was required due to the relatively low engine loads for this engine in this application.

2.1.3 Fuel/Lubricant Selection

Four fuels were utilized in this project: three fuels designed for use in the DECSE program [1] and one 2006-type refinery fuel. The DECSE fuels were used for strategy and control development, aging operation, and regulated emissions testing. The DECSE fuel is a blended fuel that was designed to have similar properties to the national average diesel fuel. While this fuel is composed of a narrower range of hydrocarbon compounds, its density, viscosity, cetane number, aromatic content, and other properties meet the specifications for a 2006 No. 2 diesel fuel. The refinery fuel, referred to as BP15, was only used during full unregulated emissions evaluations. The DECSE fuels in this project used the base DECSE fuel doped to varying sulfur levels (3, 8, and 15 ppm). The dopant mixture contains a variety of classes of sulfur containing molecules that are in the same boiling range as diesel fuel, with an emphasis on thiophenes. The refinery fuel used had a nominal 15-ppm sulfur level. A complete summary of the fuel properties for the DECSE fuel, the refinery fuel, and dopants are presented in Tables 3 and 4.

Table 3. Test Fuel Properties

Fuel Property	ASTM Method	Base Fuel	BP15
Density (kg/m^3)	D4052	826.2	837.1
Viscosity @40^{o}C (mm^2/s)	D445	2.3	2.5
Distillation			
IBP (^{o}C)	D86	180	164
10% recovery (^{o}C)	D86	203	201
20% recovery (^{o}C)	D86	219	218
30% recovery (^{o}C)	D86	233	233
40% recovery (^{o}C)	D86	244	246
50% recovery (^{o}C)	D86	251	259
60% recovery (^{o}C)	D86	257	272
70% recovery (^{o}C)	D86	265	286
80% recovery (^{o}C)	D86	279	302
90% recovery (^{o}C)	D86	312	322
FBP (^{o}C)	D86	352	346
Cloud point (^{o}C)	D2500	-26	-12
Pour point (^{o}C)	D97	-23	-18
Flash point, PMCC (^{o}C)	D93	69	64
Sulfur (ppm)	D5453	0.6	13.3
Aromatics (vol. %)	D1319	23.9	29
Olefins (vol. %)	D1319	4.6	
Saturates (vol. %)	D1319	71.4	
Aromatics (vol. %)	D5186	26.9	25
Polyaromatics (vol. %)	D5186	8.4	4.2
Non-aromatics (vol. %)	D5186	64.7	70.8
Cetane number	D613	42.5	51.1
Cetane index	D976	51.5	48.8

Table 4. Properties of Sulfur Doping Compounds

Concentration (mass %)	Compound	Chemical Formula	Boiling Point (^{o}C)
50	Dibenzo[b,d]thiophene	$C_{12}H_8S$	333
30	Benzo[b]thiophene	C_8H_6S	222
10	Di-t-butyl disulfide	$C_8H_{18}S_2$	200
10	Ethyl phenyl sulfide	$CH_{10}S$	206

BP15 is a 15-ppm sulfur fuel prepared by processing straight-run distillate stocks through a commercial single-stage hydrotreater employing a high-activity catalyst at maximum severity. This fuel was prepared in a commercial refinery unit (not a pilot plant), but cracked stocks were

excluded from the feed because the specification sulfur level could not have been achieved with their inclusion. In 2007, actual production will likely employ more advanced processing to allow the inclusion of cracked stocks.

All tests were conducted with Shell Rotella T 15W-40 engine lubricant. This oil meets the requirements of the API CI-4 specification for EGR-equipped engines and has a sulfur content of approximately 0.6%, which is typical of engine oils meeting this specification. This oil was used in the DECSE program and in all other APBF-DEC activities. Table 5 lists the lubricant specifications.

Table 5. Lubricating Oil Specifications

Property	Specification
Viscosity grade	15W40
Performance category	API CI-4
Sulfated ash	1.5%
Sulfur	0.65% (6500-ppm)
Calcium	0.36% (3600-ppm)
Phosphorus	0.14% (1400-ppm)
Density at 15^{o}C	868.0 kg/m^{3}
Viscosity at 40^{o}C	101 cSt
Viscosity at 100^{o}C	14.0 cSt

2.1.4 Emissions Measurements

Throughout the test program, both raw and dilute tailpipe exhaust samples were acquired to evaluate the engine-out emissions and the ECS effectiveness. These samples were analyzed for various compounds, both gaseous and solid particles.

Dilute bag samples were acquired at the tailpipe location and analyses conducted for concentrations of THC, methane, CO, carbon dioxide (CO_2), and NO_x. These dilute samples were acquired over a test cycle and represent the average concentration over that test cycle. In addition, a dilute particle sample was collected on a 90-mm Pallflex® filter and subsequently analyzed for total mass, and in certain cases for sulfate, SOF, and volatile organic fraction (VOF).

For the unregulated emission tests (conducted after 100, 300, 900, 1,500, and 2,000 hours of aging), dilute bag samples were also analyzed using methods discussed in Section 2.2.3 for the following individual hydrocarbons:

Ethane	1,3-butadiene
Ethylene	2-methylpropane (isobutane)
Propane	1-butyne
Propylene	Cis-2-butene
Acetylene	3-methyl-1-nutene
Propadiene	2-methylbutane (isopentane)
Butane	1-methylcyclopentene
Trans-2-butene	Benzene
1-butene	Cyclohexane
2-methylpropene (isobutylene)	2,3,3-trimethylpentane
2,2-dimethylpropane (neopentane)	Toluene
Propyne	2,3-dimethylhexane

In addition, dilute exhaust samples were collected on a 47-mm Teflo filter for metals analysis and two Oak Ridge National Laboratory (ORNL)-supplied sampling cartridges connected in series for nitroxy-alkane analysis.

An additional dilution tunnel incorporating a 50-cm x 50-cm Pallflex filter (for capturing particle-bound and solid phase components) and two cartridges of polyurethane foam (PUF) media (connected in parallel, for gaseous phase components) were utilized to collect exhaust samples for subsequent PAH/NPAH analysis. These samples were analyzed for the following individual PAH:

Naphthalene	Chrysene
2-methylnaphthalene	Benzo(b)fluoranthene
Acenaphthylene	Benzo(k)fluoranthene
Acenaphthene	Benzo(e)pyrene
Fluorine	Benzo(a)pyrene
Phenanthrene	Perylene
Anthracene	Indeno(1,2,3-cd)pyrene
Fluoranthene	Dibenzo(a,h)anthracene
Pyrene	Benzo(g,h,i)perylene
Benzo(a)anthracene	

In addition, the samples were analyzed for the following individual NPAH:

1-nitronaphthalene	4-nitropyrene
2-me-1-nitronaphthalene	1-nitropyrene
2-nitronaphthalene	7-nitrobenzo(a)anthracene
2-nitrobiphenyl	6-nitrochrysene
4-nitrobiphenyl	1,3-dinitropyrene
5-nitroacenaphthene	1,6-dinitropyrene
2-nitrofluorene	1,8-dinitropyrene
9-nitroanthracene	6- nitrobenzo(a)pyrene
3-nitrofluoranthene	

Raw tailpipe emissions were continuously sampled at 10Hz for THC, CO, CO_2, and NO_x concentration. In addition, during the unregulated emission sampling events, raw exhaust samples were acquired utilizing a bubbler technique for later determination of SO_2 and hydrogen sulfide (H_2S) concentration over the test cycle; impingers were used with a Fourier Transform Infrared (FTIR) analyzer to sample and analyses the raw exhaust for determining the concentration of the following compounds on a second-by-second basis:

NO	Formaldehyde
NO_2	Acetaldehyde
NO_x	Benzene
N_2O	Ammonia
1,3-butadiene	

Raw, continuous exhaust samples were also taken at the engine-out location and after each NAC for determination of THC, CO, and NO_x concentration. These samples were recorded at 10Hz and were instrumental in providing feedback during the development of the ECS strategy. Oxygen and NO_x sensors also were recorded at 10Hz, and utilized at the engine-out location after each NAC and at the tailpipe location.

Table 6 provides a summary of the different types of emission samples and the sample locations for the emission evaluations.

Table 6. Summary of Emission Measurements Performed during Emission Evaluations

	Raw Engine-Out	Raw after NAC1	Raw after NAC2	Raw Tailpipe	Dilute Tailpipe
Average THC, Methane, NO_x, CO, CO_2					X
Continuous THC, NO_x, CO, CO_2	X			X	X
Continuous THC, NO_x, CO		X	X		
Average SO_2 and H_2S Mass				X	
Total PM Mass and Avg. Sulfate, SOF, and VOF					X
Hydrocarbon Speciation					X
FTIR				X	
Metals Analysis					X
Nitroxy-alkanes					X
PAH/NPAH					X
Oxygen and NO_x Sensors	X	X	X	X	

2.1.5 Test Matrix

Table 7 summarizes the emissions evaluations that were performed during the study using 15-ppm DECSE fuel. Each evaluation was a duplicate or triplicate test consisting of a Cold-Start UDDS followed by Hot-Start UDDS, US06, and HFET test cycles. PM samples were collected and weighed between each test cycle; however, when testing with the ECS, the SOF and sulfate measurements were made only when triplicate tests were performed. For those tests separate composite samples were made from the triplicate runs of the Cold-Start UDDS, Hot-Start UDDS, US06, and HFET cycles. Duplicate and triplicate tests alternated every 100 hours.

Duplicate measurements were taken using 8-ppm DECSE and 15-ppm BP fuel at engine-out. Triplicate measurements were taken using 15-ppm BP fuel at 100, 300 (pre- and post-desulfurization), 900 (post-desulfurization), 1,500 (post-desulfurization), and 2,000 (post-desulfurization). Triplicate unregulated emissions samples were collected at specified aging points (100, 300, 900, 1,500, and 2,000-hours); however, each sample consisted of composite materials collected across the four test cycles. Section 2.1.4 contains a complete list of emissions parameters that were measured.

Table 7. Test Matrix

			Number of Samples or Analyses[1]		
System	**Age from-to [by] hrs)**	**Fuel**	**Regulated Gases and Total PM**	**SOF & Sulfate**	**Unregulated Gases or Filters**
Engine-Out		D8,	2	2	
	n/a	D15	2	2	
		BP15	2	2	2
NAC + DPF	0-300 [50]	D15	2 or 3 each	0 or 1 each	
	400-2,000 [100] pre-desulfurization	D15	2 or 3 each	0 or 1 each	
	200-2,000 [100] post-desulfurization	D15	3 or 2 each	1 or 0 each	
	100	BP15	3	1 each	3
	300, 900, 1,500, 2,000 post-desulfurization	BP15	3 each	1 each	3 each

[1]See Section 2.1.4 for a complete list of emissions parameters measured.

2.2 Experimental Procedures

This section describes the experimental (laboratory setup, testing, sampling, and analysis) and data (handling and analysis) procedures that were followed.

2.2.1 Laboratory Setup

The laboratory setup involved both initial vehicle tests and an ECS configuration, as described below.

Initial Vehicle Tests. Initial testing was conducted on-vehicle utilizing a 48" single-roll, Horiba Chassis Dynamometer (Model LDV-48-86-125HP). This chassis dynamometer utilizes a feed-forward control system for inertia and road-load simulation. The dynamometer electrically simulates vehicle tire/road interface forces, including parasitic and aerodynamic drag. The vehicle experiences the same speed, acceleration/deceleration, and distance traveled as it would on the road. A preprogrammed road-load curve is the basis for the required force during each second of the driving schedule. For light-duty passenger cars, observed road load and simulated inertia errors on this chassis dynamometer are typically less than ± 0.15%.

In order to provide necessary engine related data (i.e., exhaust flow rates, temperatures, engine-out emissions, etc.) to the designated MECA member supplying all the ECS components, an estimated road-load was utilized for chassis dynamometer testing prior to conducting the on-road coast-downs for the test vehicle supplied. As the emission targets for this program related to the light-duty FTP test, and the US06 cycle was the most aggressive driving schedule, the results from these two test cycles defined the exhaust environment.

As this program was intended to address the fast-growing SUV market, an appropriate inertia weight at which to test the supplied pick-up truck was determined by calculating the average of the lightest and heaviest SUVs in which this engine could be theoretically offered. The lightest vehicle used in this determination was a 2002 Chevrolet Suburban 2500, two-wheel drive, LT, four door, 6.0L V8, 4A with a curb weight of 5,447 lb. The heaviest vehicle used in this determination was a 2002 Ford Excursion Limited Ultimate, four-wheel drive, four-door, 7.3L TDI V8, 4A with a curb weight of 7,688 lb. The average of these two values resulted in a curb weight of 6,568 lb. Adding an additional 300 lb for a driver and passenger, and rounding to the nearest 125 lb increment, resulted in a dynamometer inertia weight of 6,875 lb.

Three vehicle tests were conducted over the light-duty FTP-75 and US06 cycles at the selected inertia weight of 6,875 lb using dynamometer road-load curve shown in Figure 4. This estimated road-load curve was determined by averaging the road-load curves of four vehicles of similar size and weight. The purpose of these initial tests was only to provide the initial engine-out data needed by the ECS supplier to properly size the individual components of the proposed ECS system. In addition, an appropriate transmission shift schedule was developed for the different test cycles. During the vehicle tests, raw NO_x and CO_2 concentrations were measured (after the oxidation catalyst) along with three exhaust temperatures (downpipe, after oxidation catalyst, and muffler inlet), engine back pressure, voltage output from the stock mass airflow (MAF) sensor, intake manifold vacuum/pressure, and EGR valve vacuum signal. Based on a calculated estimate of intake flow (using engine rpm, and intake pressure and temperature) and NO_x concentration, a rough estimation of instantaneous and accumulated engine-out/tailpipe NO_x mass was made. Figures 4 and 5 show the estimated accumulated engine-out NO_x mass over the

FTP and US06, respectively. The exhaust temperatures (measured in the downpipe and after the stock oxidation catalyst) are shown in Figures 6 and 7 for the FTP and US06, respectively.

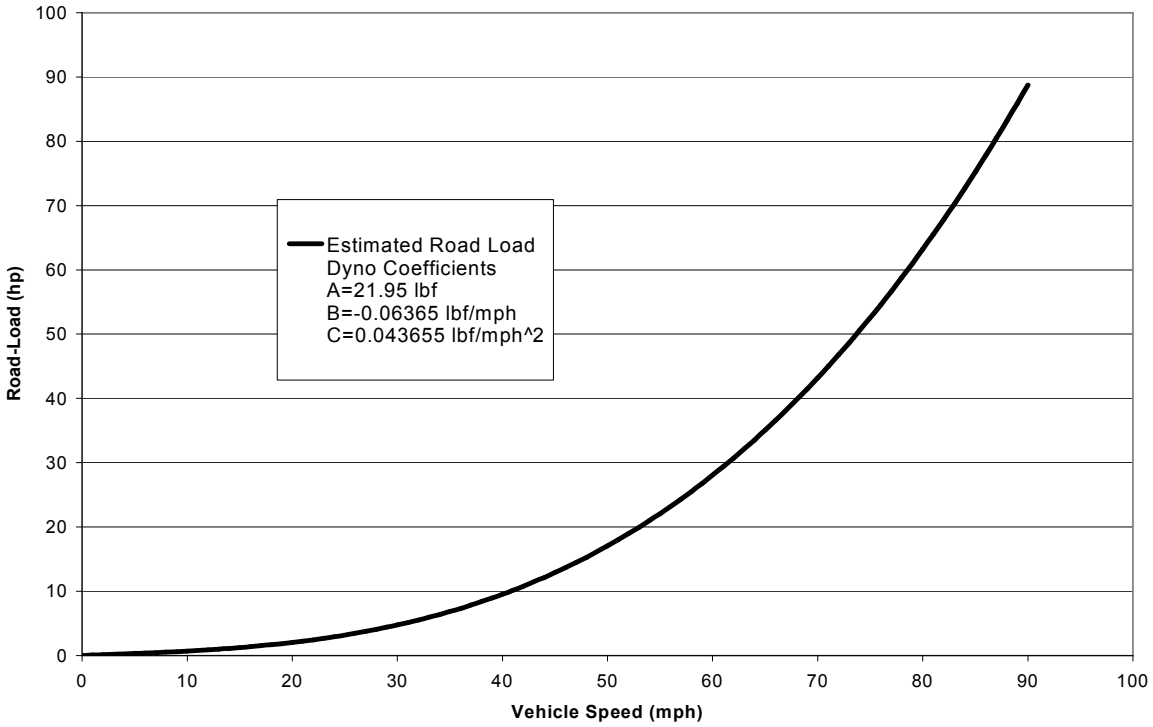

Figure 4. Initial road-load curve utilized for 2002 Chevrolet Silverado test vehicle

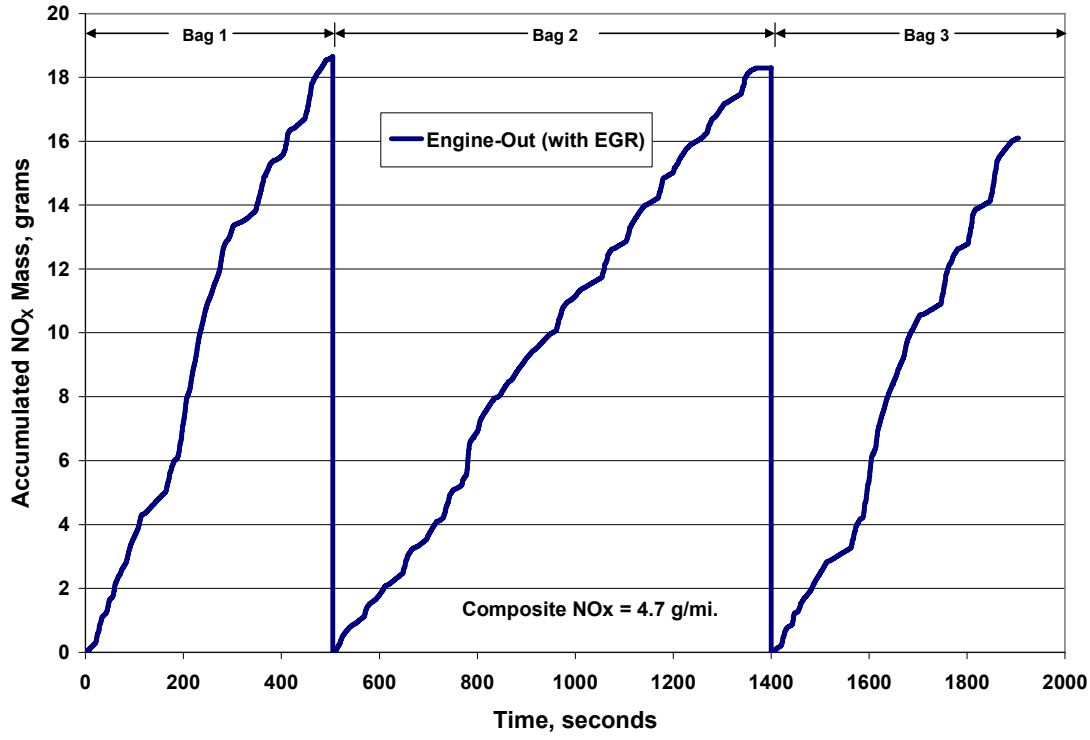

Figure 5. Accumulated NO_x mass over the FTP

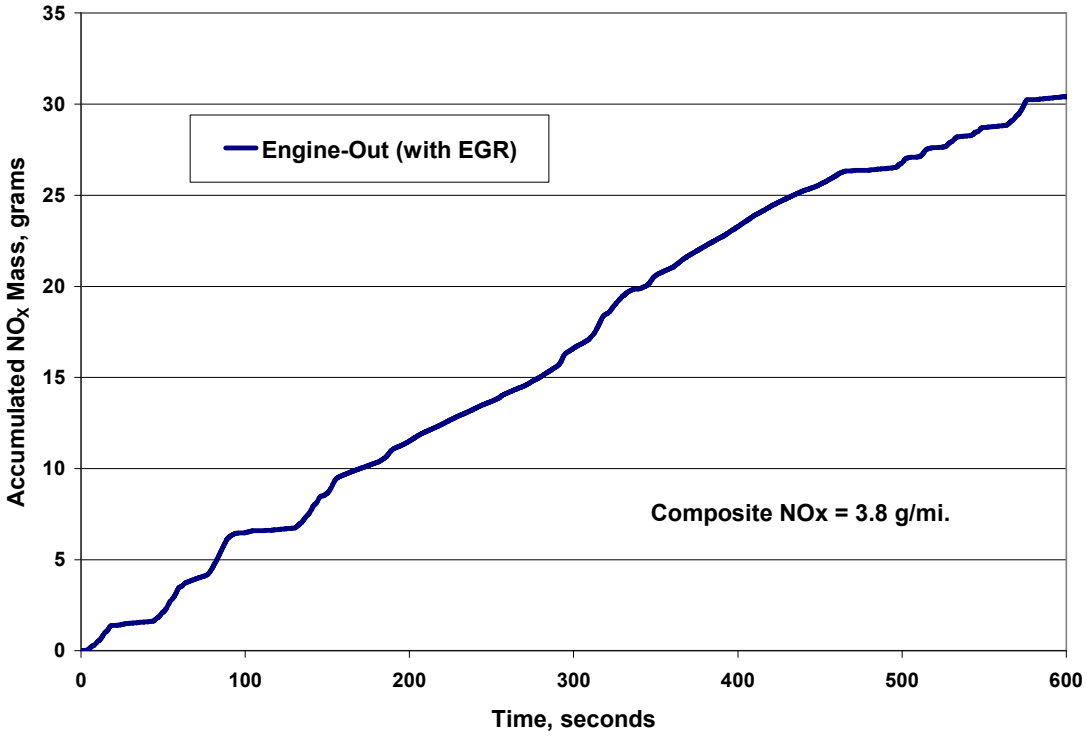

Figure 6. Accumulated NO_x mass over the US06

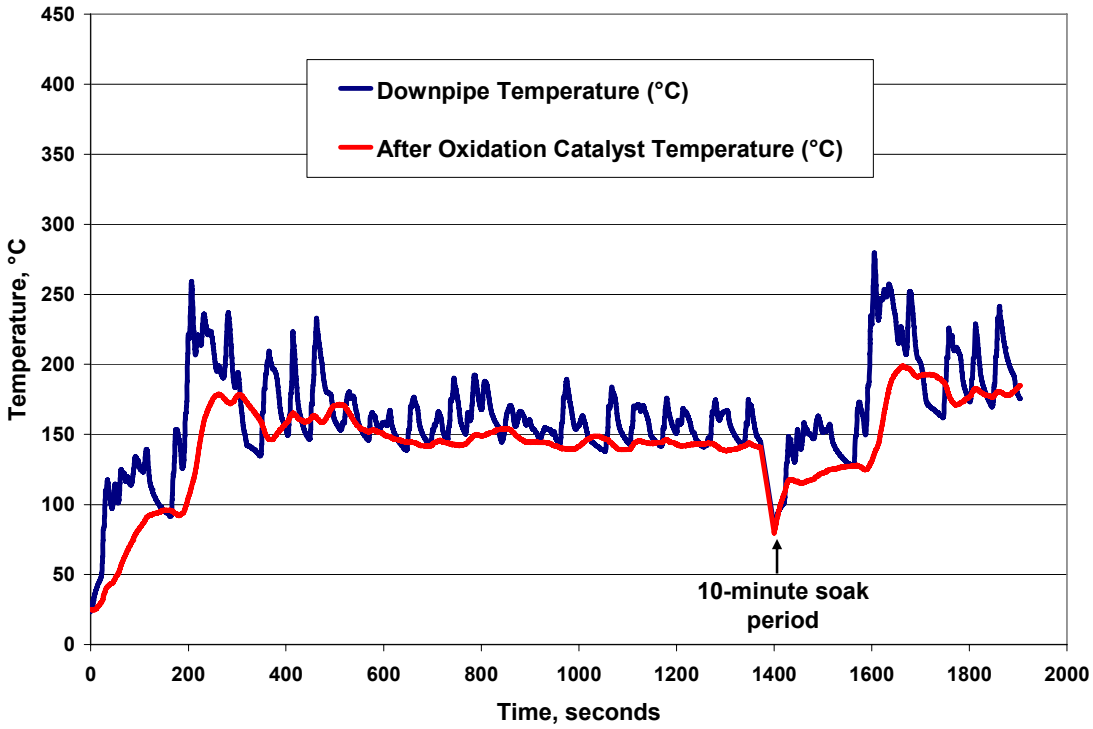

Figure 7. Exhaust gas temperatures over the FTP

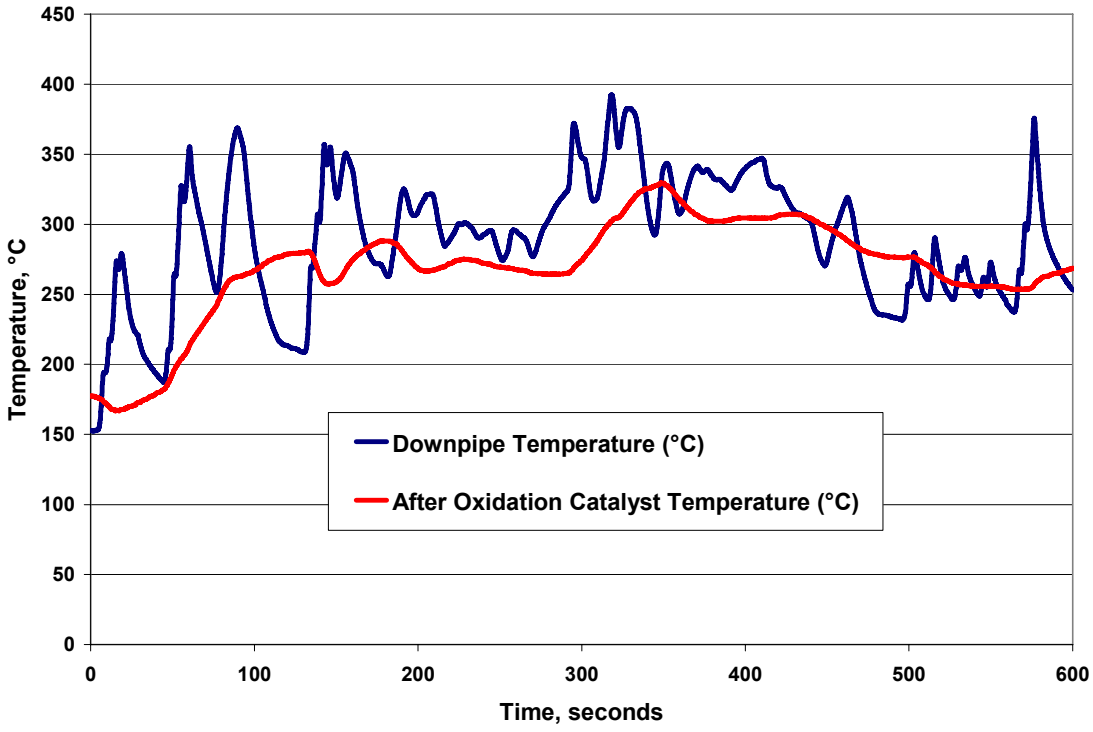

Figure 8. Exhaust gas temperatures over the US06

ECS Configuration. Based upon the initial, "quick-look" vehicle test results, it was obvious that an extremely high level of NO_x reduction would be required to meet the program goal (>98% over the FTP for the given level of engine-out NO_x with the stock EGR calibration). Also, additional heat beyond that supplied by the engine would be required in order for any NO_x adsorber system to function well (NACs typically require operating temperatures >275°C for greater than 90% NO_x reduction efficiency).

The original program plan was to examine two significantly different ECSs in order to gain a better understanding of the impact and trade-offs between the two systems. However, due to the extremely high level of NO_x reduction required, availability of system components, and the desire to investigate the performance of the system after 2,000 hours of aging, only one system (System B described below) was ultimately utilized in this program.

The first system to be studied (System A, shown in Figure 9) was a single, in-line DPF and NO_x adsorber system utilizing known and available components. Configuration A represented the smallest physical package with the least complexity. In addition, as regeneration and desulfurization would occur under full-flow conditions, it would require the least amount of additional equipment to control the system. However, full-flow regeneration and desulfurization had the potential of incurring a large fuel economy penalty and provided no additional means for NO_x adsorption when the efficiency of the NO_x adsorber was low or regenerating.

The second system to be studied (System B, variations shown in Figures 10a, 10b, 10c) was to be a dual-leg NO_x adsorber-DPF system potentially utilizing more research-oriented components (i.e., sulfur traps, CO-generating catalysts). Configuration B would be physically larger than A, and would require exhaust valves to direct flow during regeneration and desulfurization. Additionally, supplemental exhaust fuel injection (SFI) would be required to provide reducing conditions to the regenerating leg. However, as regeneration would occur under partial flow conditions, and adsorption would continue during regeneration (in the opposite leg), System B had the potential for a lower fuel economy penalty and higher efficiency. The use of sulfur traps was intended to extend the time between regenerations, reducing the fuel economy penalty associated with desulfurization. A patent application was filed for System B3 and received on June 1, 2004 (US Patent No. 6,742,328). However, due to the desire to utilize known components (for durability purposes), the final version of System B, shown in Figure 11, was more similar to the version shown in Figure 10 b.

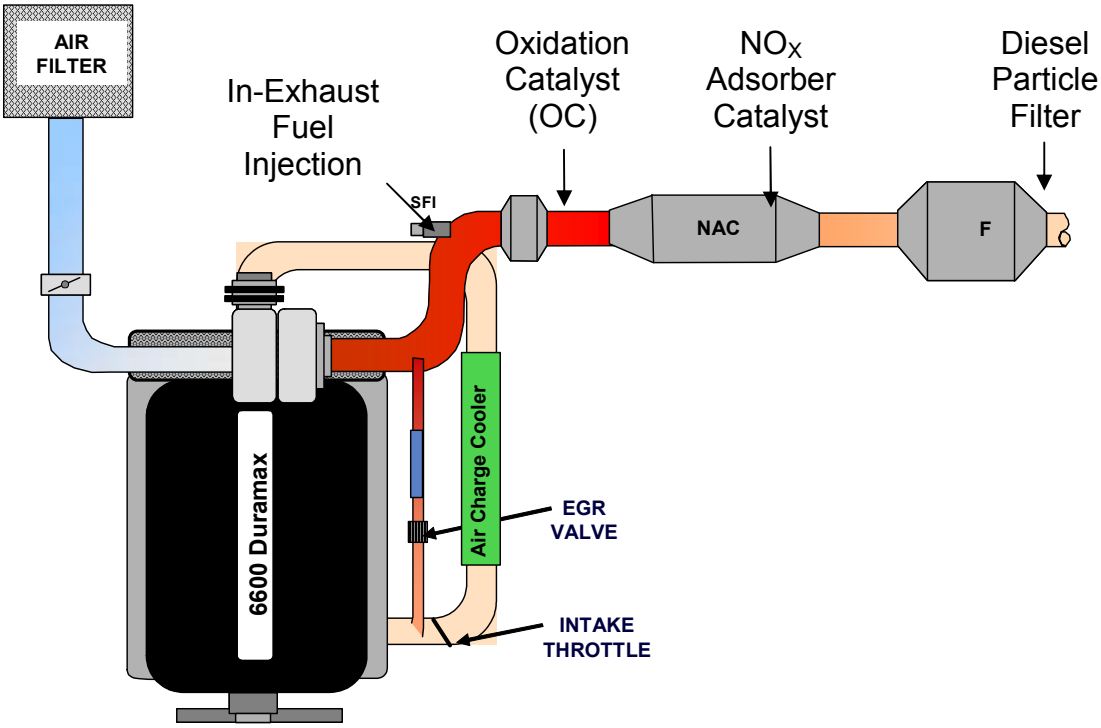

Figure 9. Proposed System A ECS configuration (single, in-line system)

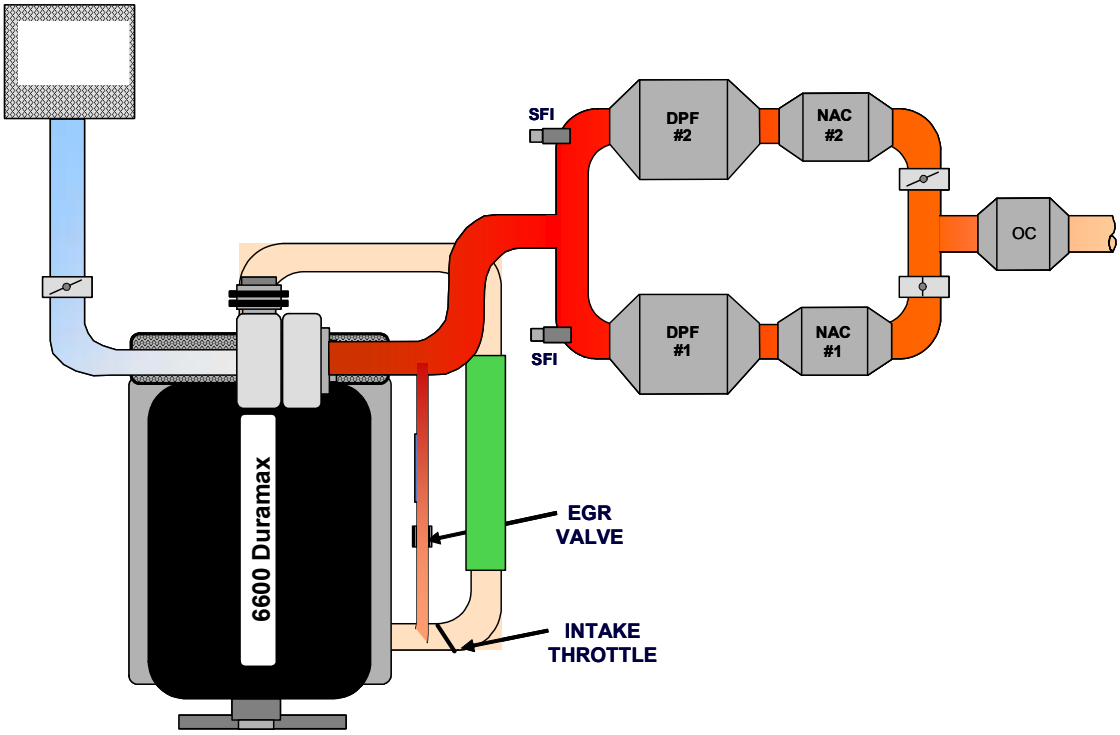

Figure 10a. Proposed System B1 ECS configuration (dual-leg system)

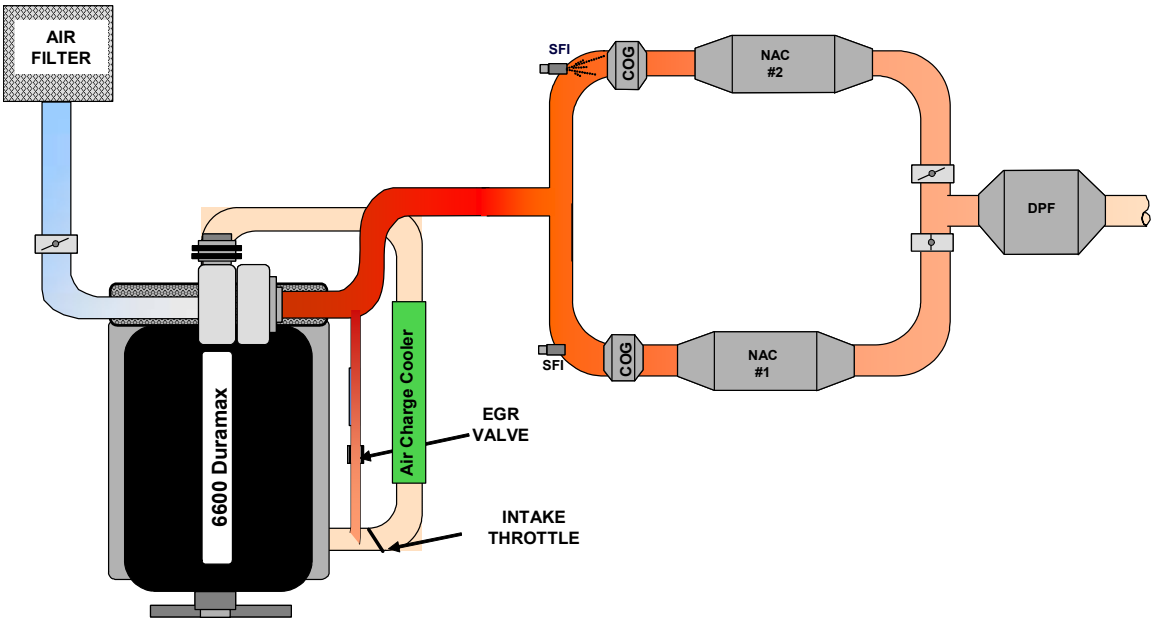

Figure 10b. Proposed System B2 ECS configuration (dual-leg system)

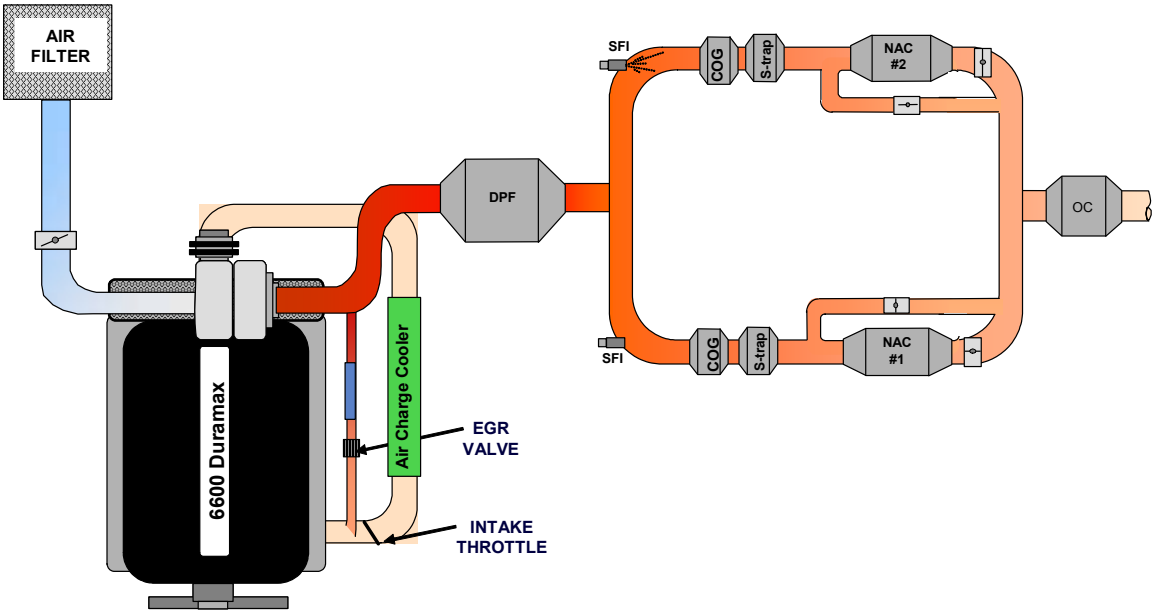

Figure 10c. Proposed System B3 ECS configuration (dual-leg system)

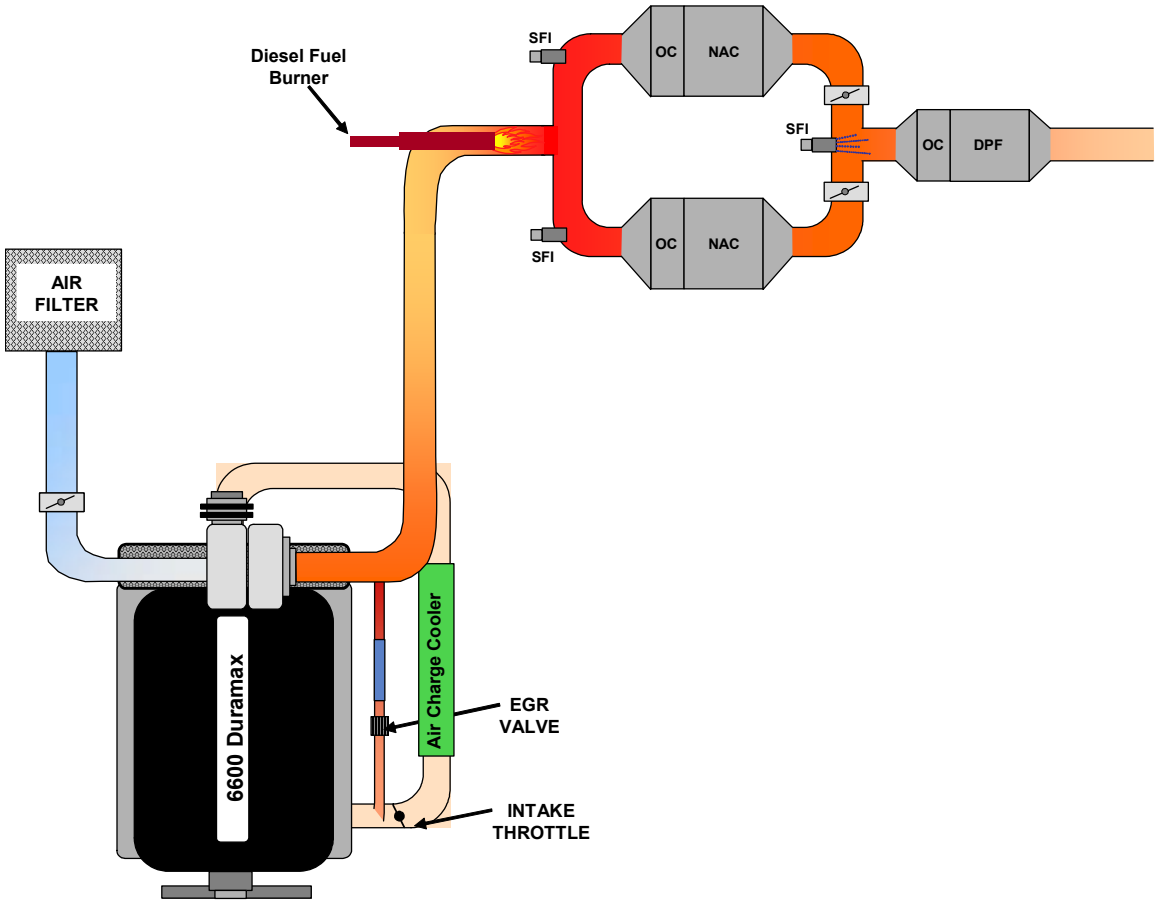

Figure 11. System B, final ECS configuration utilized

2.2.2 Test Procedures

Test procedures included chassis dynamometer test cycles; the development of equivalent test cell cycles to duplicate engine operation in the vehicle; an aging cycle; and tests of oil changes, additions, and sampling.

Chassis Dynamometer Test Cycles. Four different vehicle-based transient test cycles were utilized in this project for evaluating the ECS effectiveness. The four cycles were the cold and hot portions (Cold-Start UDDS and Hot-Start UDDS) of the light-duty FTP-75 referred to as the Urban Dynamometer Driving Schedule (UDDS), the Highway Fuel Economy Test (HFET), and the US06 portion of the Supplemental FTP. The Cold-Start UDDS cycle is conducted after a vehicle ambient soak period of 12-36 hours, while the Hot-Start UDDS cycle is conducted after a 10-minute soak period immediately following the Cold-Start UDDS (repeat of driving cycle). The HFET is conducted after operating over an HFET prep cycle, regardless of vehicle soak-time, while the US06 is conducted after completing one of a number of allowable different prep cycles. For this program, the US06 test cycle was preceded by a US06 prep cycle. The corresponding indicated vehicle speed versus time schedules for the different driving cycles (including the prep sequence) are shown in Figure 12 for the Cold -Start UDDS and Hot-Start UDDS cycle, Figure 13 for the HFET, and Figure 14 for the US06.

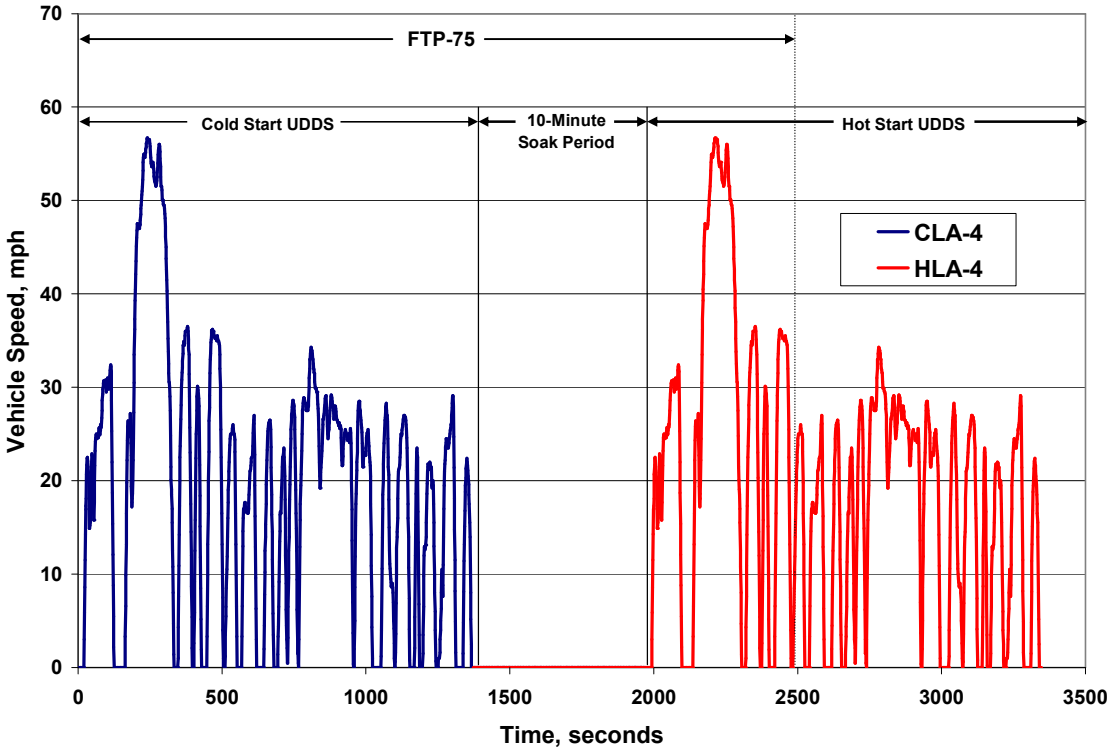

Figure 12. Indicated vehicle speed versus time for Cold-Start UDDS and Hot-Start UDDS driving schedules

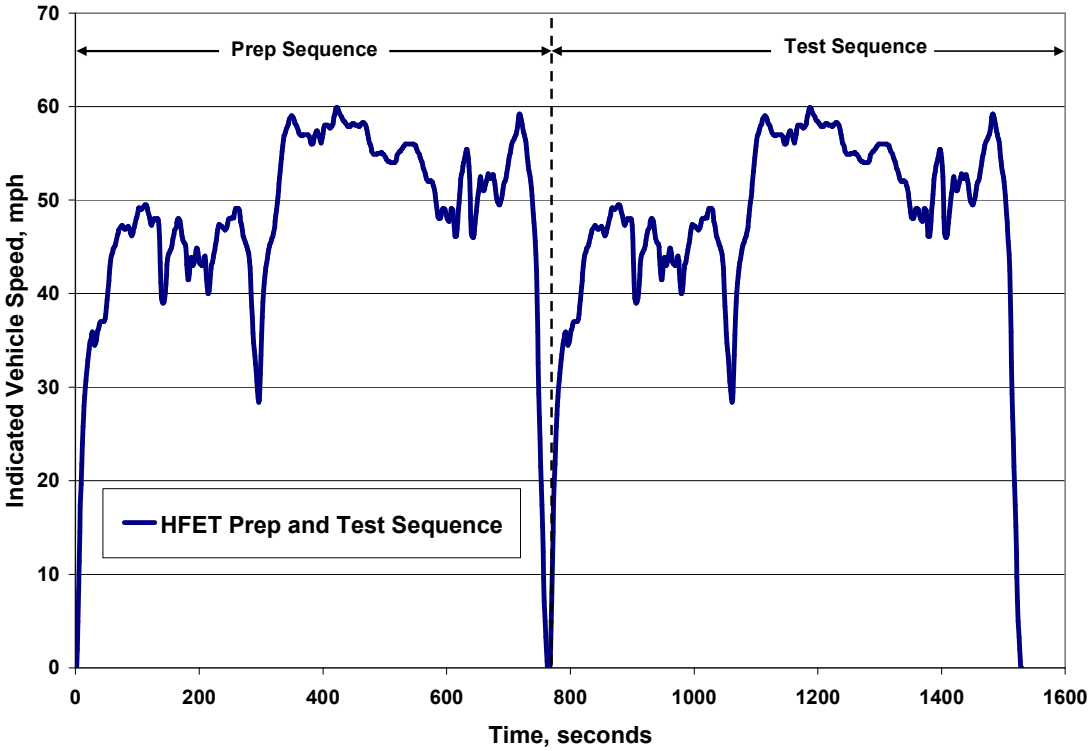

Figure 13. Indicated vehicle speed versus time for HFET prep and test driving schedule

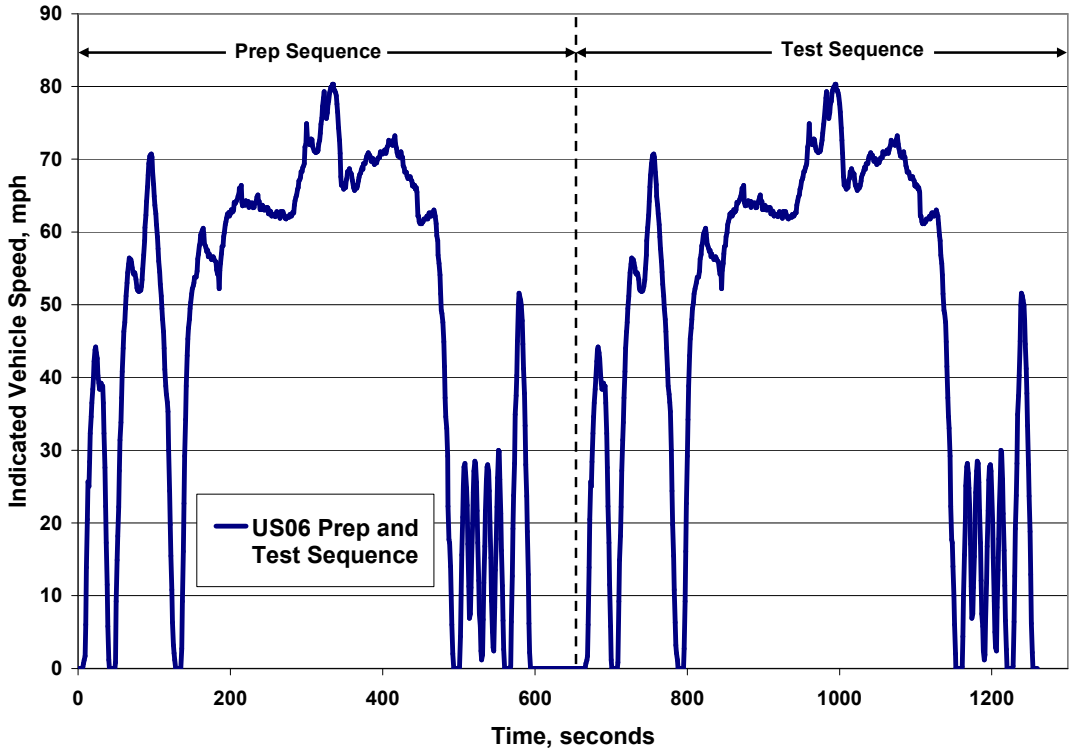

Figure 14. Indicated vehicle speed versus time for US06 prep and test driving schedule

A comparison of the maximum speed, average speed, maximum acceleration, distance traveled and time for the different cycles is shown in Table 8. As can be seen in this table, the UDDS is a lightly loaded cycle where the engine spends significant time at idle conditions.

Table 8. Operational Characteristics of Select Light-Duty Chassis Dynamometer Test Cycles

Test Cycle	UDDS	HFET	US06
Average Speed, mph	19.5	48.2	48.0
Maximum Speed, mph	56.7	59.9	80.3
Maximum Accel, mph/s	3.6	3.2	8.4
Duration, sec	1372	765	600
Distance, mi.	7.5	10.26	8.01
Idle Time, %	19.0	0.8	7.3

Development of Equivalent Test Cell Cycles to Duplicate Engine Operation in the Vehicle. In order to speed the development of the NAC system control strategy, provide more repeatable test conditions, and allow multiple cold-start tests to be conducted in a single day, it was determined to be more efficient to forgo testing on the vehicle and move into a test cell environment. Different test cell control cycles for the Cold-Start UDDS, Hot-Start UDDS,

HFET, and US06 were developed in order to duplicate engine operation in the vehicle. The vehicle was operated on the chassis dynamometer over the test cycles of interest while recording important operational information such as engine speed, accelerator pedal position (APP), manifold absolute pressure, intake MAF, exhaust temperatures, etc. (with EGR disabled). Graphical representations of the resultant engine speed and torque output versus time for the Cold-Start UDDS (with increased cold-idle speed), Hot-Start UDDS, HFET, and US06 are shown in Figures 15, 16, 17, and 18, respectively. These control cycles resulted in engine-out emissions, fuel consumption, and exhaust gas temperatures similar to those observed on-vehicle. A comparison of the engine-out accumulated NO_x mass, CO_2 mass, and exhaust gas temperature for a Cold-Start UDDS on the vehicle and in the test cell is shown in Figures 19, 20, and 21, respectively. A more complete description of the test cell control cycles developed and comparisons of various engine parameters can be found in Section 3.1 of this report.

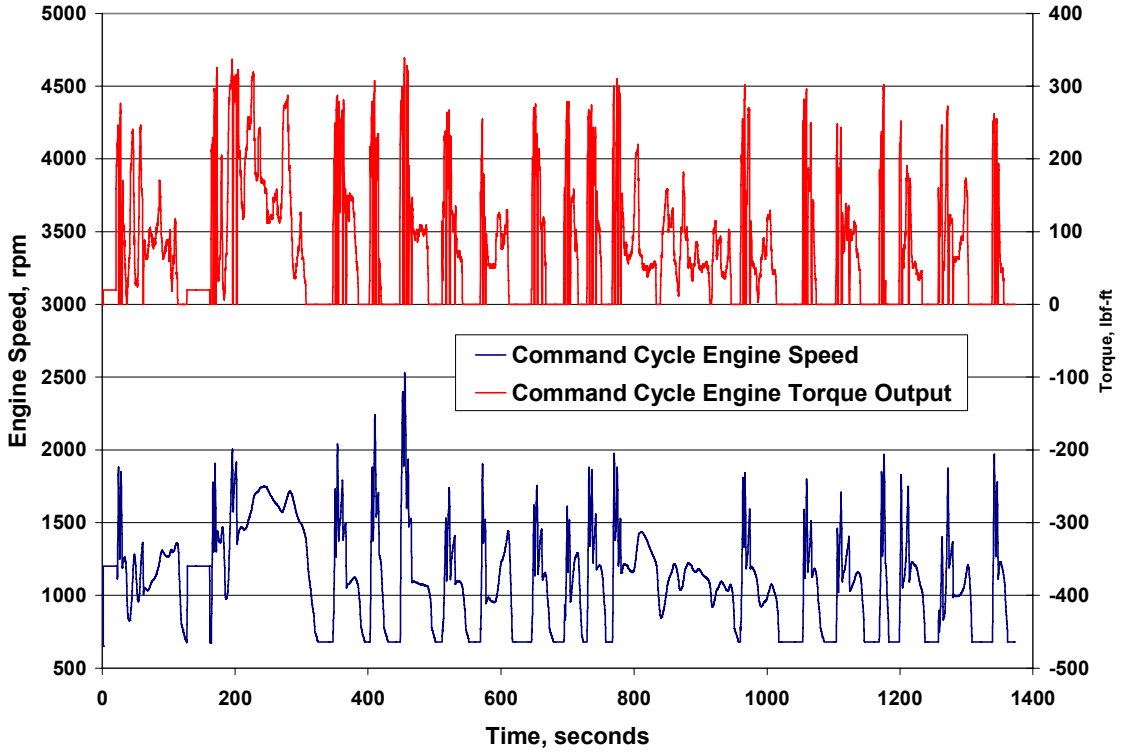

Figure 15. Test command cycle (engine speed and torque) for Cold-Start UDDS cycle

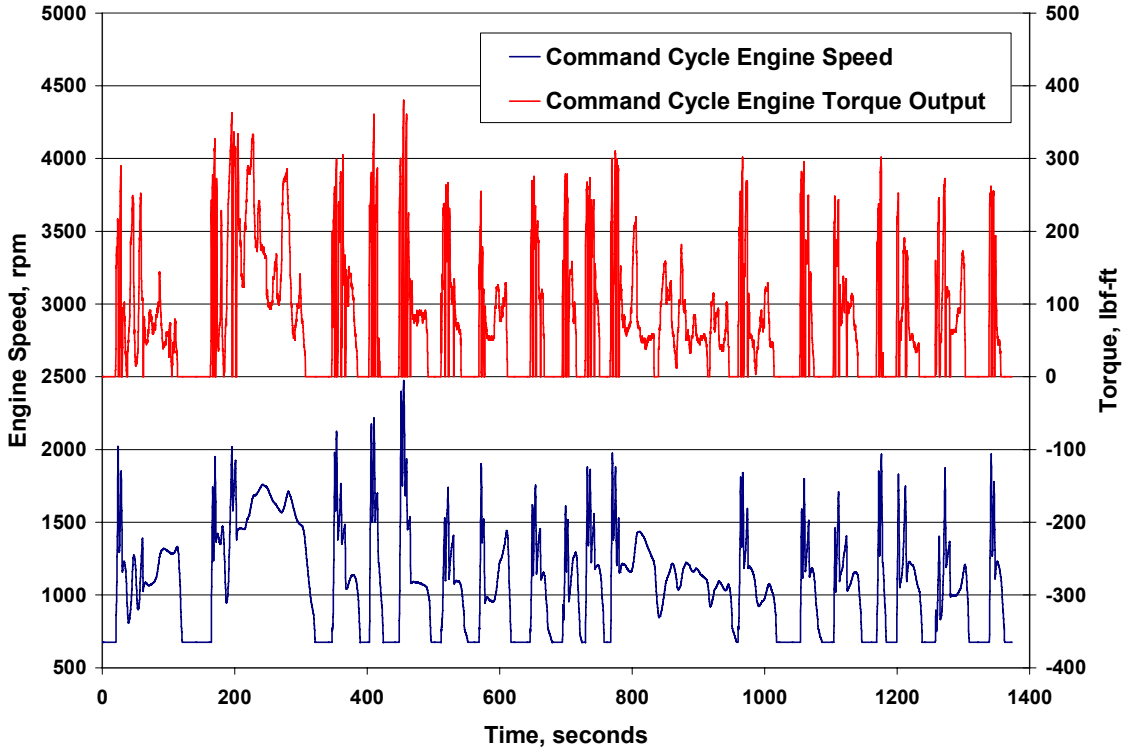

Figure 16. Test cell command cycle (engine speed and torque) for Hot-Start UDDS

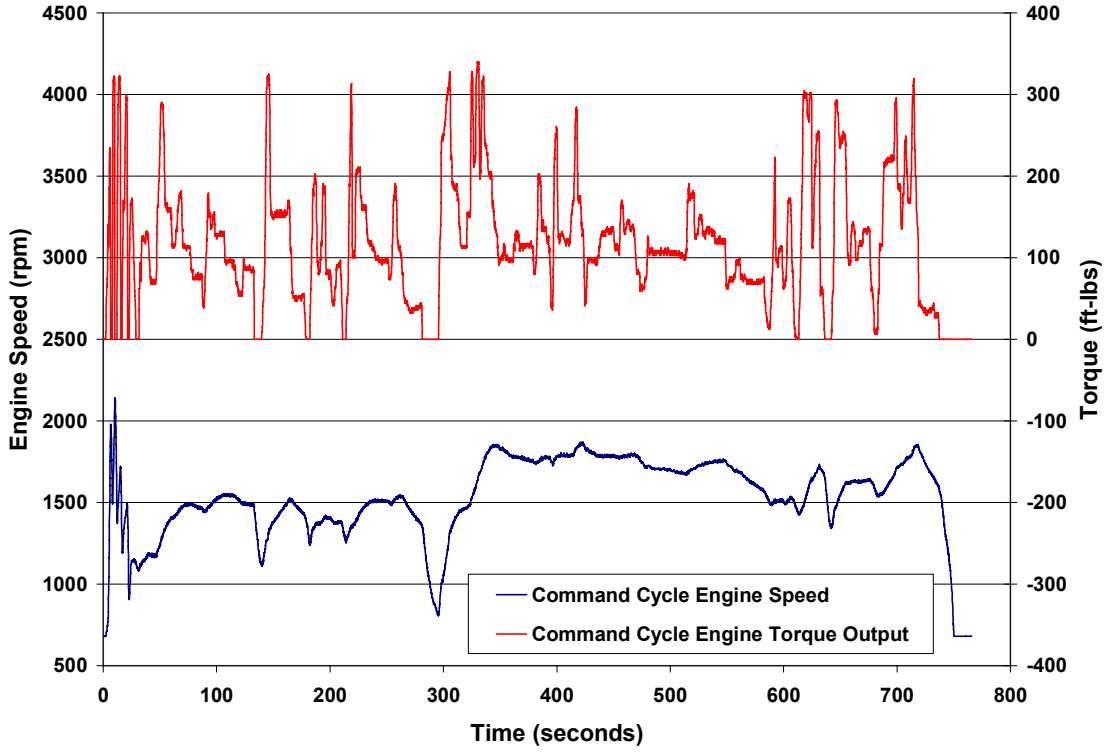

Figure 17. Test cell command cycle (engine speed and torque) for HFET cycle

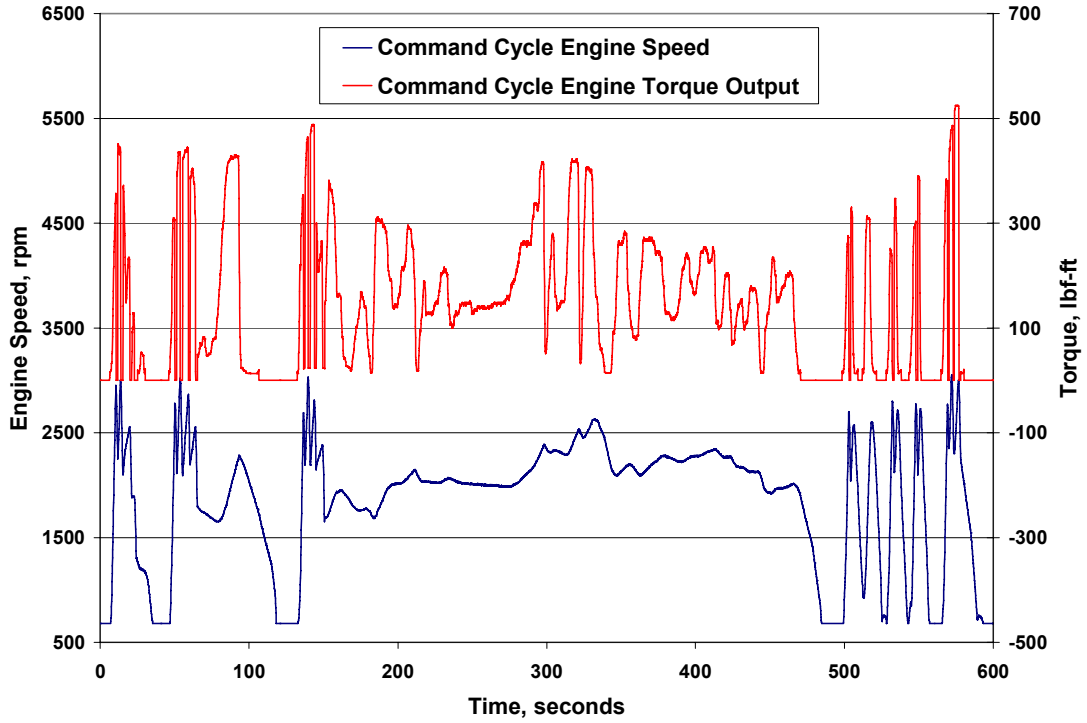

Figure 18. Test cell command cycle (engine speed and torque) for US06 cycle

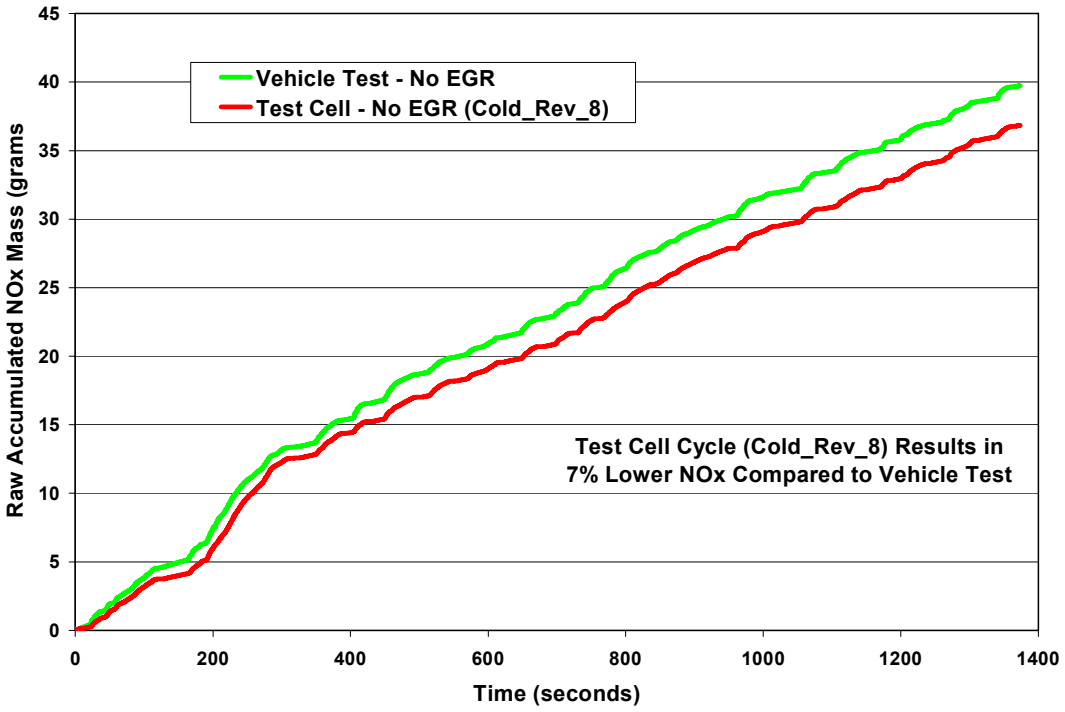

Figure 19. Comparison of accumulated engine-out NO_x mass over the Cold-Start UDDS for a vehicle test and test cell run

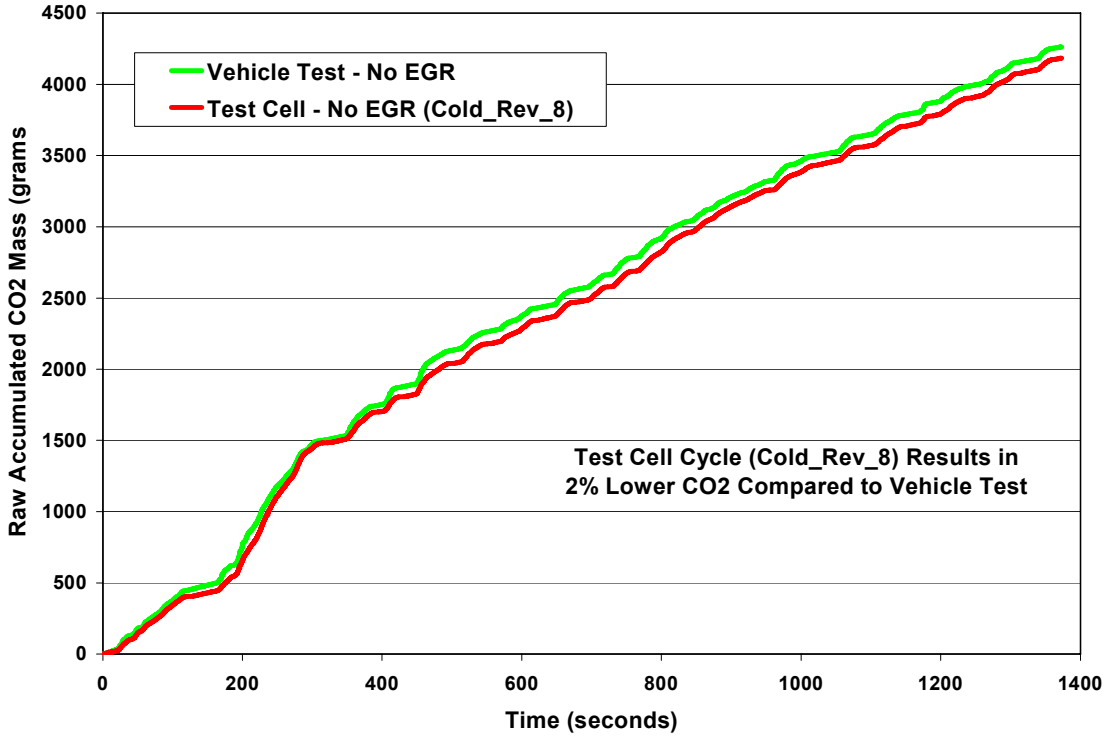

Figure 20. Comparison of accumulated engine-out CO_2 mass over the Cold-Start UDDS for a vehicle test and test cell run

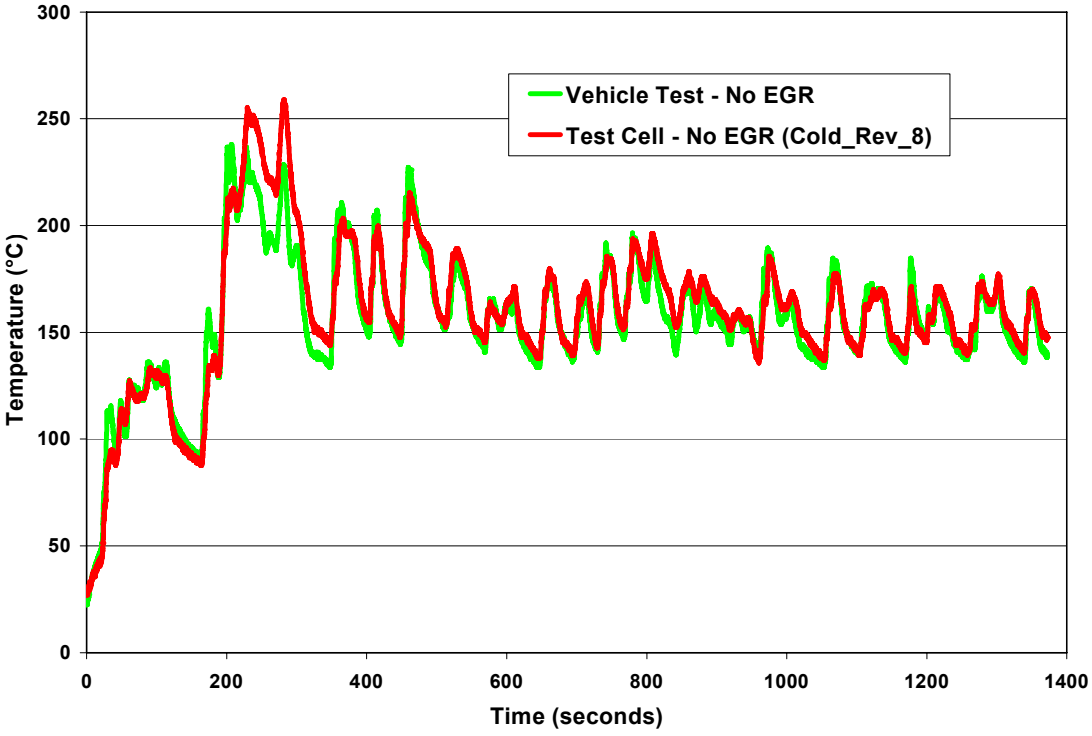

Figure 21. Comparison of exhaust gas temperature over the Cold-Start UDDS for a vehicle test and test cell run

Aging Cycle. In order to evaluate the impact of long-term operation on the ability of the NAC system to achieve high levels of NO_x reduction, it was necessary to develop an aging cycle as there are no industry standards for aging NO_x adsorber systems. As this program was a light-duty-based program, an aging cycle was developed that reflected more on light-duty-type operation (i.e., no extended high-load operation). Also, since the primary functions of the NAC are to adsorb, desorb, and reduce NO_x, it was not known exactly how the aging of this device could be accelerated while still exercising these functions. Aging at elevated temperature is known to deactivate the NAC, but a correlation of elevated temperature exposure to miles was not known. Also it was not clear that thermal acceleration of aging alone would adequately simulate the aging process of the NAC. In addition, sulfur exposure of the NAC is a critical issue, and the frequency of desulfurization events was unknown at the start of testing. Therefore, the aging cycle was not intended to be an accelerated-type aging cycle; instead the cycle was to focus on exercising the emissions control system in a manner similar to what would be expected in-use. In the interest of repeatability and unmanned operation, a stepped, steady-state mode type of cycle was deemed appropriate (as opposed to a transient-type cycle).

The aging cycle developed in this program was obtained by examining the most frequent 10 modes of operation (engine speed and APP) during a vehicle test operating over the CARB Unified Driving cycle, also referred to as the LA92 cycle (speed versus time trace shown in Figure 22). This cycle was expected to expose the engine/vehicle to more "real-world" type driving conditions than seen on the FTP. The test vehicle was operated over the CARB Unified cycle on a chassis dynamometer to obtain engine operating information (i.e., speed, APP, exhaust temperatures, etc.). A summary of the frequency of operation for various engine speed and APP "bins" is shown in Table 9 where the 11 most frequent bins of operation are highlighted. The 1,350 rpm / 5% APP point was determined to be a motoring phase and was not included in the aging cycle. An engine dynamometer-based aging cycle was developed utilizing the remaining 10 bins of most frequent operation. The cycle was developed by fixing the desired total cycle length at 10 minutes, and basing each mode length on its corresponding percentage of total operation over the CARB Unified Driving cycle. Table 10 shows the various operating modes and their corresponding time duration. A ramp time of 5 seconds was incorporated between each mode where a change in engine speed was required.

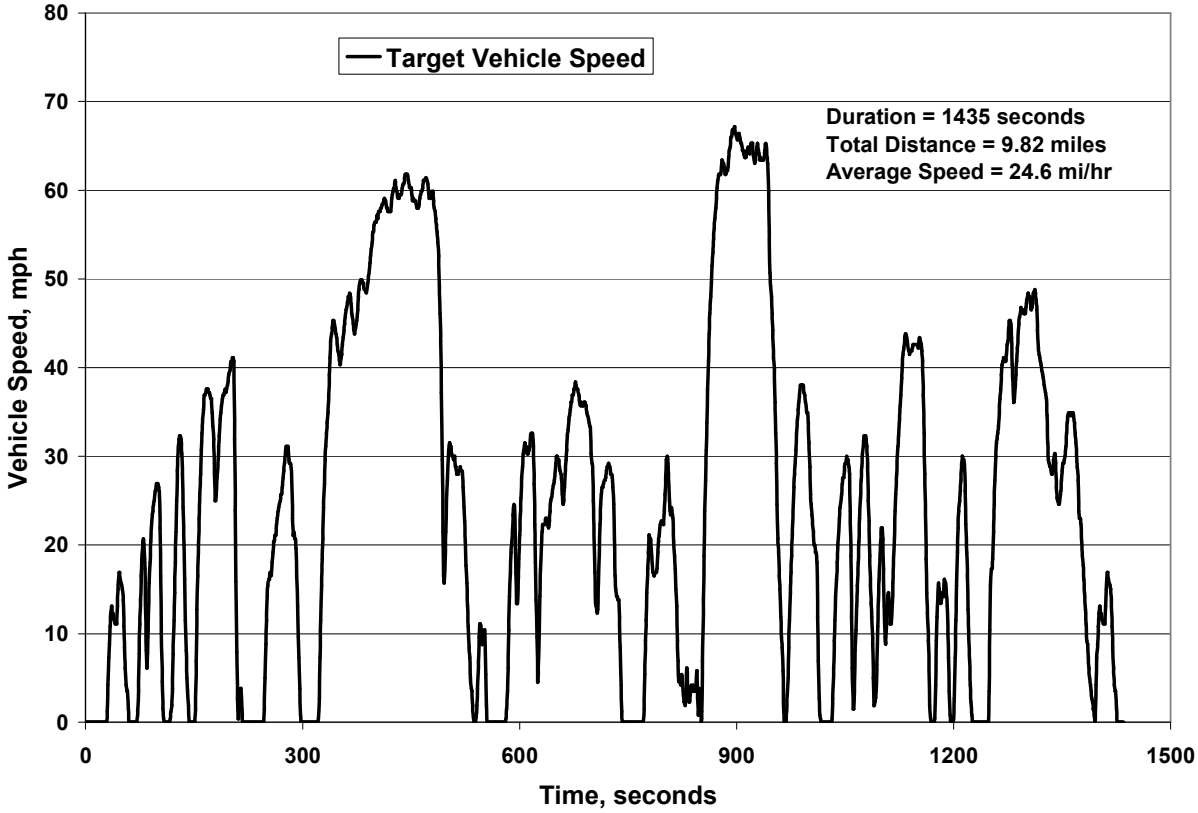

Figure 22. Vehicle speed versus time for CARB Unified Driving Schedule

Table 9. RPM and APP Analysis of the CARB Unified Driving Cycle

Engine Speed RPM	*Accelerator Pedal Position (APP)*									
	5	*15*	*25*	*35*	*45*	*55*	*65*	*75*	*85*	*95*
450	***0.2%***	***0.1%***	***0.0%***	***0.0%***	***0.0%***	***0.0%***	***0.0%***	***0.0%***	***0.0%***	***0.0%***
750	*9.2%*	***1.7%***	***0.8%***	***0.0%***	***0.0%***	***0.0%***	***0.0%***	***0.0%***	***0.0%***	***0.0%***
1,050	***2.7%***	*3.6%*	*4.0%*	***2.7%***	***0.8%***	***0.3%***	***0.0%***	***0.0%***	***0.0%***	***0.0%***
1,350	*4.0%*	*6.0%*	*8.0%*	*8.2%*	*6.8%*	***3.7%***	***0.3%***	***0.0%***	***0.0%***	***0.0%***
1,650	***1.6%***	***1.5%***	***1.5%***	***2.4%***	***3.1%***	*4.3%*	***1.1%***	***0.1%***	***0.0%***	***0.0%***
1,950	***0.6%***	***0.3%***	***1.7%***	*5.5%*	*5.7%*	***3.1%***	***1.1%***	***0.4%***	***0.0%***	***0.0%***
2,250	***0.1%***	***0.1%***	***0.1%***	***0.4%***	***0.4%***	***0.2%***	***0.3%***	***0.3%***	***0.1%***	***0.0%***
2,550	***0.0%***	***0.0%***	***0.0%***	***0.0%***	***0.0%***	***0.1%***	***0.0%***	***0.2%***	***0.1%***	***0.0%***
2,850	***0.0%***	***0.0%***	***0.0%***	***0.0%***	***0.0%***	***0.0%***	***0.0%***	***0.0%***	***0.1%***	***0.0%***
3,150	***0.0%***	***0.0%***	***0.0%***	***0.0%***	***0.0%***	***0.0%***	***0.0%***	***0.0%***	***0.0%***	***0.0%***

Table 10. Frequency of RPM and APP Combinations over the CARB Unified Driving Cycle

	Speed, rpm	**APP**	**Percent of CARB Unified Cycle**	**Percent of Aging Cycle**	**Mode Time, sec**
Mode 1	680	0%	9.2%	14.2%	86
Mode 2	1050	15%	3.6%	5.7%	34
Mode 3	1050	25%	4.0%	6.3%	38
Mode 4	1350	15%	6.0%	9.4%	56
Mode 5	1350	25%	8.0%	12.5%	75
Mode 6	1350	35%	8.2%	12.8%	77
Mode 7	1350	45%	6.8%	10.6%	54
Mode 8	1650	55%	4.3%	6.7%	40
Mode 9	1950	35%	5.5%	8.7%	52
Mode 10	1950	45%	5.7%	8.9%	53
Ramps	---	---	---	4.2%	25
Totals	---	---	61.3%	100.0%	600

In an effort to harmonize the aging cycle developed for the medium-duty SUV and light-duty passenger car APBF-DEC programs, the aging cycle was modified to include a 20-minute, steady-state evaluation mode. The final aging cycle maintained the original 10 steady-state points (shown in Figure 23) and their relative weighting, but was expanded to include a steady-state evaluation point. The selected steady-state evaluation point was the highest speed and load point of the 10 cycle modes (1,950 rpm and 45% APP or 180 lb-ft torque). The steady-state evaluation point chosen had the highest space velocity and was expected to magnify any loss in performance of the NAC due to sulfur accumulation. In addition, this point had one of the highest fuel consumption rates and increased the sulfur mass exposure of the system. The evaluation point was also used to verify continuous DPF regeneration throughout the aging

cycle. This point was run for 20 minutes, once every 4 hours (22, 10-minute cycles followed by the 20-minute, steady-state point). Table 11 provides the operating characteristics of the steady-state evaluation point. Figure 24 shows the percentage of time spent at each operating point for the aging cycle as a 4-hour set (22, 10-minute cycles plus one 20-minute evaluation).

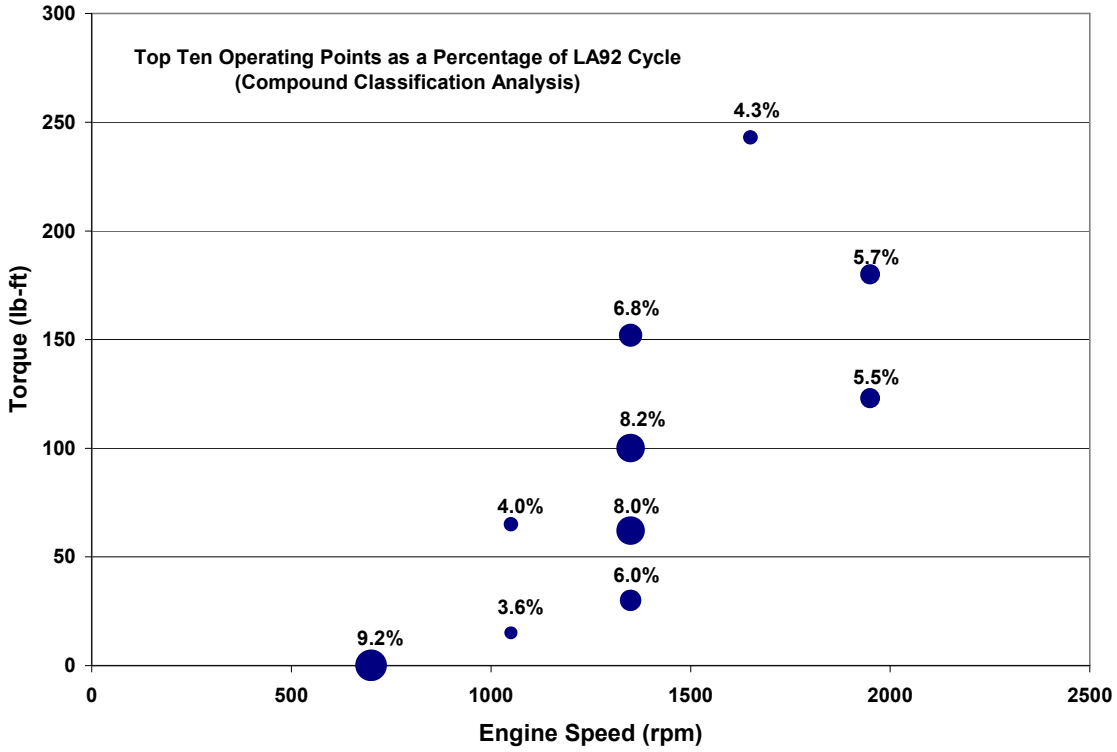

Figure 23. Ten most frequent operating points over CARB Unified Driving cycle

Table 11. Steady-State Evaluation Point Information

Engine Speed (rpm)	1950
APP (Percent)	45
Torque (lb-ft)	180
Power (hp)	67
Intake MAF Rate (g/s)	73
EGR Rate (Percent)	24
Fuel Consumption (lbs/hr)	27.8
Engine Back Pressure (inHg)	2.4
DPF DeltaP (inH2O)	17.2
Exhaust Temp @ Manifold (ºC)	446
Oxi1 – 1" (ºC)	370
Oxi2 – 1" (ºC)	355
NAC1 – 1" (ºC)	389
NAC1 –5" (ºC)	394
NAC2 – 1" (ºC)	405
NAC2 – 5" (ºC)	416
Oxi3 - 1" (ºC)	362
DPF – 1" (ºC)	364
DPF – 11" (ºC)	361
Engine-Out NO_x Concentration (ppm)	200

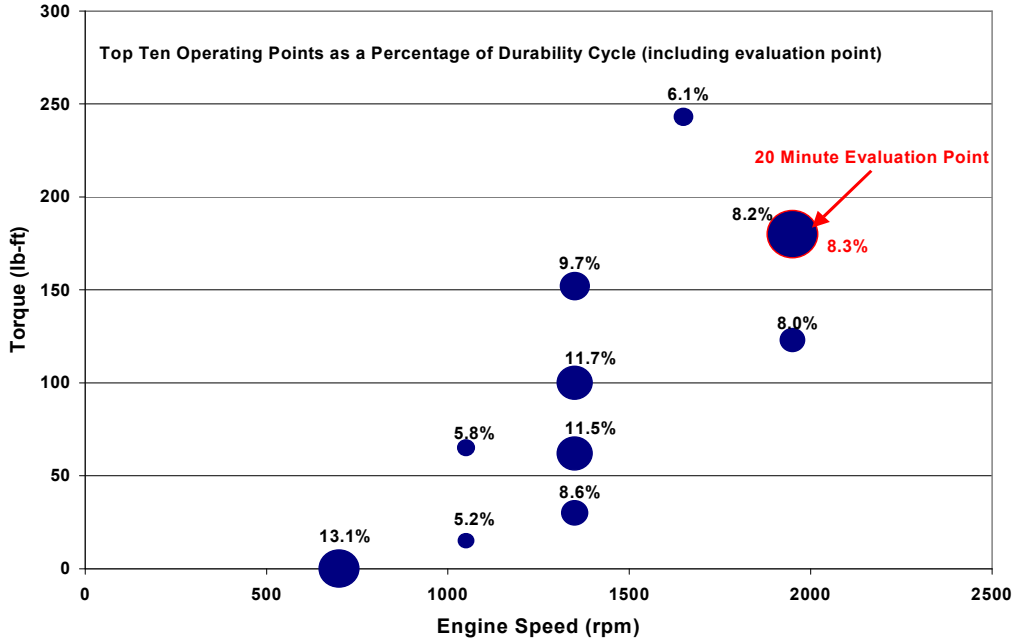

Figure 24. Aging cycle operating points with steady-state evaluation point (based on CARB Unified Driving cycle)

The order of the modes was changed after 400 hours of aging due to undesirably high NAC bed temperatures and recurring oxidation catalyst face plugging. As a result, the time of operation at each mode was slightly modified to account for the additional time required to ramp between the modes. The new order of modes alternated the engine operation between high and low speeds/loads. A comparison of engine speed and load for the original aging cycle and the modified cycle is shown in Figure 25, while a comparison of oxidation and NAC bed temperature for the two different cycles is shown in Figure 26. A summary of the modified

aging cycle (including the weighting of the steady-state evaluation point, Mode 10, and ramps between modes) is shown in Table 12.

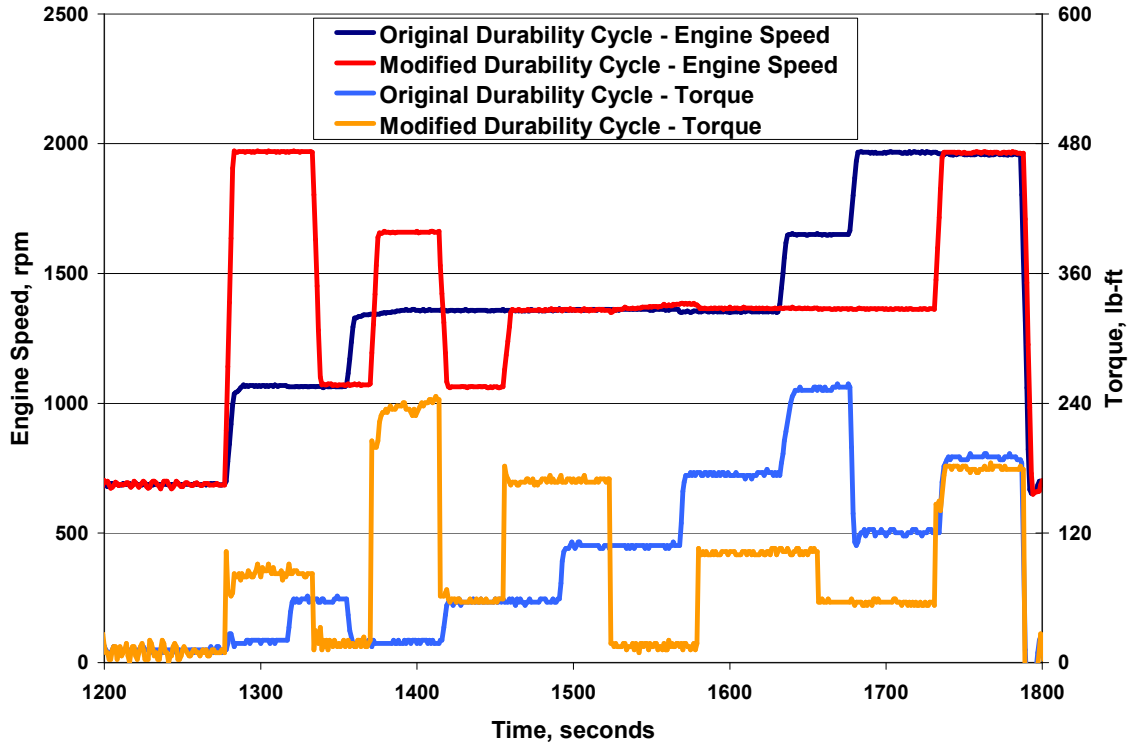

Figure 25. Comparison of engine speed and load for the original and modified aging cycles

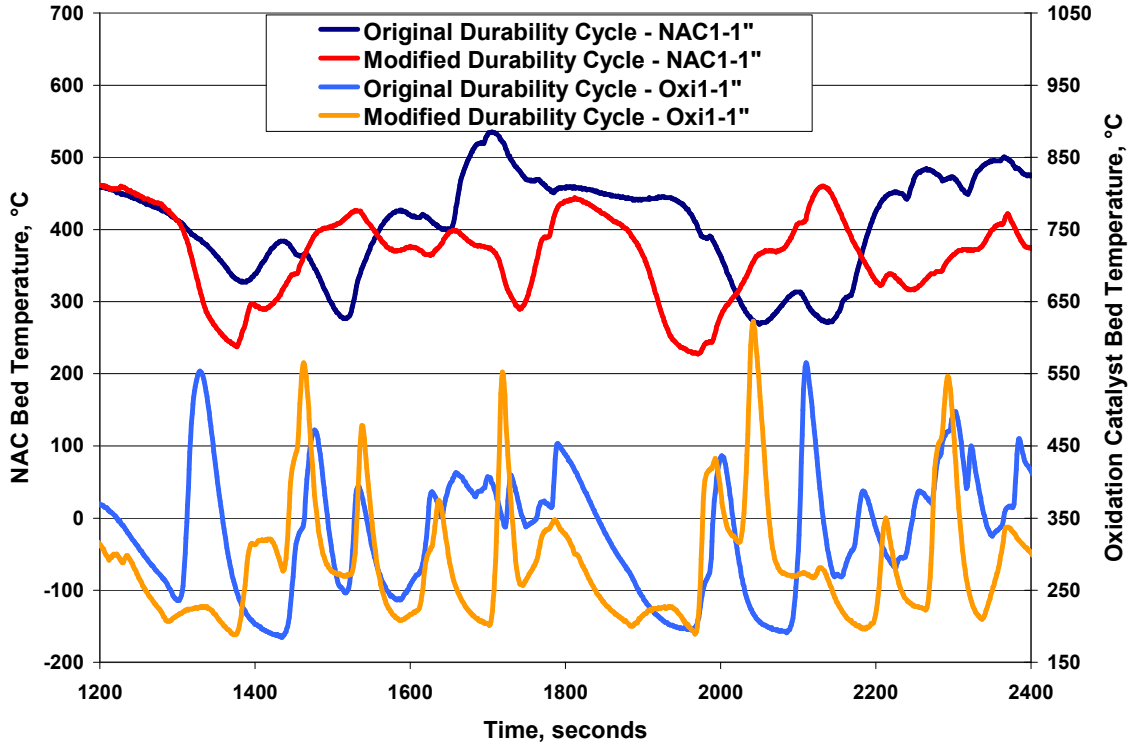

Figure 26. Comparison of oxidation and NAC bed temperatures over the original and modified aging cycles

Table 12. Summary of Modified CARB Unified Cycle Based on Aging Cycle Operating Conditions and Mode Order

Step	Original Mode Number	Engine Speed, rpm	APP	Percent of CARB Unified Cycle	Percent of Aging Cycle	Mode Time, sec
1	1	680	0%	9.2%	12.8%	84
2	Ramp	680-1,950	0-35%	- - -	0.8%	5
3	9	1,950	35%	5.5%	7.8%	51
4	Ramp	1,950-1,050	35-15%	- - -	0.8%	5
5	2	1,050	15%	3.6%	4.9%	32
6	Ramp	1,050-1,650	15-55%	- - -	0.8%	5
7	8	1,650	55%	4.3%	6.0%	39
8	Ramp	1,650-1,050	55-25%	- - -	0.8%	5
9	3	1,050	25%	4.0%	5.5%	36
10	Ramp	1,050-1,350	25-45%	- - -	0.8%	5
11	7	1,350	45%	6.8%	9.6%	63
12	Ramp	1,350-1,350	45-15%	- - -	0.2%	1
13	4	1,350	15%	6.0%	8.4%	55
14	Ramp	1,350	15-35%	- - -	0.2%	1
15	6	1,350	35%	8.2%	11.6%	76
16	Ramp	1,350	35-25%	- - -	0.2%	1
17	5	1,350	25%	8.0%	11.3%	74
18	Ramp	1,350	25-45%	- - -	0.2%	5
19	10 (SS)	1,950	45%	5.7%	16.3%	52
20	Ramp	1,950-680	45-0%	- - -	0.8%	5
	Totals	- - -	- - -	61.3%	100%	600

Oil Changes/Additions/Sampling. As the program fuel sulfur level was very low (15 ppm), there was concern that engine oil consumption could have a significant impact on sulfur deposition on the NACs, and as such, it would be necessary to accurately monitor oil consumption throughout the test sequence. However, there was also a desire to accelerate the time frame of the program, and a decision was made to allow force-cooling between sets of tests to allow multiple cold starts in a single day, reducing the time required to conduct the emission evaluations by 50%. The force-cooling approach necessitated pumping the engine oil from the sump, through a cooler and back into the sump. This approach resulted in eliminating the possibility of accurately tracking oil consumption during the emission evaluation sequences. However, oil consumption and addition were monitored during the 100-hour aging sequences. The engine exhibited extremely low oil consumption throughout the aging, consuming approximately 7 liters of oil over the course of 2,000 hours of operation at a relatively constant rate.

Oil samples were acquired after every 100-hour emission evaluation sequence. A portion of these samples were utilized for the VOF analysis detailed in Section 2.2.3. The engine oil was changed every 300 to 400 hours of aging (after the emission evaluations had been conducted, approximately 350 or 450 hours of total run time). This oil change interval was determined earlier in the project by conducting oil analyses at various intervals during aging and observing no significant change in oil properties after 300 hours of operation. Table 13 provides a summary of select engine oil properties after various aging hours.

Table 13. Select Engine Oil Properties after Various Aging Hours

Property	0 Hours	148 Hours	221 Hours	277 Hours
Fuel Dilution (D322FD), wt.%	0	0	0	0
Viscosity (D445, 100C), cSt	14.55	14.23	14.42	14.72
Viscosity (D445, 40C), cSt	108.46	106.47	106.87	106.92
Base Number (D4739 TBN), Inflect, mg KOH/g	10.4	10.32	9.98	10.05
Base Number (D4739 TBN), Buffer, mg KOH/g	10.25	9.49	8.75	8.37
Residue (D86), wt.%	1.2	1.3	1.3	1.39
Volatile (D5480-93), wt.%	98.5	98.1	98.2	97.9
Soot (Soot TGA), wt.%	0.286	0.557	0.539	0.855
P (X-Ray SemiQ), wt.%	0.15	0.15	0.16	0.15
S (X-Ray SemiQ), wt.%	0.64	0.62	0.52	0.59
Ca (X-Ray SemiQ), wt.%	0.35	0.36	0.36	0.35
Zn (X-Ray SemiQ), wt.%	0.14	0.16	0.16	0.15

2.2.3 Sampling and Analysis Procedures

The sampling system utilized in the test cell for obtaining exhaust samples is shown in Figure 27. The system was a constant volume sampling (CVS) system using positive displacement pumps. Engine exhaust traveled through a 102-mm diameter transfer pipe to a 58.4-cm diameter by 5.5-m long, stainless-steel dilution tunnel (Figure 27), which was used to ensure proper mixing of gaseous and particle emissions prior to being sampled. The CVS system was operated at a nominal volumetric flow rate of 33.4 m^3/min, ensuring that the sample zone temperature remained below 51°C during the FTP-75, HFET, and US06 evaluations. Total dilute exhaust volume was determined for each test cycle given ambient and tunnel conditions (temperature, pressure, humidity) and blower counts. The calculated dilute exhaust volume from each test cycle was used to convert concentration values to mass values for the dilute exhaust samples.

Sampling and analysis procedures included regulated gases such as THC, CO, and NO_x in dilute bags; particle mass determination; tailpipe raw samples analyzed by an FTIR analyzer; speciation of volatile hydrocarbon compounds in dilute bags; H_2S; SO_2; PAH and NPAH; metals such as aluminum, silicon, and phosphorus; and total nitrogen compounds from nitroxy-alkane samples.

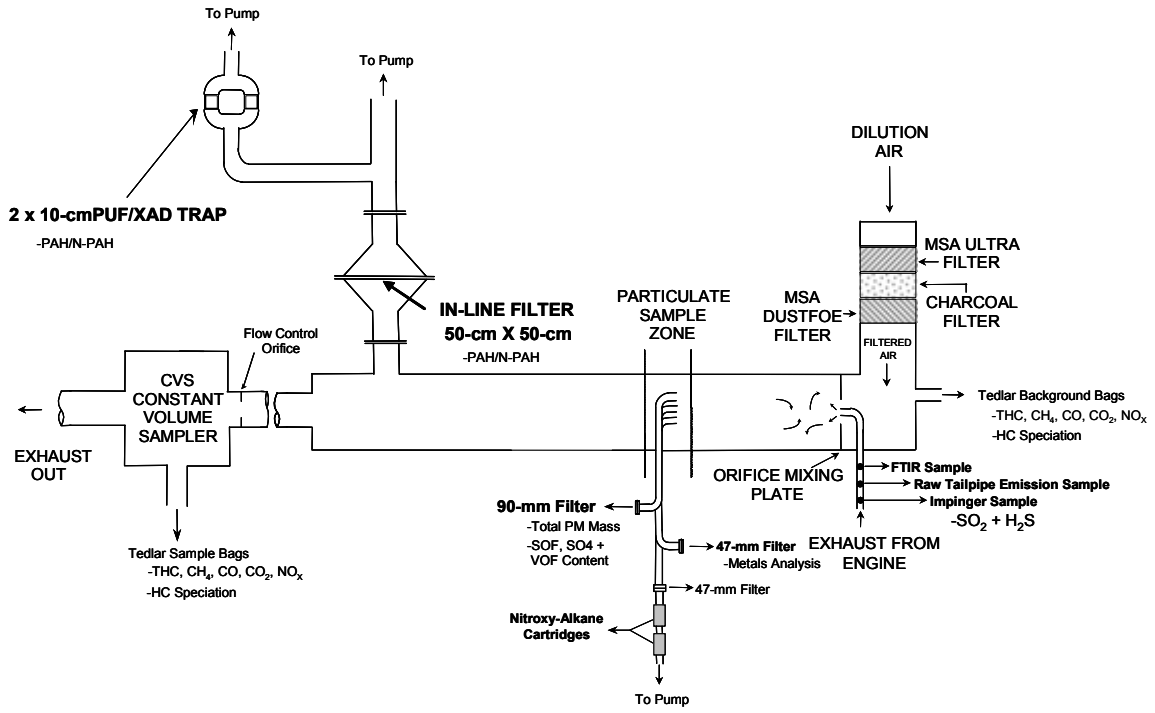

Figure 27. Test cell emissions sampling system

Regulated Gases (THC, methane, CO, CO_2, NO_x) – Dilute Bags. Proportional dilute exhaust samples, as well as ambient samples for the determination of THC, methane, NO_x, CO, and CO_2 concentration, were collected in Tedlar® bags for analysis. THC concentration was measured using a flame ionization detector (FID). CO and carbon dioxide (CO_2) were determined using nondispersive infrared instruments. NO_x was measured using a chemiluminescent instrument. Methane was quantified using a gas chromatograph (GC) equipped with a FID. The dilute bag samples were taken over a given test cycle (i.e., Cold-Start UDDS, Hot-Start UDDS, HFET, or US06) at the location shown in Figure 27.

Particle Mass Determination. A 12.7-mm diameter probe was used to collect a proportional sample of dilute exhaust from the dilution tunnel for gravimetric determination of total part PM exhaust emissions at the location shown in Figure 27. PM samples were collected on both a primary and backup 90-mm Pallflex® filter (glass fiber filter coated with fluorocarbon). The filters were weighed before and after use on a microbalance of 1-microgram sensitivity. Before weighing, the filters were properly conditioned in a temperature- and humidity-controlled chamber which also housed the microbalance. The controlled airflow, temperature, and humidity provided an absolute humidity of 10.7 ± 0.66 grams water per kilogram of dry air in the chamber.

The volumetric flow rate of the 90-mm sampling system was approximately 177 l/min. For the engine-out tests, a new 90-mm filter pair was used for each test cycle. For the tests with the NAC/DPF system installed, a 90-mm filter pair was used for duplicate or triplicate tests for a given test cycle (i.e., three Cold-Start UDDS cycles collected on a single 90-mm filter). This approach was used in an attempt to collect a sufficient mass of sample to obtain a meaningful weight gain after installing the highly efficient DPF in the exhaust stream.

Methods included direct filter injection (DFI)/GC for VOF determination; sulfate analysis; and SOF analysis.

- ***DFI/GC for VOF Determination.*** Diesel exhaust PM is composed of elemental carbon and organic compounds derived from the combustion of diesel fuel and lubricating oil. A DFI/GC method was used to quantitatively measure and characterize the VOF of diesel exhaust PM collected on a 90-mm diameter Pallflex® filter media. This method employed a novel injection port into which 10% of the 90-mm filter media (pie-shaped portion) was placed, and thermally desorbed onto a non-polar column to separate the volatile hydrocarbons according to their boiling point. Chromatograms of the VOF from the actual lubricating oil and the VOF of PM samples were compared to determine the percent VOF and percent unburned oil. The difference was the remaining VOF, which may be attributed to fuel and partially burned fuel and lubricating oil.
- ***Sulfate Analysis.*** Sulfuric acid was collected on the 90-mm Pallflex® filter media and converted to ammonium sulfate by exposure to ammonia vapor. The soluble sulfates were leached from the filter media (40%, pie-shaped portion of total filter) with a measured volume of 60% isopropanol/40% water solution. An aliquot of this extract was injected via an autosampler into an ion chromatograph. Anions were separated by an analytical column, and passed through a conductivity detector. The retention time on the analytical column provided identification of the anion, and the intensity of the signal corresponded to the concentration detected. This method was capable of detecting sulfate at levels lower than 0.02 µg/mL.
- ***SOF Analysis.*** The remaining 50% of the 90-mm Pallflex® filter was extracted with a toluene/ethanol binary solvent (32/68% wt/wt and boiling point of 76.6°C) in a Soxhlet extraction apparatus for 8.5 hours with a solvent cycle about every 15 minutes. After drying the filters for approximately 6 hours at room temperature, the filters were reweighed at a constant temperature and humidity. The loss of weight after this extraction was the mass of the SOF. A Coordinating Research Council (CRC) round-robin interlaboratory program has established a relative standard deviation of ±15% for a minimum sample of 1 mg for SOF. For samples of 10 mg and larger, precision within the laboratory should be ±10% or less.

FTIR Analyzer—Tailpipe Raw Sample. A raw exhaust sample was taken at the tailpipe location (as shown in Figure 27) utilizing a Nicolet REGA 7000 RT Exhaust Gas Analyzer which incorporates a high-performance FTIR spectrometer (NEXUS 670). These data were recorded on a second-by-second basis and were acquired during the unregulated emission sampling tests (zero-hour engine-out tests; and 100-hr, 300-hr, 900-hr, 1,500-hr, and 2,000-hr aging points) as detailed in Section 2.1.5. The lowest and highest calibration points (multiple calibration points between) for the various compounds analyzed are shown in Table 14. Due to the known limitations of the analyzer, and the availability of alternate sampling procedures, separate analyses (based on average concentration over a given test cycle – dilute bag) were conducted for benzene, 1,3-butadiene, and SO_2.

Table 14. Low- and High-Span Gas Concentrations

Compound	Low- / High-Span Points (ppm)
Acetaldehyde	1 / 8
Ammonia	1 / 104
Benzene	2 /100
1,3-Butadiene	10 / 100
Formaldehyde	8 / 79
NO_2	9 / 1,000
Nitric Oxide	1 / 10,000
Nitrous Oxide	5 / 50
SO_2	1 / 7

Speciation of Volatile Hydrocarbon Compounds—Dilute Bag. Volatile hydrocarbon compounds were determined by hydrocarbon speciation. Analytical procedures for conducting the hydrocarbon speciation (C1 to C4 hydrocarbons, plus select C6 hydrocarbons) were similar to the CRC Auto/Oil Phase II methods.1 Three GC procedures and one high-performance liquid chromatograph procedure were used to identify and quantify specific compounds. One GC was used for the measurement of methane, a second for C2-C4 species; and a third GC was used to measure 1-methylcyclopentane, benzene, toluene, and 2,3,3-trimethylpentane, which co-elute and cannot be accurately quantified by other methods. The dilute tailpipe samples collected in Tedlar® bags for regulated emissions were also utilized for hydrocarbon speciation determination. In general, all emission "sample" bags were analyzed before the "background" bags, so that reactive exhaust compounds could be analyzed as quickly as possible.

A brief description of these procedures is given below. These included methane speciation; C_2–C_4 species; and benzene and toluene.

- ***Methane Speciation.*** A GC equipped with a FID was used for the analyses and in accordance with Society of Automotive Engineers' J1151 procedures. The GC system was equipped with a packed column to resolve methane from other hydrocarbons in the sample. Samples were introduced into a 5-mL sample loop via a diaphragm pump. For analysis, the valve was switched to the inject position, and the helium carrier gas swept the sample from the loop toward the detector through a 61 cm × 0.3 cm Porapak N column in series with a 122 cm × 0.3 cm molecular sieve 13X column. As soon as the methane peak passed into the molecular sieve column, the helium flow was reversed through the Porapak N column to vent. For quantification, sample peak areas were compared to those of external calibration standards.
- ***C_2-C_4 Species.*** With the aid of a DB-WAX pre-column and a 10-port switching valve, the second GC procedure allows the separation and determination of exhaust concentrations of C_2-C_4 individual hydrocarbon species, including: ethane; ethylene; acetylene; propane; dimethylpropane; propyne; 1,3-butadiene; 2-methylpropane; 1-butyne; and cis-2-butene. Bag samples were analyzed with a GC system, which utilizes a Hewlett-Packard Model 5890 Series II GC with an FID; two pneumatically operated and electrically controlled valves; and two analytical columns. The carrier gas was helium. One column is utilized to separate the C_2-C_4 hydrocarbons from the higher molecular weight hydrocarbons and the polar compounds. These higher molecular weight hydrocarbons (and water and alcohols) are retained on the pre-column while the C_2-C_4 hydrocarbons are passed through to the analytical

column. While the C_2-C_4 hydrocarbons are separated on the analytical column, the pre-column is back-flushed with helium to prepare for the next run. The column flow was set by fine-tuning the column head pressure to give butane a retention time of 5.25 ± 0.05 minutes. The GC was calibrated daily using a CRC Auto/Oil 23-component calibration mixture. Detection limits for the procedure were on the order of 5 ppbC in dilute exhaust for all compounds.

- ***Benzene and Toluene.*** Dilute bag samples were analyzed using a GC equipped with a FID. The GC system utilized a Hewlett-Packard Model 5890 Series II GC with a FID; a pneumatically operated and electrically controlled valve; and a DB-5 fused silica, open tubular column. The carrier gas was helium. Gaseous samples were pumped from the bag through a sample loop and then introduced into a liquid nitrogen-cooled column. The column oven was then programmed to a maximum temperature of 200°C. The analog signal from the FID was sent to a networked computer system via a buffered analog to digital converter. Column flow was set by fine-tuning the column head pressure to give propane a retention time of 5.40 ± 0.10 minutes using a temperature program. Detection limits for the procedure were on the order of 10 ppbC in dilute exhaust for all compounds. Separation of benzene and toluene from co-eluting peaks was carried out by fine-tuning the column head pressure to give benzene a retention time of 22 to 23 minutes. The GC was calibrated daily using a CRC 7-component calibration mixture consisting of propane; 1-methyl cyclopentene; cyclohexane; benzene; 2,3,3-trimethylpentane; 2,3-dimethylhexane; and toluene.

Hydrogen Sulfide. The collection of H_2S was accomplished by bubbling raw exhaust sampled at the tailpipe location through glass impingers containing a buffered zinc acetate solution at a nominal flow rate of 4 lpm (sample transported through a heated sample line). This solution traps the sulfide ion as zinc sulfide. The absorbing solution was then treated with N,N-dimethyl-para-phenylene diamine sulfate and ferric ammonium sulfate. Cyclization occurs, forming the highly colored, heterocyclic compound methylene blue (3,9-bisdimethylaminophenazothionium sulfate). The resulting solution was analyzed with a spectrophotometer at 667nm in a 1-cm cell. Sample responses were then compared to a Beer's Law curve, which was standardized from known concentrations of a standard sulfide ion solution. The minimum detectable concentration was 0.01 ppm.

-

Sulfur Dioxide. The collection of SO_2 was accomplished by bubbling raw exhaust sampled at the tailpipe location through glass impingers containing a 3% solution of hydrogen peroxide at a nominal flow rate of 4 lpm (sample transported through a heated sample line).The temperature of the absorbing solution was kept at 0°C by means of an ice water bath. This solution trapped the SO_2 as sulfate ion, and the samples were analyzed directly in an ion chromatograph and compared to external standards of known sulfate concentration.

PAH/NPAH Sampling and Analytical Procedures. Dilute exhaust samples were acquired for the determination of PAH and NPAH. An additional sampling system was utilized for acquiring the samples as shown in Figure 27. Particle-bound PAH/NPAH were trapped on the 50-cm x 50-cm Pallflex filter, and gaseous PAH/NPAH were trapped in the PUF cartridges. The 50-cm x 50-cm filter sampling system had a nominal volumetric flow rate of 6371 L/min, while the PUF system flow rate was 708 l/min. For the engine-out only tests, a new 50cm x 50cm filter was installed before each individual test cycle to minimize the potential of the filter tearing due to the pressure drop across a loaded filter. The four filters for a set of tests (Cold-Start UDDS, Hot-Start UDDS, HFET, and US06) were extracted, combined, and analyzed as a single sample.

With the NAC/DPF system in place, a single 50cm x 50cm filter was utilized across the four test cycles in an attempt to collect sufficient mass on the filter to provide for a meaningful analysis.

These procedures included sampling media preparation; sample storage and extraction; sample extracts cleanup for PAH and NPAH analyses; GC/mass spectrometry (MS) analyses of PAHs and NPAHs; and quality control sample analysis.

- ***Sampling Media Preparation.*** The PUF circles (10.8cm OD, 3.2cm thickness) were cleaned by extraction using a 15-liter Soxhlet extractor with acetone for 72 hours. At the end of the extraction, the acetone in the 22-liter round-bottom flask was replaced with new acetone, and the PUF circles were extracted for another 72 hours. One PUF circle was then extracted for a quality control (QC) check. The QC check was considered to have failed if total nanograms of naphthalene exceeded 400 ng or all other PAHs combined exceeded 200 ng, or if there were sizable interfering peaks in the PAH chromatogram. The PUF circles were then re-cleaned with new acetone for another 72 hours before the next QC check took place. This process was repeated until the PUF QC check sample had passed the above-mentioned criteria. A lot number was assigned to the batch of PUFs that had passed the QC check. The cleaned PUF circles were used once only and then discarded.
- The XAD-2 synthetic resin was cleaned using a 5-liter Soxhlet extractor with deionized water (4 siphons), methanol (72 hours), and acetone (72 hours). The XAD-2 was then purged dry with nitrogen, removed from the 5-liter Soxhlet extractor, and put into multiple one-liter Soxhlet extractors. The XAD-2 was further cleaned with dichloromethane (DCM) for 72 hours. Twenty grams of XAD-2 was removed, put into a 250 mL Soxhlet extractor system, spiked with PAH international standard (IS) mixture, and extracted for 6 hours. The resulting extract was cleaned up and subject to GC/MS analysis for PAHs. If total nanograms of naphthalene exceed 200 ng, all other PAHs combined exceed 100 ng, or if there were sizable interfering peaks in the PAH chromatogram, the XAD-2 QC check was considered to have failed. The XAD-2 resin was re-cleaned for another 72 hours before another QC check took place. This process was repeated until the XAD-2 QC check sample passed the above-mentioned criteria. A lot number was assigned to the new XAD-2 resin that had passed the QC check.
- The used XAD-2 was cleaned using one-liter Soxhlet extractors with DCM for 72 hours. At the end of cleaning, a 20-gram aliquot of XAD-2 was taken for a QC check. It had to pass the above-mentioned QC check for the XAD-2 before it was re-used for field sampling; otherwise, a repeated cleaning and QC check was performed. A lot number was assigned to the clean, used XAD-2 resin that had passed the QC check.
- Each 10.2-cm, stainless-steel PUF/XAD-2 trap was packed in the following order: one piece of 10.8-cm PUF, 40 grams of clean XAD-2, and one piece of 10.8-cm PUF. Each trap was labeled with PUF and XAD-2 lot numbers; date of preparation; and the name of the person who prepared it. The prepared traps were then wrapped in aluminum foil, sealed in Ziplok bags, and kept in a freezer until the time of their use.
- ***Sample Storage and Extraction.*** After sampling, all PUF traps and filters (after weighing) were stored in a freezer at -15°C in the dark until the time of extraction. At the time of extraction, the PUF and XAD-2 of each PUF trap were removed and loaded into a one-liter Soxhlet extractor with the XAD-2 resin sandwiched between the two PUF

circles. The PUF on the top was then spiked with 20 uL each of PAH and NPAH internal standard (IS) mixtures with their compositions listed in Table 15. With a one-liter flask attached to the Soxhlet extractor, solvent (750 mL of DCM) was poured into the Soxhlet to initiate the extraction. The extraction process continued for 8 hours by using a heating mantle and a condenser. At the end of extraction, the 1-liter flask containing sample extract was allowed to cool down. The sample extract was carefully concentrated down to about 23 mL by distillation using a heating mantle, a six-bulb Snyder column, a condenser, and a solvent receiver. The sample extract was transferred into a labeled vial and stored in a freezer.

- The filter samples were extracted using a microwave extractor (Milestone, ETHOS E Microwave Extraction Labstation) as follows: one quarter of each 50-cm x 50-cm FIFG filter was put into a 100-mL extraction rotor with interior tube made of Teflon. The filter sample was spiked with PAH and NPAH IS mixtures as listed in Table 15 and extracted with 30 mL of DCM. The temperature and energy program of the microwave extractor was as follows: at room temperature (~20ºC) to 75ºC at 5.5ºC/minute with 800 watts energy, held at 75ºC for 7.5 minutes using 500 watts, and naturally cooled down to room temperature (~30 minutes). The filter extract was piped out of the rotor and transferred into a labeled vial. The extraction process was repeated once more with 25 mL of fresh DCM. The two extracts were combined and blown down to about 20 mL, transferred into a labeled vial, and stored in a freezer.

Table 15. Composition of IS Spiking Solutions for PUF Traps and TIGF Filters

Compound	IS mixture for PUF trap spiking (20 μL/trap)	IS mixture for TIGF filter spiking (20 μL/sample)
Deuterated PAH	ng/μL	ng/μL
Naphthalene-d_8	1000	60
2-Methylnaphthalene-d_{10}	1000	60
Acenaphthylene-d_8	300	30
Phenanthrene-d_{10}	100	10
Fluoranthene-d_{10}	100	10
Benzo[a]anthracene-d_{12}	5	5
Chrysene-d_{12}	5	5
Benzo[b]fluoranthene-d_{12}	5	5
Benzo[k]fluoranthene-d_{12}	5	5
Benzo[a]pyrene-d_{12}	5	5
Perylene-d_{12}	5	5
Indeno(1,2,3-cd)pyrene-d_{12}	5	5
Dibenz(a,h)anthracene-d_{14}	5	5
Benzo[g,h,i]perylene-d_{12}	5	5
Deuterated NPAH	ng/μL	ng/μL
1-Nitronaphthalene-d_7	5	5
5-Nitroacenaphthene-d_9	5	5
2-Nitrofluorene-d_9	5	5
9-Nitroanthracene-d_9	5	5
3-Nitrofluoranthene-d_9	5	5
6-Nitrochrysene-d_{11}	5	5
1-Nitropyrene-d_9	5	5
6-Nitrobenzo(a)pyrene-d_{11}	5	5

- ***Sample Extracts Clean Up for PAH and NPAH Analyses.*** One-third of each of the PUF trap extracts and one-half of each of the filter extracts were taken for PAH analysis. A 25 uL aliquot of alternate standard, Anthracene-d10 at 2.0 ng/uL was spiked to the sample extract just prior to the solvent exchange from DCM to mostly hexane. The solvent exchange was carried out by blowing down the sample extract to 0.5 mL and then brought back up to 3.0 mL with hexane in a 3-dram vial. Two mL of diluted sulfuric acid (25%) was added to the vial, and the two liquids were thoroughly mixed for 20 seconds using a vortex mixer (Fisher). A glass column (10-mm OD x 350-mm L) was packed with 5.0" silica gel (Fisher, Davisil Silica Gel 32 Sorbent, Grade 923, 100-200 mesh). The column was pre-cleaned with 15 mL of DCM and then 5 mL of hexane. The hexane layer of the acid washed sample extract was then transferred onto the column. Ten mL of hexane was used to elute the column, and the hexane eluate was discarded. The PAH fraction was collected by eluting the column with 23 mL of DCM/pentane (60/40, v/v). This fraction was carefully blown down, in three steps, to a final volume of 100 uL (toluene) in a labeled sample injection vial.

- The same amount of PUF and filter extracts from each sample was solvent exchanged for NPAH cleanup as described above. A glass column (10 mm OD x 350mm L) was packed with 2.54cm silica gel (Fisher, Davisil Silica Gel 32 Sorbent, Grade 923, 100-200 mesh). The column was pre-cleaned with 6 mL of DCM and then 2 mL of hexane. The sample extract was then loaded onto the column. Ten mL of hexane was used to elute the column, and the eluate was discarded. The NPAH fraction was collected by eluting the column with 23 mL of DCM. This fraction was carefully blown down, in three steps, to a final volume of 100 uL (toluene) in a labeled sample injection vial.

- ***GC/MS Analyses of PAHs and NPAHs.*** The PAH sample extracts were analyzed using an Agilent 6890N GC in conjunction with an Agilent 5973N mass selective detector (MSD) in the positive ion electron ionization mode. Two characteristic ions of each PAH were monitored. Prior to any sample analysis, an initial calibration (ICAL) consisting of five calibration standards were analyzed to establish the relative response factor (RRF) of the PAH target compounds relative to their corresponding deuterated PAHs. All RRFs must have had their percentage relative standard deviations (RSDs) at or below 25% before the ICAL was considered successful. For every subsequent 12-hour GC/MS sample analysis period, a continuing calibration (CC)—midpoint calibration standard, 300 pg/uL—was analyzed, and the RRFs of the PAHs were calculated and compared with the mean RRFs of the ICAL. The %Ds (% difference) of the RRFs of the PAHs must be at or below 25%. The same RRF criteria for the deuterated PAHs (i.e., IS, relative to their corresponding deuterated PAH recovery standards) must also be met. These criteria must be met before a CC was considered acceptable and used for PAH sample extract analysis.
- Just prior to PAH analysis by GC/MS/selected ion monitoring, each PAH sample extract was spiked with 10 uL of PAH recovery standard mixture containing three deuterated PAHs [Acenaphthene-d10, Pyrene-d10, and Benzo(e)pyrene-d12], each at 10 ng/uL. The PAH concentrations in the sample extracts were quantified using the RRFs of the CC as picograms (10-12 grams)/μL, which was later converted to total nanograms (10^{-9} grams) per sample. For all samples, the PAH extracts were solvent-diluted 20 times and analyzed to bring the lighter PAHs (naphthalene through pyrene) within calibration range. All PUF sample extracts were further analyzed by a high-resolution GC/MS for accurate quantification of the heavier PAH [benzo(a)anthracene through benzo(g,h,i)perylene].
- The NPAH sample extracts were analyzed using the same GC/MS except in the negative ion-chemical ionization mode using methane as chemical ionization reagent gas. All ICAL and CC criteria used on PAH analysis applied to the NPAH analysis.
- ***QC Sample Analysis.*** For each set of field sample extraction, a solvent blank, a matrix blank (PUF/XAD-2, or filter), a lab control sample (LCS), and LCS duplicate (LCSD) were extracted. The LCS and LCSD were QC samples made up of clean sampling media (PUF/XAD-2 or filter) and spiked with known amounts of PAH and NPAH target compounds. All QC samples were spiked with PAH and NPAH IS mixtures, like the field samples, and were extracted, cleaned up, and analyzed using GC/MS alongside the field samples. The advisory recovery range for each PAH and NPAH in LCS/LCSD was set at 50% to 150%. Any outliers on the LCS/LCSD report were evaluated and corrective actions taken, when deemed necessary, to improve their percentage recoveries. The IS recoveries for the PAHs and the NPAHs were also tabulated and evaluated. Most IS

recoveries fell within 30% to 150%. Corrective actions were taken when low IS recoveries were encountered to improve IS recoveries in future analyses.

Metals Analysis. A proportional exhaust sample was pulled through a 47-mm Teflo™ filter at a volumetric flow rate of 50 lpm across four consecutive test cycles (i.e., Cold-Start UDDS, Hot-Start UDDS, HFET, and US06) at the location shown in Figure 27. The filter was weighed to determine the mass gain over the test duration and subsequently subjected to metals analysis by X–ray fluorescence. Aluminum, silicon, phosphorus, sulfur, chlorine, potassium, and calcium values determined by XRF were adjusted for large particle, self-absorption using the theoretical formulation developed by Dzubay and Nelson (1975). This adjustment is a function of particle-size distribution and composition. Because the actual particle size distribution and composition is unknown, the uncertainty of these adjustments is up to ± 25%, and is reflected in the reported uncertainty. Particle-size effects for sodium and magnesium are so large and variable that accurate corrections cannot be made for these two elements. Their raw, uncorrected concentrations are included in the data files, but they should not be considered quantitative.

Toxic Nitrogen Compounds (Nitroxy-Alkane Samples). A proportional exhaust sample was pulled through another 47-mm Teflo™ filter, which was followed by two ORNL-supplied, nitroxy-alkane sampling cartridges in series (primary and secondary). The 47-mm filter was used only to avoid contaminating/plugging the sampling cartridge. This sample was also obtained across four consecutive test cycles (i.e., Cold-Start UDDS, Hot-Start UDDS, HFET, and US06) at the location shown in Figure 27 with a volumetric flow rate of 1.25 lpm.

2.2.4 Data Handling

Data provided by the test laboratory included measurements of NO_x, THC, NMHC, CO, and PM using D15 fuel taken at engine out with and without EGR. Tailpipe measurements using D15 fuel were taken every 50 hours between 0 and 300 hours, with measurements made before and after desulfurizations at 200 and 300 hours. Between 300 and 2,000 hours, desulfurizations occurred every 100 hours; measurements using D15 fuel taken before and after each desulfurization. Measurements using BP15 fuel were taken at engine out, 300 hours pre- and post-desulfurization, 900 hours post-desulfurization, 1,500 hours post-desulfurization, and at 2,000-hours post-desulfurization. The laboratory also measured nonregulated emissions using a continuous FTIR instrument, the analysis of speciation dilute bag samples, and by bubbling raw exhaust through a heated sample line. Metal emissions were measured using a Teflo™ filter, and PAH and NPAH emissions were measured using a GC in conjunction with a MSD.

Prior to conducting the statistical analysis, a data review was conducted to ensure data completeness and accuracy. After comparing the data received with the data collection plan, the data were stored in a controlled database. Changes, updates, and corrections were carefully monitored and controlled. To identify gross outliers (unusual and unexplained emissions results) and unexplained variations or trends associated with laboratory procedures, plots of emission data versus time were prepared and shared with the laboratories and the technical committee.

Lists of outliers identified from the outlier analysis were sent to the laboratory with instructions to check for clerical errors, equipment failures, or other external factors that could explain the deviation in results. Clerical errors were corrected, and outliers due to known problems were corrected whenever possible. If the data could not be corrected, or the outliers were found to be

associated with documented testing or measurement issues, they were eliminated from the analysis.

2.2.5 Statistical Analysis and Modeling

The statistical analysis approaches to address the study questions posed in Section 1.3 are as follows: initial performance; durability and desulfurization; sulfur mass balance; fuel effects on regulated emissions; and unregulated emissions.

Initial Performance

Q1.1 Can the system meet the 2007-2010 regulated emissions levels for NO_x, NMHC, and PM?

Q1.2 What is the impact on other regulated emissions (THC, CO, PM, and NMHC) and fuel economy?

Q1.3 How does system performance change during the early life (under 300 hours) of the system?

Q1.4 Are there similar patterns for various transient duty cycles (Cold- and Hot-Start UUDS, US06, HFET)

In order to address study questions Q1.1 and Q1.2, the average composite FTP emissions from the seven engine-out tests (six without EGR and one with EGR) and from 18 tailpipe tests—conducted prior to the first desulfurization at 200 hours—and their corresponding 95% confidence intervals were produced. A standard t-test was used to determine if there were statistically significant differences between the average tailpipe emissions and the regulated emissions standards. Emission reductions were also calculated relative to engine-out emissions obtained both with and without EGR. The performance of the system before 300 hours was characterized by a series of plots for these emissions by mode.

Durability and Desulfurization

Q2.1 How do NO_x emissions change as the system ages? Specifically, how do the maximum (pre-desulfurization), minimum (post-desulfurization), and average NO_x levels change?

Q2.2 Is the increase in NO_x emissions between consecutive desulfurizations constant over time?

Q2.3 How effective is desulfurization at restoring the initial NO_x reduction performance of the system (initially and over time)?

Q2.4 Does the performance of the system stabilize within the first 2,000 hours? If so, at what point does this occur?

Q2.5 Are there temporal trends with respect to other regulated emissions or fuel economy?

These questions were addressed through a series of plots of the observed FTP Composite NO_x data. Trend lines using log-linear regression models were produced and analyzed to assess the behavior of NO_x emissions over time. To account for the effects of desulfurization process, separate log-linear models were fit to three sets of NO_x emissions data: (1) measurements made before a desulfurization event, (2) measurements made after a desulfurization event, and (3) the average of measurements made at the beginning (post-desulfurization) and end (pre-desulfurization) of each 100-hour aging period. To address the question of whether the performance of the system stabilizes over time, the left-most data from each of the three data sets were iteratively truncated; then the regression model was refitted, and the significance of the regression slope parameter was evaluated. This same process was applied to the other regulated emissions and fuel economy.

Sulfur Mass Balance

Q3.1 How much sulfur is emitted during the desulfurization process?

Q3.2 How does the amount of sulfur emitted during the aging cycle compare to the amount emitted during desulfurization process? Do these rates change over time?

Q3.3 What happens to the differences between these amounts?

A table of summary calculations was used to answer these study questions**.** A series of special tests were performed periodically to measure the mass of SO_2 and H_2S emitted during desulfurization. These results were used to estimate total sulfur accumulation on the catalysts for comparison with the estimated engine-out emissions based on measured fuel and oil consumption.

Fuel Effects on Regulated Emissions

Q4.1 Are there differences in emissions from DECSE and BP fuels?

Q4.2 If such differences exist, are they consistent over time?

Analysis of variance models was used to determine if there were statistically significant differences between the two test fuels in terms of the average emissions of NO_x, hydrocarbon, and PM and fuel economy. The models, which accounted for the effects of aging and test mode (Cold-Start UDDS, Hot-Start UDDS, US06, and HFET), were also used to produce 95% confidence intervals for the average emissions and fuel economy.

Unregulated Emissions

Q5.1 Which unregulated toxic (or potentially toxic) compounds are present in tailpipe emissions?

Q5.2 How do the levels compare to engine-out emissions?

Q5.3 How do unregulated emissions change with time?

Unregulated emissions results are being presented in a separate report.

Section 3: System Development

The following section details the system development for this project. This includes a discussion of the baseline engine and EGR calibration, and emission systems calibration and control, including a discussion of the diesel fuel burner, NO_x management, and cold-start strategies. In addition the section also covers the development of the NAC desulfurization strategy.

3.1 Baseline Emissions and Exhaust Gas Recirculation Calibration

To set an appropriate baseline for assessing the ECS performance, the emissions from the Duramax engine were measured as received and after EGR calibration changes. Since this engine was retrofitted with an EGR systems for this project, two baselines were established. That is, for the purpose of comparison, it was necessary to have two baselines for this project: one with an optimized EGR strategy and one with out EGR (i.e., original equipment manufacturer calibration). The following section details the baseline emissions and the EGR calibration process.

3.1.1 Baseline Emissions

After the initial "quick-look" vehicle tests were completed on the chassis dynamometer, the vehicle was ballasted to the previously determined test weight of 6,568 lbs and taken on the road for vehicle coast-downs to generate a vehicle road-load curve. After determining the actual on-road power requirements, the vehicle was placed on the chassis dynamometer, and the parasitic losses of the drive axle were determined. The dynamometer road-load curve was generated by subtracting the drive axle losses from the actual on-road power curve. The three individual curves are shown graphically in Figure 28. Figure 29 shows a comparison of the dynamometer load curve used for the quick-look emission tests and the actual dynamometer load curve determined. Due to the close similarity between the two curves, it was decided that the data previously provided to the ECS supplier were still a valid representation of the actual engine operating conditions.

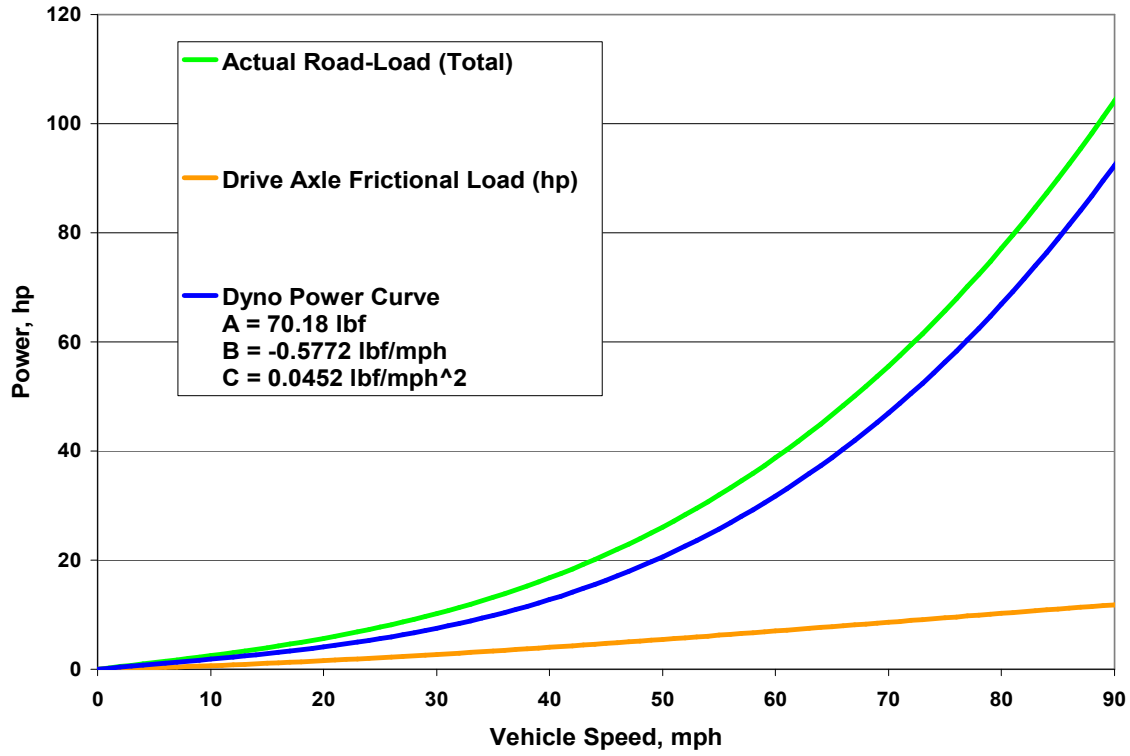

Figure 28. Power curves for 2002 Chevrolet Silverado test vehicle

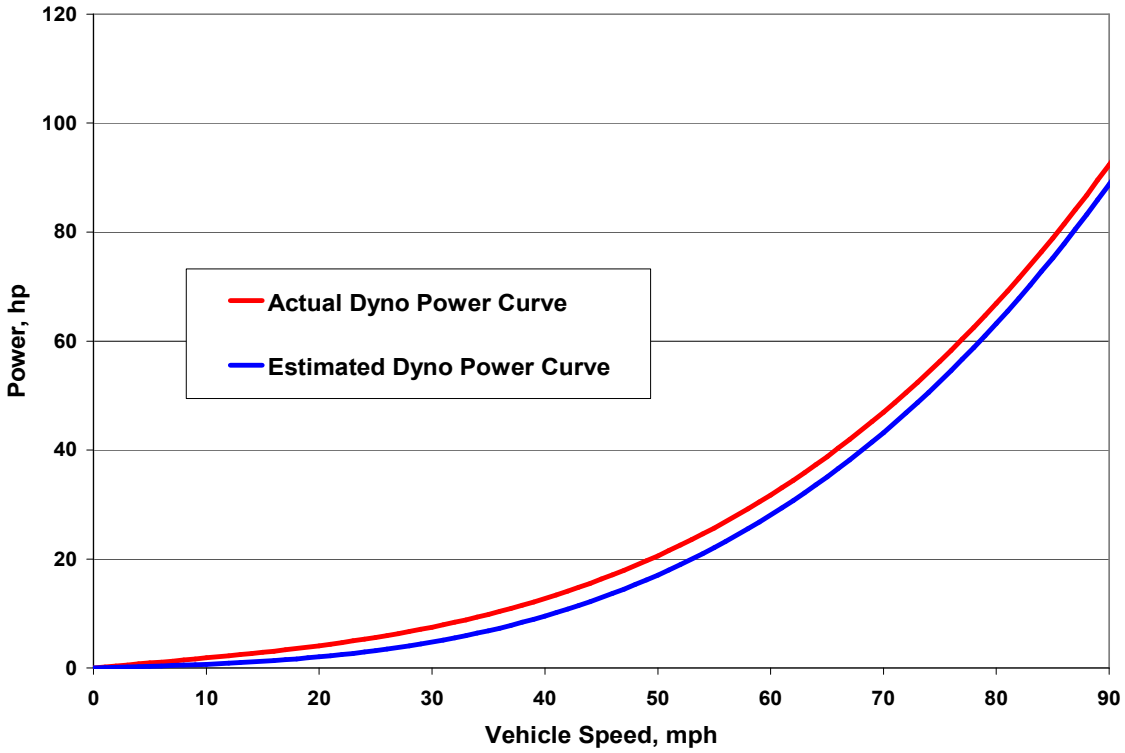

Figure 29. Estimated and actual chassis dynamometer power curves

Using the newly established road-load curve, the vehicle was operated on the chassis dynamometer over the FTP and US06 test cycles. Data collected during these cycles (triplicate runs) were used to develop vehicle-based maps. The maps were generated from the fully warmed-up data (i.e., the first 200 seconds of the cold-start FTP were dropped from the analysis). Maps of exhaust gas temperature; NO_x; CO_2 concentration and instantaneous mass; and EGR rate as a function of engine speed (rpm) and load (assumed to be a function of APP in volts) were developed. It was agreed that the EGR maps (and all other engine calibration related maps) would remain confidential to the manufacturer and not for public release. Figures 30, 31, and 32 show the resultant exhaust gas temperature, NO_x, and CO_2 concentration and instantaneous mass maps, respectively. The zeroes on the edge of the tables result from a lack of data in the region (i.e., the engine does not operate in this region in the vehicle over the drive cycles tested). Figure 33 shows a scatter plot of engine speed and APP over the FTP and US06. This figure provides information on the operating region for the Duramax across the light-duty drive cycles. As observed in this figure, the engine operates the vast majority of the time at low speeds and low loads over these test cycles.

NOx, ppm -- STOCK MAP, FTP+US06
HOLES FILLED, SMOOTHED

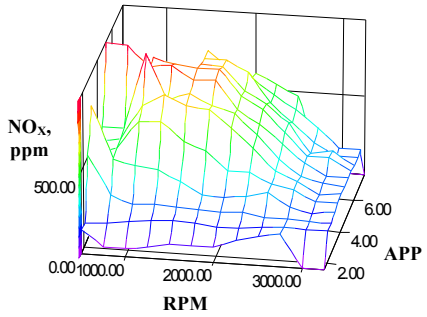

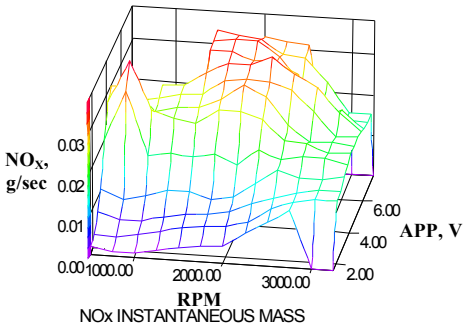

APP1

ENGINE SPEED, RPM	0.53	0.70	0.87	1.03	1.20	1.37	1.53	1.70	1.87	2.03	2.20	2.37	2.53
500	147	140	516	779	419	450	497	973	0	0	0	0	0
750	54	151	282	456	475	480	497	973	0	0	0	0	0
1000	54	168	230	421	648	700	974	842	858	0	0	0	0
1250	71	186	236	408	659	776	695	859	820	0	0	0	0
1500	96	193	229	337	543	720	744	781	803	785	772	766	0
1750	97	185	220	263	493	707	683	786	811	778	767	673	0
2000	97	175	217	255	378	595	641	617	646	636	704	620	601
2250	146	173	225	275	379	479	517	530	576	555	519	518	542
2500	184	193	204	313	315	348	375	411	438	451	404	435	473
2750	211	201	205	229	285	286	275	309	300	270	285	328	0
3000	0	192	195	191	220	212	239	228	302	290	208	214	0
3250	0	193	193	212	218	234	227	234	228	208	211	211	0

Figure 30. Exhaust gas temperature after oxidation catalyst over the FTP and US06 test cycles

CO_2, % -- STOCK MAP, FTP + US06
HOLES FILLED, SMOOTHED

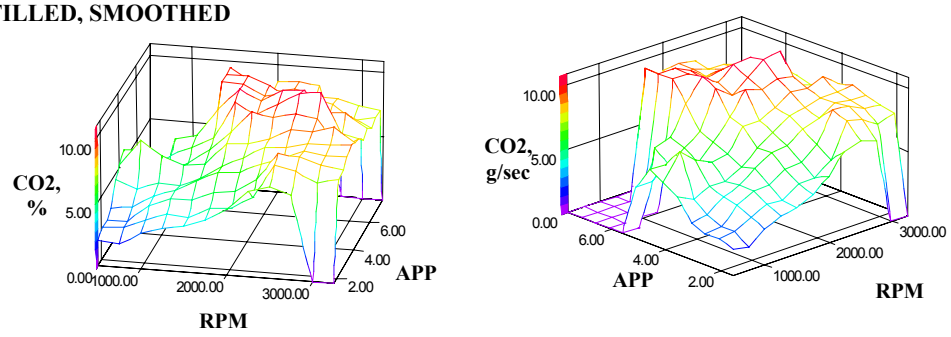

APP, volts

ENGINE SPEED, RPM	0.53	0.70	0.87	1.03	1.20	1.37	1.53	1.70	1.87	2.03	2.20	2.37	2.53
500	2.0	2.4	2.4	2.9	4.5	5.2	5.8	4.1	0.0	0.0	0.0	0.0	0.0
750	1.8	2.6	2.5	3.0	3.9	7.2	5.8	4.1	0.0	0.0	0.0	0.0	0.0
1000	2.8	3.3	3.8	4.0	4.5	6.2	4.1	5.0	5.8	0.0	0.0	0.0	0.0
1250	3.3	3.9	4.5	4.6	4.4	5.5	5.1	5.8	6.3	0.0	0.0	0.0	0.0
1500	3.6	3.7	4.6	5.5	5.1	5.8	6.3	6.7	8.5	10.0	10.0	10.1	0.0
1750	4.2	4.6	5.3	6.3	6.2	7.5	7.8	9.6	10.1	9.9	10.1	9.1	0.0
2000	5.1	4.7	5.5	6.4	7.0	7.5	9.5	8.7	9.3	9.1	9.5	8.4	8.7
2250	6.7	5.7	6.5	7.2	7.9	8.1	9.2	9.7	10.3	9.4	8.6	8.7	8.8
2500	7.2	8.3	8.7	7.7	8.1	9.0	9.6	10.6	10.4	8.8	8.7	8.4	8.6
2750	6.7	8.0	8.6	8.5	8.5	8.9	9.4	10.9	8.8	8.1	8.3	8.3	0.0
3000	0.0	7.2	8.0	8.2	8.5	9.4	7.1	7.8	8.9	8.1	7.3	7.9	0.0
3250	0.0	7.6	7.8	8.3	8.7	8.3	8.1	7.4	7.8	7.3	7.6	7.6	0.0

Figure 31. Engine-out NO_x concentration and instantaneous mass map over light-duty FTP and US06 test cycles

EXH-T after OC -- STOCK MAP, COURSE GRID
HOLES FILLED, SMOOTHED

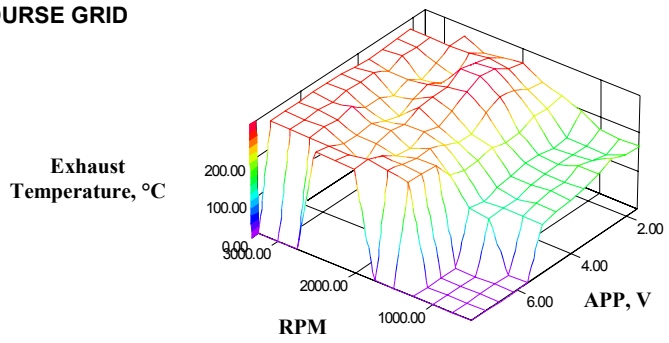

APP1

ENGINE SPEED, RPM	APP, volts												
	0.53	0.70	0.87	1.03	1.20	1.37	1.53	1.70	1.87	2.03	2.20	2.37	2.53
500	165	166	181	165	152	144	141	130	0	0	0	0	0
750	163	147	154	165	147	148	141	130	0	0	0	0	0
1000	167	148	149	149	148	145	131	133	127	0	0	0	0
1250	196	151	145	154	156	147	141	127	135	0	0	0	0
1500	216	205	208	191	187	201	188	188	200	251	252	255	0
1750	230	235	255	262	246	215	217	233	247	249	256	264	0
2000	259	268	290	296	279	254	238	247	228	234	257	272	273
2250	251	274	285	294	272	270	267	248	254	243	219	264	274
2500	242	268	233	238	257	244	225	235	254	245	249	266	275
2750	268	267	246	226	250	234	251	249	278	266	272	267	0
3000	0	268	268	269	251	271	271	274	267	271	270	270	0
3250	0	268	268	263	263	264	272	273	274	270	270	270	0

Figure 32. Engine-out CO_2 concentration and instantaneous mass map over light-duty FTP and US06 test cycles

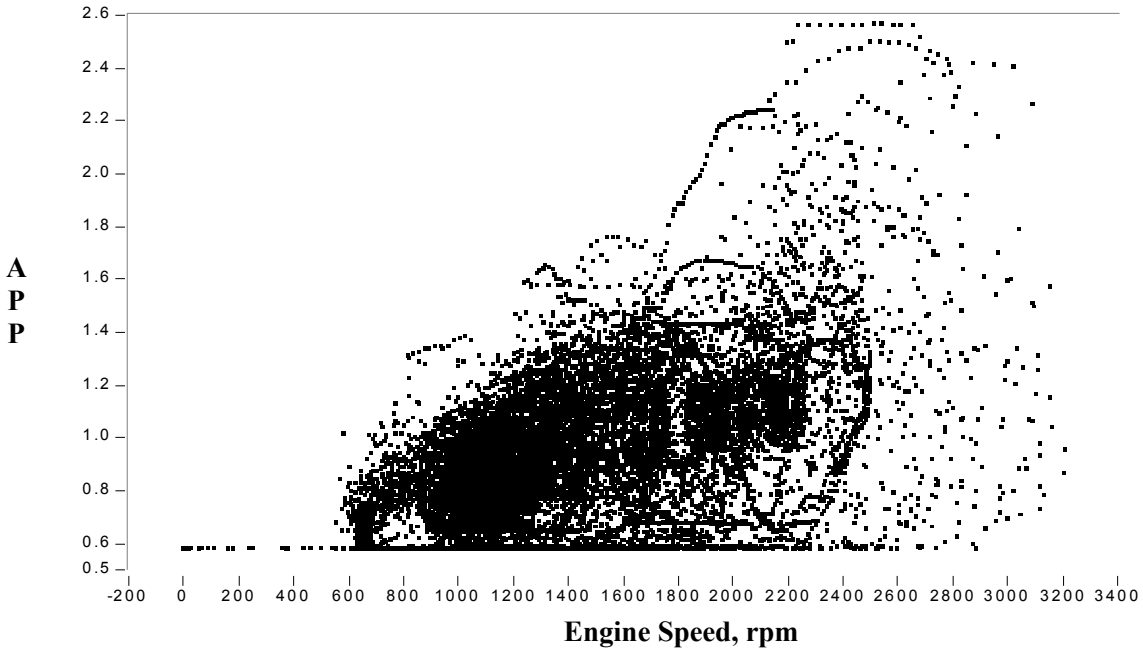

Figure 33. Range of APP (volts) and engine speed (RPM) across the light-duty FTP and US06 test cycles

A summary of the baseline, as-received, engine-out emissions over the light-duty FTP cycle, with and without EGR, is shown in Tables 16 and 17, respectively. The standard weighting of 43% for the cold-start and 57% for the hot-start was used in calculating the composite FTP values. The calculated Cold-Start UDDS (Bags 1 and 2) and Hot-Start UDDS (Bags 3 and 2) results are also shown as it was decided to utilize these test cycles after the baseline tests had already been conducted. A comparison of the regulated engine-out emissions and the program goals (i.e., EPA Tier 2 Bin 5) are shown in Figure 33. As can be seen from this figure, meeting the 50K mile program goals required a 99% NO_x reduction, an 84% hydrocarbon reduction, and an 89% PM reduction over the engine-out (no EGR) emission levels. Figures 34 through 37 show the continuous engine-out NO_x emissions and exhaust gas temperature (with and without stock EGR calibration) for the Cold-Start UDDS (Bags 1 and 2 of the FTP) and US06 tests, respectively. Given the 120,000-mile program goal of 0.07 g/mile NO_x, it can be seen in Figure 38 that the NO_x target is exceeded approximately 27 seconds after the engine started. In order to come close to meeting the program goals, it became obvious that the system would require significant additional exhaust temperature (immediately after engine-start and also throughout the low-load operating regime) and extraordinarily high levels of emission reduction. In addition, it would be necessary to reduce the engine-out NO_x levels to lessen the burden on the ECS. In order to reduce engine-out NO_x levels it was decided to pursue a new EGR calibration.

Table 16. Light-Duty FTP As-Received, Engine-Out Emissions with EGR

	Bag 1 (grams)	Bag 2 (grams)	Bag 3 (grams)	FTP Composite (g/mi)	Cold-Start UDDS (g/mi)	Hot-Start UDDS (g/mi)
THC	1.709	1.932	1.184	0.448	0.487	0.418
NO_x	17.468	16.150	13.928	4.233	4.500	4.032
CO	18.074	11.371	8.302	3.198	3.942	2.637
CO_2	2066	2138	1848	546	563	534
PM	0.287	0.338	0.272	0.083	0.084	0.082
Distance (Miles)	3.60	3.87	3.59	11.06 (total)	7.47 (total)	7.46 (total)

Table 17. Light-Duty FTP As-Received, Engine-Out Emissions without EGR

	Bag1 (grams)	Bag 2 (grams)	Bag 3 (grams)	FTP Composite (g/mi)	Cold-Start UDDS (g/mi)	Hot-Start UDDS (g/mi)
THC	1.629	2.025	1.310	0.468	0.491	0.450
NO_x	18.740	20.98	18.14	5.304	5.346	5.272
CO	25.918	18.120	17.460	5.282	5.927	4.795
CO_2	2138	2124	1843	551	574	535
PM	0.360	0.311	0.335	0.088	0.090	0.087
Distance (Miles)	3.58	3.85	3.57	11.00 (total)	7.43	7.42

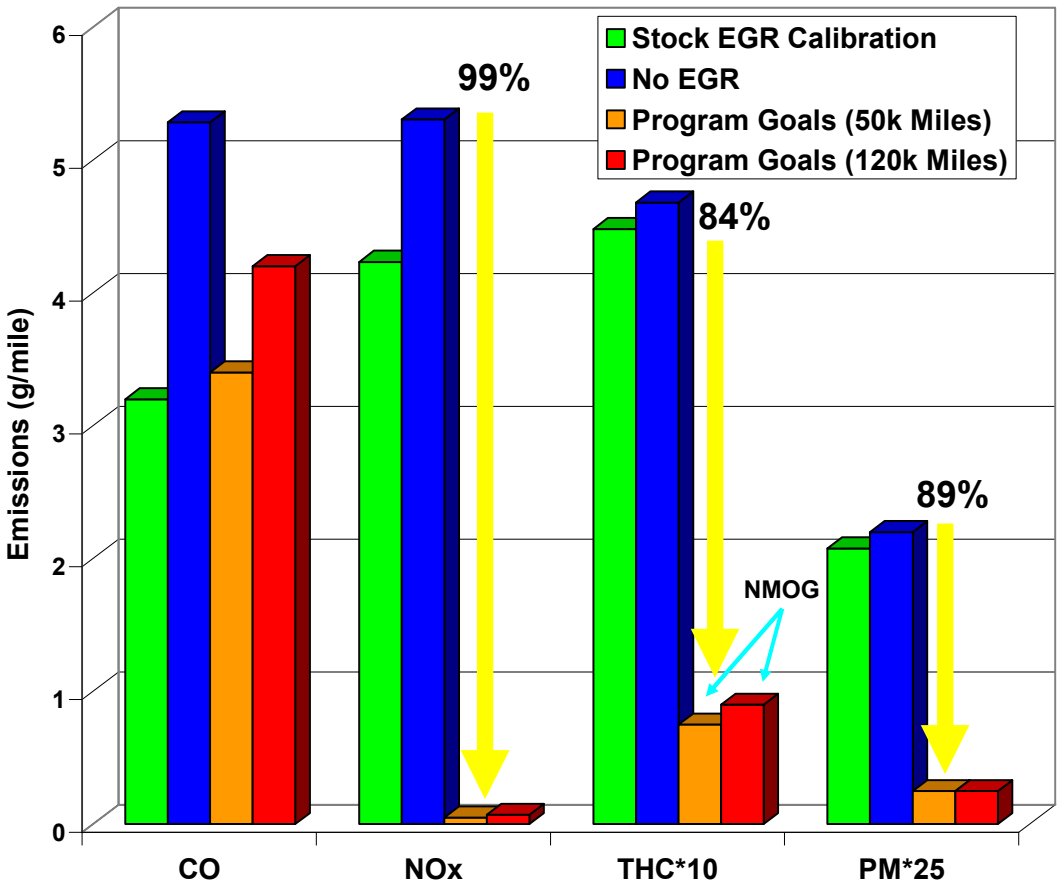

Figure 33. Comparison of regulated engine-out emissions to program goals (EPA Tier 2 Bin 5) for the light-duty FTP

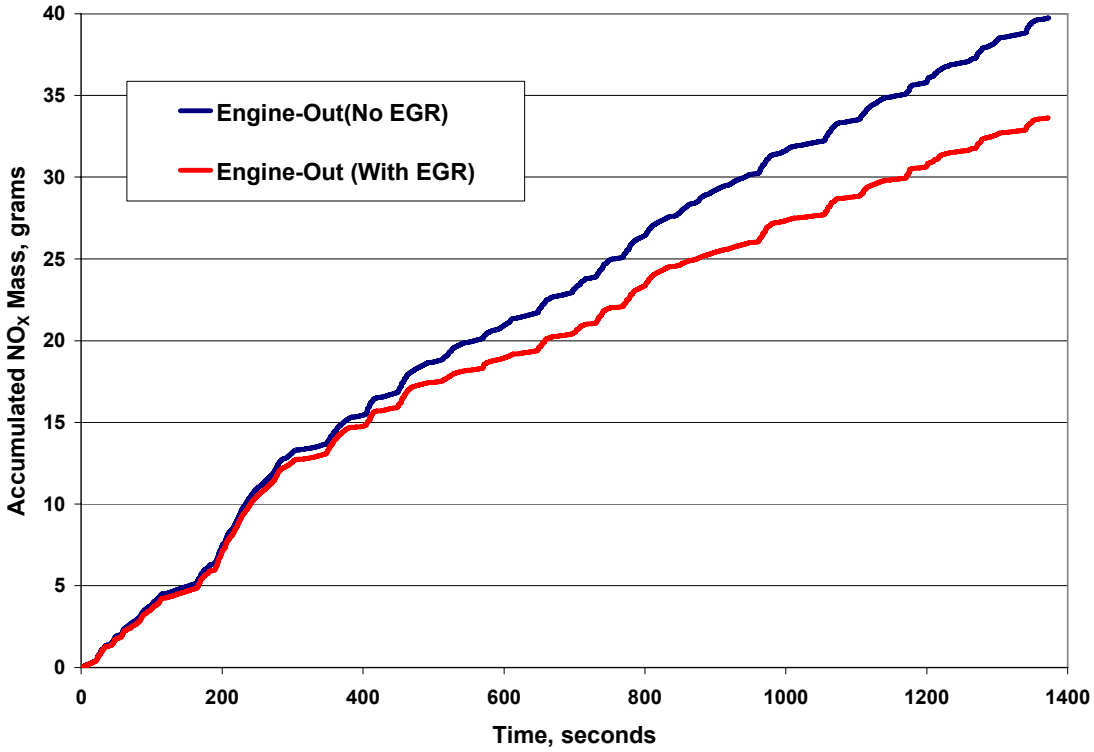

Figure 34. Accumulated engine-out NO_x mass over the Cold-Start UDDS cycle

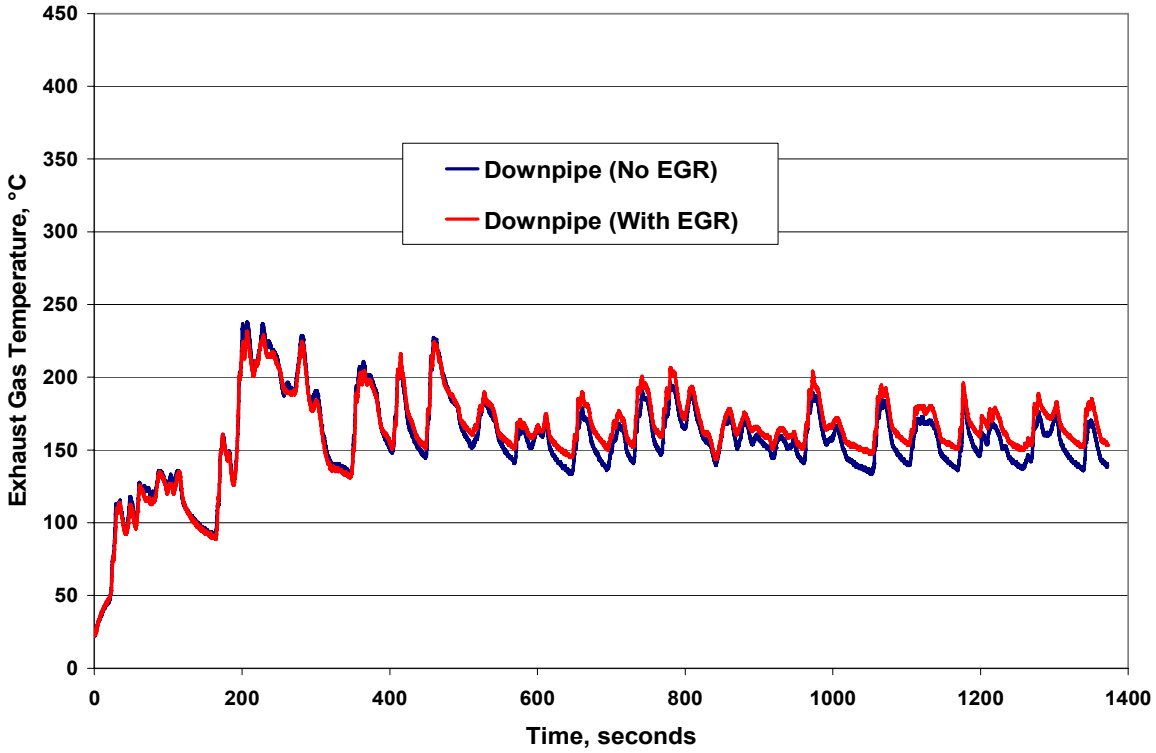

Figure 35. Exhaust gas temperature (downpipe location) over the Cold-Start UDDS cycle

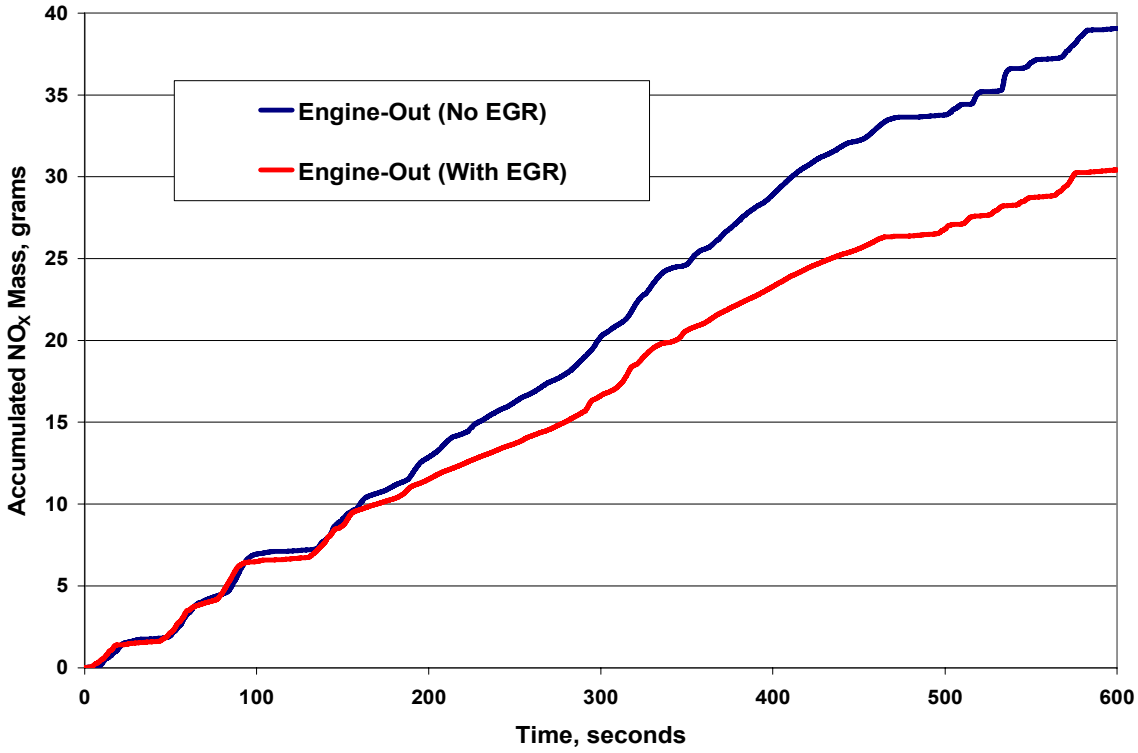

Figure 36. Accumulated engine-out NO_x mass over the US06 cycle

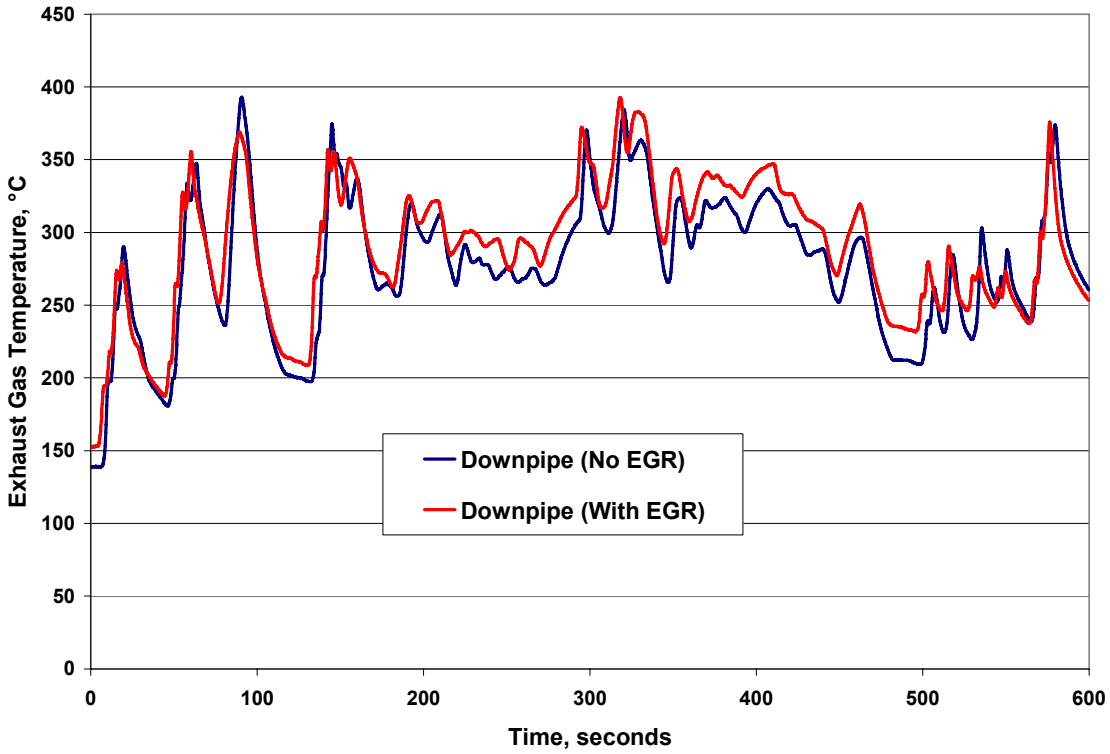

Figure 37. Exhaust gas temperature (downpipe location) over the US06 cycle

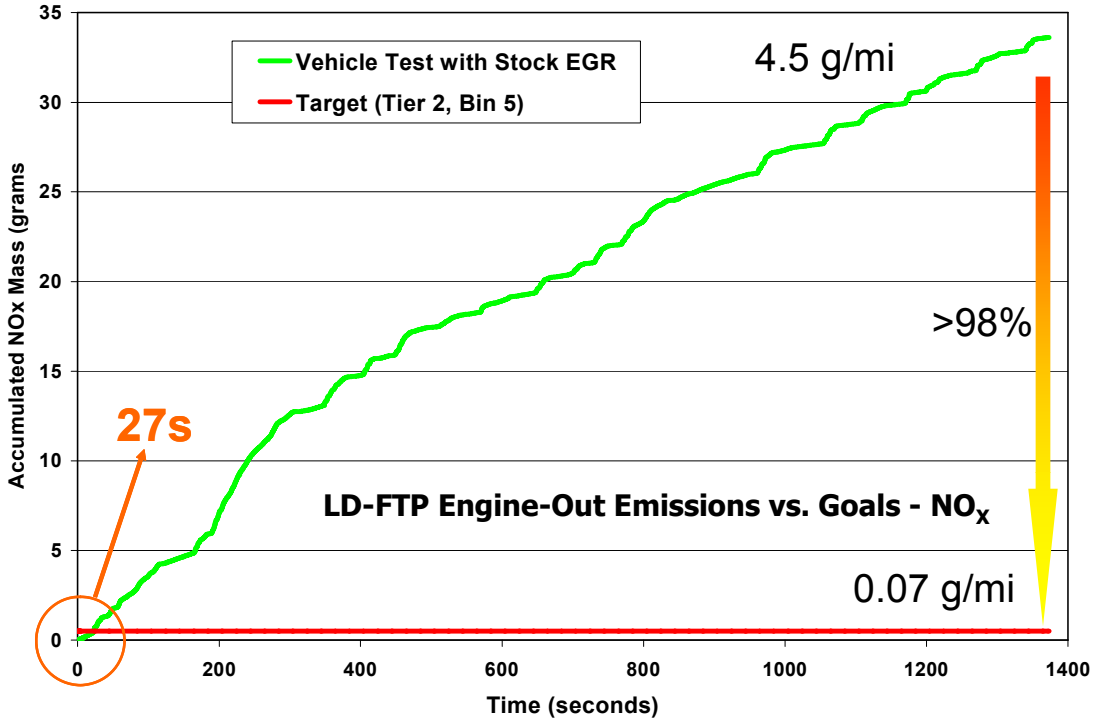

Figure 38. Continuous engine-out NO_x mass and program goal over the Cold-Start UDDS Test cycle

Prior to beginning any EGR calibration, testing was moved from the vehicle chassis dynamometer test environment to a dedicated engine test cell. This move allowed accelerated development of the EGR calibration and ECS control strategies; provided more repeatable test conditions; and shortened the test plan time line. In addition, the inherent repeatability issues of a human driver operating a manual transmission-equipped vehicle were eliminated. Working in a dedicated test cell also provided the ability to force-cool the engine, accelerating cold-start strategy development. However, before this move was made, it was necessary to create test cell control cycles that would duplicate vehicle engine operation in the test cell over the cycles of interest (Cold-Start UDDS, Hot-Start UDDS, HFET, and US06).

To create an equivalent motoring dynamometer test cell cycle for the engine, data generated from previous light-duty vehicle tests without EGR were used to define the engine speed and APP signal versus time schedule (as opposed to an engine speed and torque cycle, as in the heavy-duty FTP test cycle). This approach was used because engine-out torque was not readily measurable on the vehicle chassis dynamometer; therefore, using APP as an indicator of load was determined to be the best alternative. The APP signal was converted to an equivalent indicated throttle angle for the test cell electronic control module. As the drivetrain in the vehicle utilizes a manual transmission, some smoothing of the engine speed trace was required to avoid high, transient current spikes in the dynamometer at certain shift points. The goal of the test cell control cycle was to operate the engine at similar conditions observed on the chassis dynamometer for generating similar exhaust gas temperatures, exhaust mass flow rate, engine-out emissions, and fuel consumption, and thereby emulating the vehicle test.

The final test cell command cycles were presented in Section 2.2.2. After the test cell command cycles were deemed acceptable, corresponding cycle statistics (speed, torque, and power) were used as a comparison for all future tests. These statistics were used to verify that the engine was able to follow the speed and/or torque command cycles, and to check the driveability of various strategy changes. The cycle statistics also provided a continual feedback of engine repeatability over the cycles of interests. A summary of the work for each command test cycle is shown in Table 18.

Table 18. Test Cycle Work for Drive-Cycle Emulation on Motoring Dynamometer

	Cold-Start UDDS	Hot-Start UDDS	HFET	US06
Cycle Work, kW-hr	5.03	4.87	5.50	7.14

3.1.2 Exhaust Gas Recirculation Calibration

Prior to mapping the stock EGR calibration, a map of the engine-out NO_x concentration as a function of speed and load was derived by operating the engine across a series of steady-state points. This map was used to identify engine operating points that would produce high levels of engine-out NO_x (areas where increased EGR would be most beneficial). Figures 39 and 40 show maps of engine-out NO_x concentration versus engine speed and load.

The stock EGR system is a high-pressure loop, vacuum-actuated, cooled-EGR system, with an intake throttle for increasing EGR flow at low intake/exhaust flows. The recirculated exhaust gases pass through an EGR cooler and then enter the intake manifold downstream of the charge air cooler. The as-received EGR calibration on this engine provided a reduction in engine-out NO_x of approximately 16% over the FTP-75 test cycle and 24% over the US06. After examining the vehicle maps, it was determined that the stock calibration was not utilizing the maximum available EGR from the stock system. Therefore, it was decided to assess the EGR rate and NO_x reduction that could be achieved with the stock system.

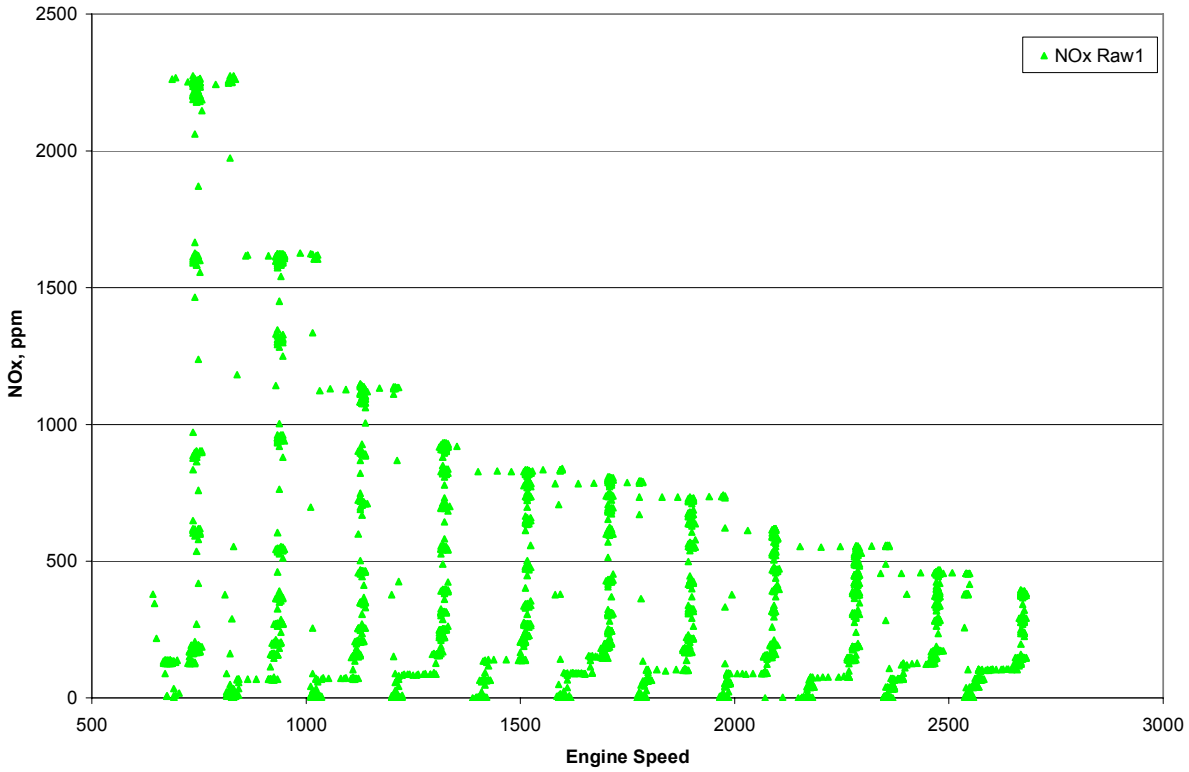

Figure 39. Measured NO_x concentration as a function of engine speed (no EGR)

NOx, ppm -- ENGINE MAP No.1: STOCK CAL, NO-EGR HOLES FILLED, SMOOTHED

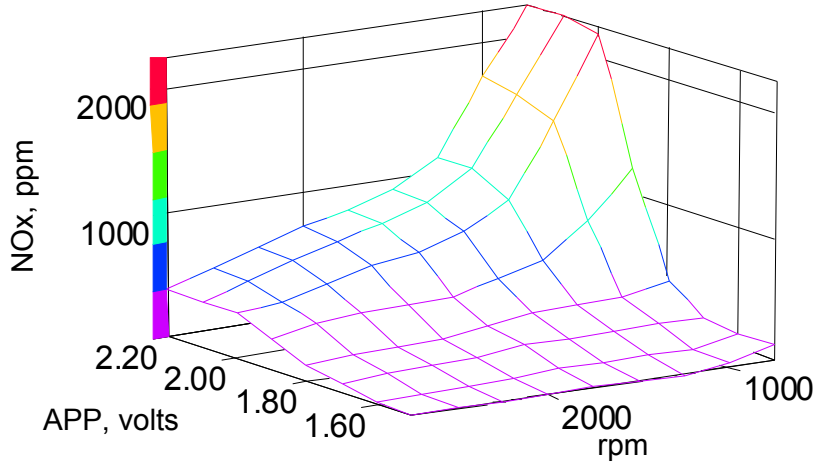

ENGINE SPEED, RPM	APP1, volts 1.40 / 500	1.50	1.60	1.70	1.80	1.90	2.00	2.10	2.20
	750	152	130	169	388	1193	2190	2248	2256
	1000	47	63	175	311	821	1542	1678	1736
	1250	8	72	171	296	574	971	1119	1127
	1500	19	59	175	278	463	756	915	916
	1750	21	82	172	232	381	658	782	807
	2000	9	54	120	191	363	587	695	733
	2250	13	39	110	174	352	494	596	611
	2500	14	36	109	158	320	405	480	504
	2750	17	38	83	135	256	373	379	379

Figure 40. NO_x concentration—stock engine calibration—no EGR

An SwRI-developed control system, called the Emissions Reduction Integration Controller (ERIC), was used to create the controls for the EGR valve and intake throttle, allowing user-controllable operation. After verifying operation of the ERIC EGR controller, sweeps of engine speed, load, and EGR rate were performed. Table 19 outlines the operating conditions that were mapped. During mapping, the following parameters were monitored: intake and exhaust CO_2 concentrations (for calculating percent EGR); engine-out NO_x concentration; exhaust gas temperature near the planned catalyst inlet location; mixed intake air temperature (after EGR added); torque; engine speed; fuel consumption; smoke opacity; and intake MAF. At each speed and load set point, the EGR rate was varied from the minimum (0% duty-cycle, valve closed) up to the maximum the valve would flow (100% duty cycle) while limiting mixed intake air temperature to a maximum of 90ºC. After stabilizing the emissions systems at each point, data were collected at 1 Hz for a minimum of 10 seconds. Figure 41 shows the minimum and maximum EGR rates achieved at each tested speed and load. Table 19 summarizes the maximum EGR rates achieved, as well as the rate-limiting factor.

Table 19. EGR Mapping Points

Engine Speed, RPM	Accelerator Pedal Position, %	Maximum EGR, %	Limiting Factor
Idle, 680	0	-	Valve Flow Limit
700	10 - with intake throttle	57	Valve Flow Limit
	20 - with intake throttle	55	Valve Flow Limit
	30 - with intake throttle	39	Valve Flow Limit
	40	21	Valve Flow Limit
	50	20	Valve Flow Limit
	60	22	Intake Air Temp.
900	10 - with intake throttle	61	Valve Flow Limit
	20 - with intake throttle	57	Intake Air Temp.
	30	32	Valve Flow Limit
	40	27	Valve Flow Limit
	50	22	Valve Flow Limit
	60	22	Valve Flow Limit
	70	22	Valve Flow Limit
1,100	10	-	Intake Air Temp.
	20	41	Intake Air Temp.
	30	36	Valve Flow Limit
	40	33	Valve Flow Limit
	50	28	Valve Flow Limit
	60	28	Valve Flow Limit
	70	29	Valve Flow Limit
1,300	11	45	Valve Flow Limit
	20	45	Valve Flow Limit
	30	40	Valve Flow Limit
	40	35	Valve Flow Limit
	50	30	Valve Flow Limit
	60	30	Valve Flow Limit
	70	25	Valve Flow Limit

Table 19. EGR Mapping Points (continued)

Engine Speed, RPM	Accelerator Pedal Position, %	Maximum EGR, %	Limiting Factor
1,500	11	45	Valve Flow Limit
	20	32	Valve Flow Limit
	30	32	Valve Flow Limit
	40	30	Valve Flow Limit
	50	26	Valve Flow Limit
	60	25	Intake Air Temp.
	70	26	Intake Air Temp.
1,700	11	37	Valve Flow Limit
	20	35	Valve Flow Limit
	30	32	Valve Flow Limit
	40	29	Valve Flow Limit
	50	25	Valve Flow Limit
	60	21	Intake Air Temp.
	70	21	Intake Air Temp.
1,900	16	33	Valve Flow Limit
	20	30	Valve Flow Limit
	30	30	Valve Flow Limit
	40	26	Valve Flow Limit
	50	24	Valve Flow Limit
	60	20	Intake Air Temp.
2,100	10	32	Valve Flow Limit
	20	32	Valve Flow Limit
	30	29	Valve Flow Limit
	40	26	Valve Flow Limit
	50	23	Intake Air Temp.
	60	23	Intake Air Temp.
	70	20	Intake Air Temp.
2,300	10	34	Valve Flow Limit
	20	31	Valve Flow Limit
	30	31	Valve Flow Limit
	40	26	Intake Air Temp.
	50	23	Intake Air Temp.
2,500	20	31	Valve Flow Limit
	30	30	Valve Flow Limit
	40	26	Intake Air Temp.
	50	23	Intake Air Temp.

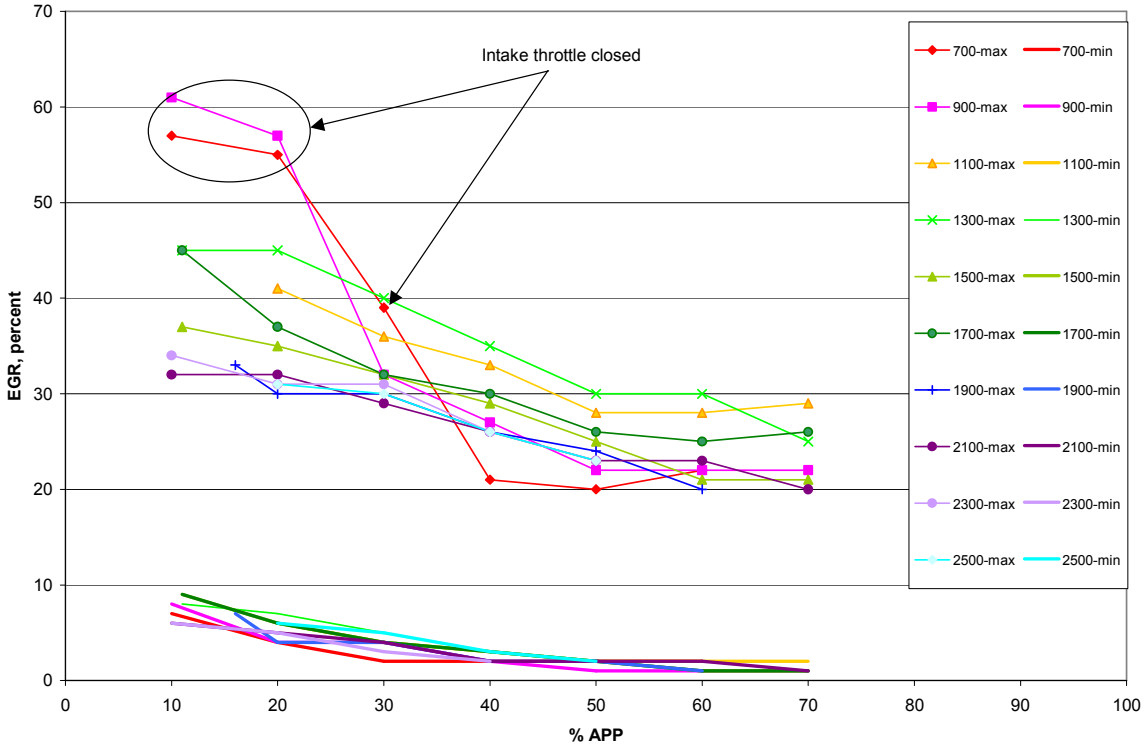

Figure 41. Maximum and minimum EGR rates as a function of engine speed and load

The results of the steady-state EGR mapping of the stock system showed potential for significantly increasing EGR rates over the stock calibration to lower engine-out NO_x levels. Another benefit of increased EGR rates would be higher exhaust gas temperatures. However, during the EGR mapping, very little of the heat generated from increased EGR rates was transferred to the catalyst inlet position. The intake manifold temperature increased up to 50ºC, but this additional heat was completely lost at low speeds due to cooling in one or more of the following: the head, exhaust manifolds in the turbocharger, and downpipe. An increase in exhaust gas temperature at the catalyst inlet location was observed at higher speeds and loads. However, as observed during the baseline tests, engine operation over the FTP-75 cycle was typified by low engine speeds and loads.

An EGR look-up table within the ERIC system was implemented to increase the amount of EGR provided to the engine at any given operating point. (From this point, the ERIC system was used to control the EGR valve and intake throttle during all engine operation.) The goal of a new EGR calibration was to reduce the engine-out NO_x levels to reduce the burden on the ECS. An engine-out NO_x level of 1.8 g/mile over the FTP-75 cycle was targeted, as this level was to be expected from typical MY 2007 engines for this type of application/engine displacement. Achieving this level of engine-out NO_x required a 66% reduction over the no EGR engine-out emissions of (13.5 grams of engine-out NO_x mass over the Hot-Start UDDS cycle).

This level of engine-out NO_x mass was achieved; however, it came at the expense of increased engine-out PM levels. Examining the continuous smoke opacity over the Hot-Start UDDS cycle (shown in Figure 42), significant increases in opacity were observed throughout the test cycle and were attributable to APP tip-in (moderate-to-hard accelerations, particularly from off-idle). In order to minimize the increase in engine-out PM while still achieving a high-level of engine-out NO_x reduction, it was decided to add a mode identification algorithm that would modify the EGR-duty cycle value in the look-up table.

The different types of engine operating modes were identified as:

- Engine crank/start
- Idle
- Acceleration
- Hard acceleration
- Cruise
- Deceleration.

Under acceleration and hard-acceleration modes, the amount of EGR called for by the look-up table was reduced in order to minimize the increase in engine-out PM. Table 20 shows a comparison of engine-out NO_x and PM mass for a number of different EGR calibrations/strategies for the Cold-Start UDDS cycle. Figure 43 shows the engine-out NO_x and PM mass measured over a Hot-Start UDDS for three different strategies employing mode identification, along with the results using only the EGR look-up table and a no-EGR test. The EGR look-up table strategy resulted in reducing the engine-out NO_x mass emissions by 64% but increased the PM mass by 93% over the base, no-EGR condition. Using the mode-modified EGR control strategy reduced the engine-out NO_x mass emissions by approximately 50% while increasing the PM mass by approximately 20%. This reduction in engine-out NO_x mass equated to approximately 2.4 g/mile over the Hot-Start UDDS cycle, short of the desired level of 1.8 g/mile, but substantially below the 4.0 g/mi noted for the as-received, engine-out level with the stock EGR calibration.

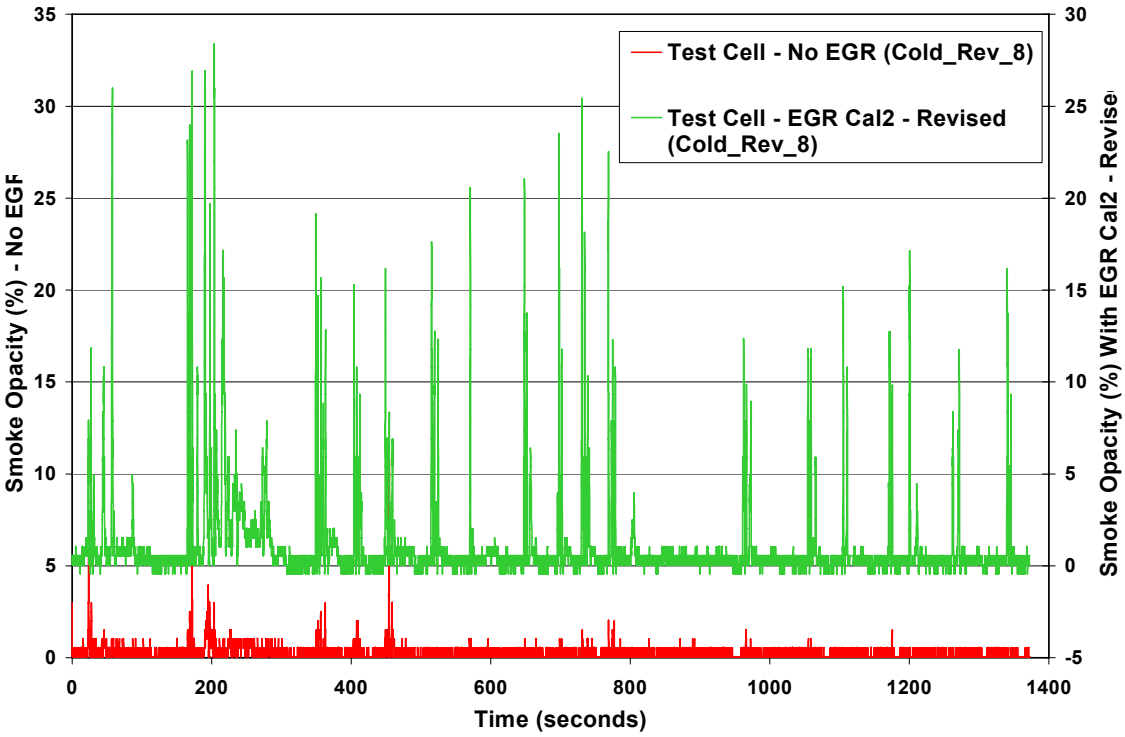

Figure 42. Engine-out smoke opacity over Hot-Start UDDS cycle for no EGR and high-EGR calibration

Table 20. NO_x and PM Mass Emissions for Different EGR Calibrations

Calibration ID	Cold-Start UDDS Mass Emissions, grams	
	NO_x	PM
Stock – No EGR	37.4	0.765
Cal1-LU Table only	13.1	1.600
Cal2 w/Mode Modification-1	19.1	0.986
Cal2 w/Mode Modification-2	18.1	1.202
Cal2 w/Mode Modification-3	17.8	1.032

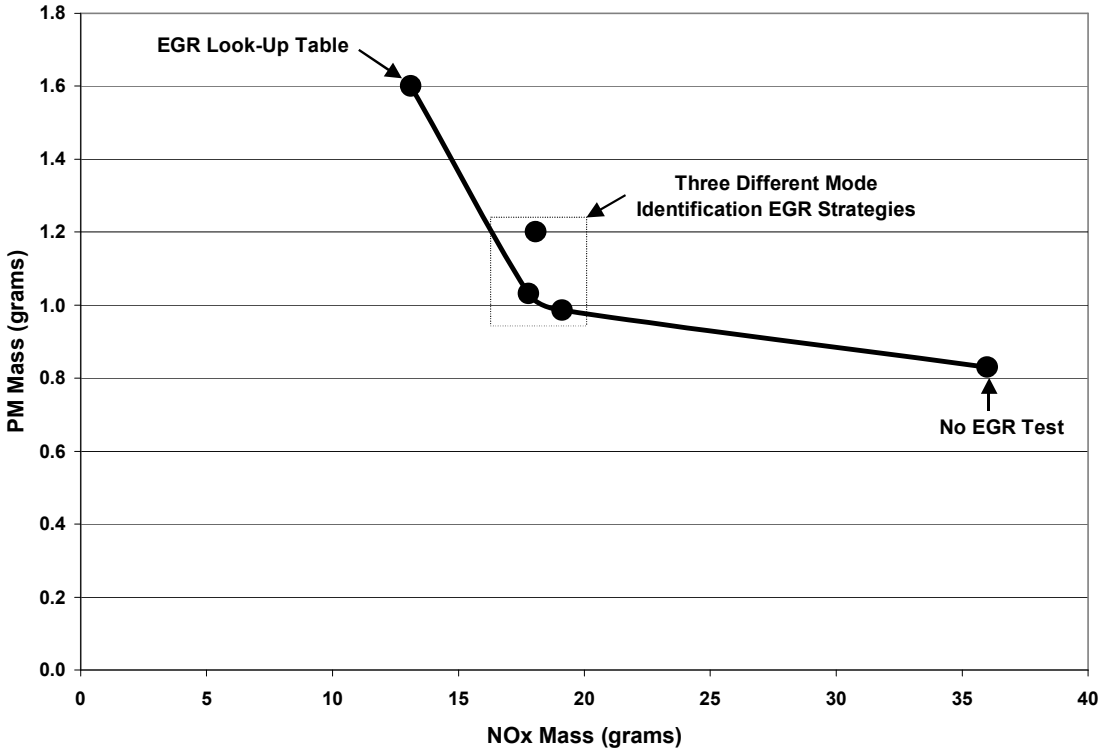

Figure 43. NO_x/PM trade-off for different EGR strategies over the Hot-Start UDDS Test cycle

3.2 Emissions System Calibration and Control (EGR+DPF+NAC)

The ECS components tested in this project consisted of NACs, oxidation catalysts, and a catalyzed DPF. These components were integrated with the engine control to form the ECS. In addition to the controls/strategy developed for the ECS, a diesel-fueled burner was utilized to provide the heat necessary for the ECS to function in its temperature operating window. Section 3.2.1 describes the burner developed in this program. The regeneration strategies and control of the ECS are described in Section 3.2.2. The resultant fuel economy penalty over the test cycles of interest is discussed in Section 3.2.3.

3.2.1 Diesel-Fueled Burner

A diesel-fueled burner was designed to provide supplemental heat to the ECS. However, because burners can typically operate across a very wide range of air-fuel ratio control, the burner can also provide a means for reducing exhaust gas O_2 content and provide reductant during emissions system regeneration. The burner was created drawing on previous gasoline-fueled burner design experience and thorough study of a commercially available fuel-oil burner system. The intent was to create a fast, simplistic solution and to utilize commercially available parts where possible. It is a tube-type burner that operates in parallel to the exhaust system, minimizing back pressure increases due to the device

installation. Some parts from a commercially available oil burner were combined with a gasoline fuel injector, an air atomizing injector holder, and a flame-stabilizing technology developed by SwRI (Active Porous Media Aftertreatment Control System – US Patent No. 5,771,68), to create the diesel burner.

When a diesel engine is operated at loads much lower than the engine is rated for, the exhaust temperatures are much lower than typically required for modern day aftertreatment devices. Under lightly loaded engine operation it will be necessary to perform general thermal management as well as regeneration management for a NAC-based system. When large levels of thermal management are necessary, transferring the supplemental heat efficiently to the catalyst system becomes the main priority in reducing the fuel economy penalty that will be incurred.

One approach to thermal management is to use modified engine calibrations to generate the supplemental heat needed (i.e., post-injection, intake throttling, EGR). Figure 44 shows the layout of a dual branch system that would incorporate only engine-based regeneration and thermal management control. For the configuration shown in Figure 44, supplemental heat generated by the engine has many potential heat loss paths. A major source of heat loss occurs in the engine during combustion of the supplemental fuel. After the exhaust leaves the engine, heat loss can occur in the exhaust manifolds and cross over pipes through the turbocharger, the downpipe, and the exhaust system that bends underbody into the catalyst. The heat loss paths in the exhaust are shown in red.

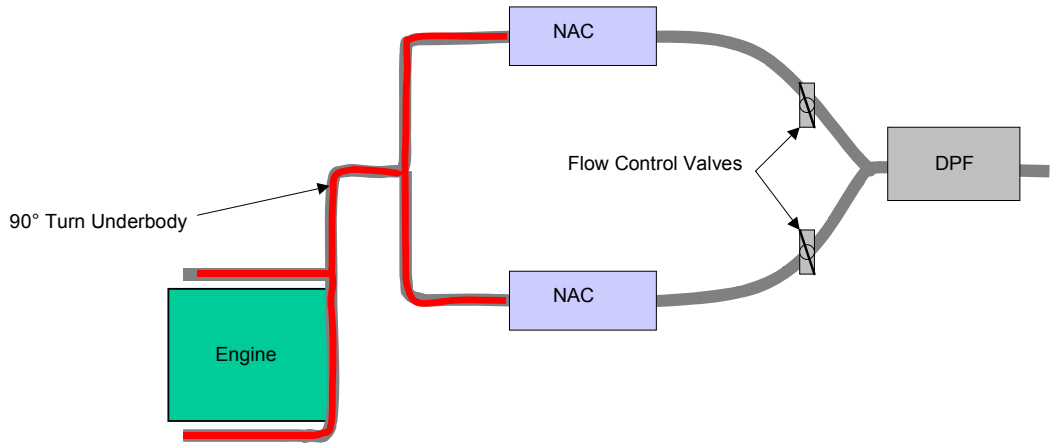

Figure 44. Heat loss paths in an engine-based regeneration and thermal management configuration

Another option for supplemental heat generation would be the use a fuel burner located in the exhaust. A fuel burner has a very high efficiency of conversion of fuel energy to heat energy, and can be located in close proximity to the emissions systems, thereby reducing heat lost between the point of generation through transfer to the emission systems. Figure 45 shows a possible emissions control system configuration using a burner-based thermal management approach. In this configuration the combustion chamber is located

inside the "Y" of the exhaust, in an underbody location. Installing the burner inside the exhaust allows the combusted fuel heat as well as the radiant heat emitted from the combustor wall to be transferred to the exhaust, limiting heat loss during the combustion process. The remaining heat loss paths are the exhaust pipe that transfers the heat to the catalyst. Figure 45 highlights this heat loss path in red. Because the heat loss path is confined to the exhaust system, double-walled pipe could be used to minimize heat loss and improve the efficiency of the heat transferred to the catalysts.

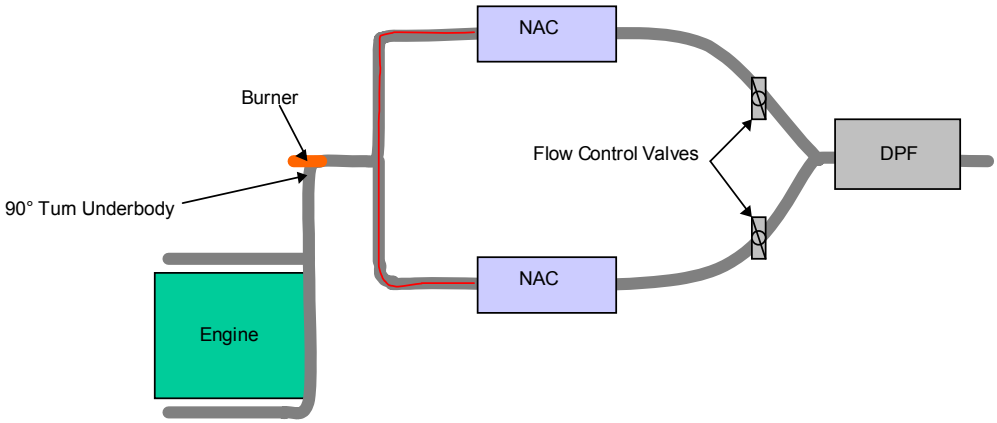

Figure 45. Heat loss paths in an In-exhaust burner-based regeneration and thermal management configuration

The use of a fuel burner to generate supplemental heat in close proximity to the ECSs creates a configuration that is more efficient at converting fuel to supplemental heat and transferring that heat to the emissions control systems than an engine-based approach. Another beneficial feature of using a fuel burner is the wide range of stable operation (both in airflow and fuel flow) that burners typically offer. This wide range of operation allows the device to provide a wide range of temperature as well as air-fuel ratio control, which may be a very useful feature in creating the exhaust gas composition needed to carry out the periodic regeneration of the NAC. The diesel engine is not well adapted to running under the rich conditions needed to regenerate the NAC; however, a burner lends itself well to rich operation. Running the burner rich will generate unburned and partially burned hydrocarbons, CO, and hydrogen. Running rich will also help reduce the overall exhaust gas oxygen content. Adding a pre-catalyst (such as a thin oxidation catalyst) can be useful in combusting some of the unburned hydrocarbons from the burner with the engine exhaust. Once overall rich conditions are achieved, the pre-catalyst can also be used to generate large amounts of CO from the unburned hydrocarbons and engine exhaust oxygen. This will help to not only create overall rich conditions, but will remove the excess O_2 from the exhaust prior to entering the NAC. Additionally, adding SFI in the exhaust, upstream of the pre-catalyst, can be used to enhance the available reductant and to accelerate the transition from lean to rich conditions. Figure 46 shows the ECS

configuration utilized in this program, which includes a burner, supplemental fuel injection, and a pre-catalyst before the NAC and DPF systems.

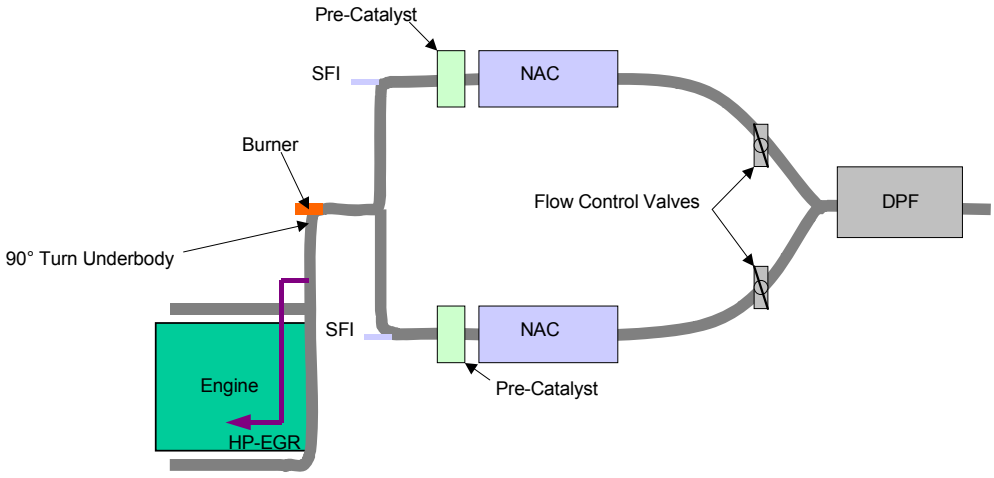

Figure 46. Emissions system configuration utilizing a fuel burner, in-exhaust supplemental fuel injection, and pre-catalyst upstream of NAC-DPF system

Figure 47 shows some photographs of the burner head. The injector selected was a Bosch K-Jetronic with fuel modulation achieved using a Bosch frequency valve. The K-Jetronic was selected because it offers rapid shutoff of fuel and has a poppet-valve design that is more heat tolerant than a needle-lift type injector. The K-Jetronic selected has an air-shroud bonnet installed on the injector, and for better atomization, compressed air flows through the bonnet while the injector is activated. To achieve this, a jacket was designed to hold and seal the injector, and to provide a means for injecting compressed air. The air jacket was also designed to provide mounting for the air-swirl bonnet and the electrodes.

The flame stabilizer is a section of ceramic-foam silicon carbide, placed between the burner flame and exhaust flow. The foam was used to stabilize and contain the flame within the burner head, thus preventing the flame from contacting the catalyst face, even if it were to be very closely coupled to the emissions systems. It is also used to provide a surface for combustion of larger fuel droplets, to reduce the impact of engine exhaust pulsations on the burner flame structure, to flatten the burner exit temperature profile, and, once hot, to reignite the burner flame, if necessary.

A control system was built to provide control over fuel injection, spark, air assist, and the main burner airflow rate. The controls were integrated into the ERIC, and three modes of operation were provided:

1. Cold-start emissions system warm-up
2. Temperature balancing
3. Manual mode.

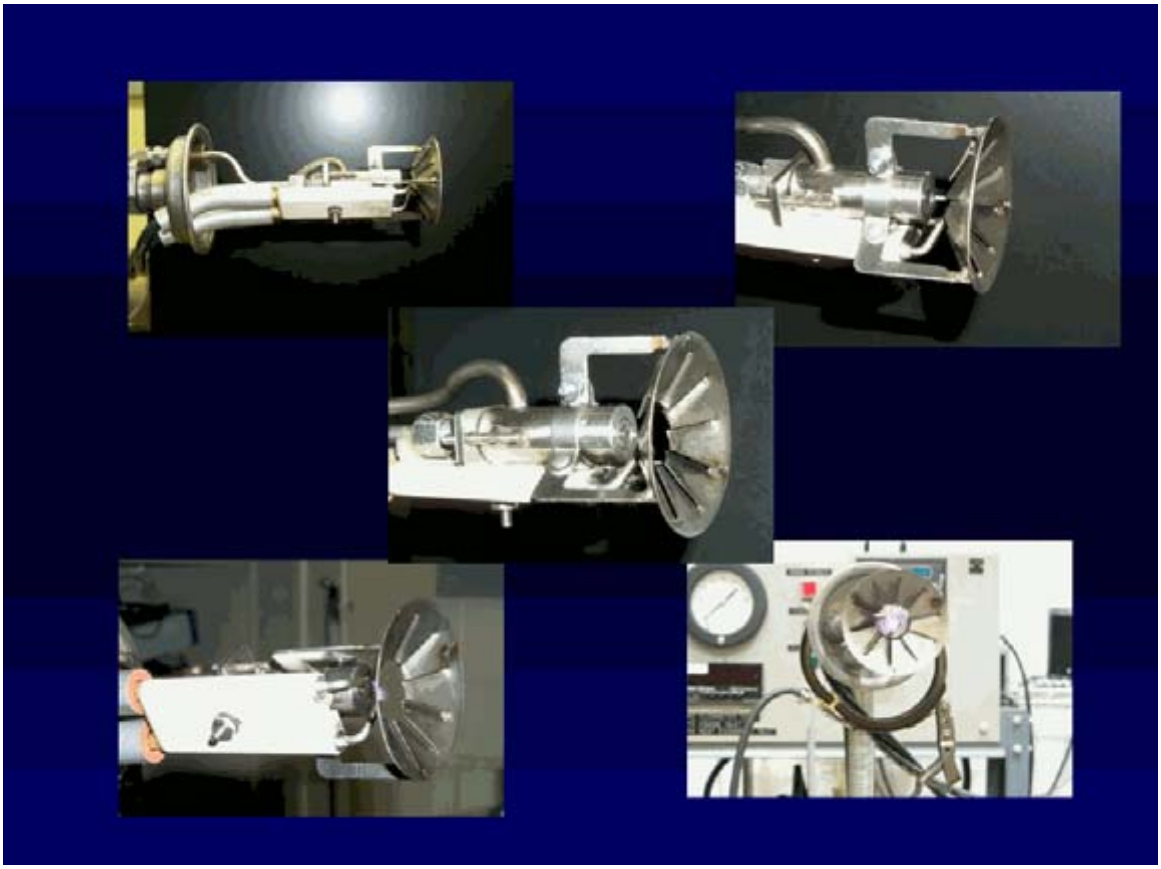

Figure 47. Photographs of the diesel fuel-burner head

The burner was installed with the combustion chamber submerged in the engine exhaust flow. This approach provides external cooling of the combustion chamber and reclaims the heat normally radiated from the combustion chamber wall, thereby improving the transfer efficiency of the supplemental heat to the catalyst. This configuration also combines all hot portions of the burner inside the exhaust. Figure 48 shows a burner system installed in a dual-branch configuration with an oxidation catalyst and one NAC catalyst. The burner is installed in a position that simulates the underbody turn of the exhaust on the vehicle.

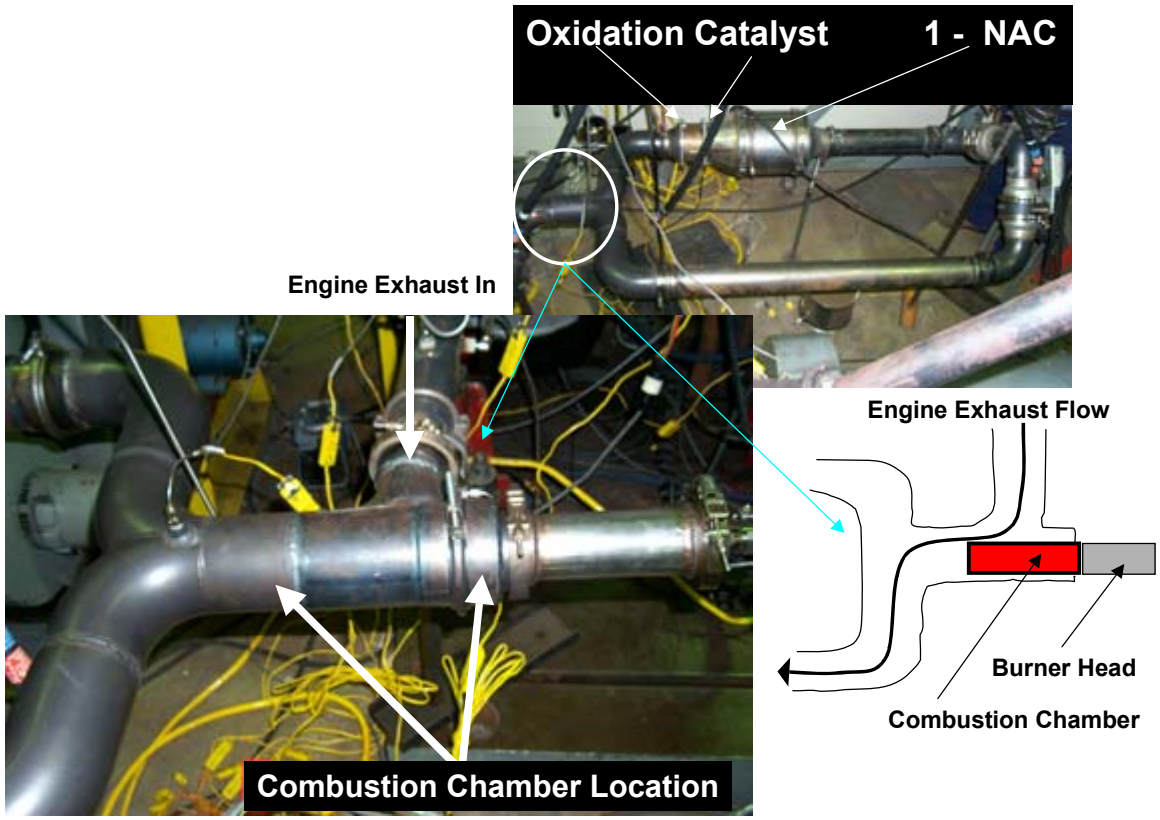

Figure 48. Photographs of the burner installed in the engine exhaust with an oxidation catalyst and one NAC

3.2.2 Emission Control System Regeneration Control/Strategy

The ECS was a dual-leg NAC with a single DPF downstream of the combined flow after the NACs. There were also oxidation catalysts installed upstream of each NAC and in front of the DPF. The dual leg NAC configuration allowed reduced flow regeneration (compared to a single leg, full-flow system), and used exhaust valves to direct flow during regeneration and desulfurization. This particular system included a single diesel fuel burner used for thermal management and to produce reductants for regeneration. SFIs were installed in each exhaust leg to allow additional control of the regeneration reductant. Figure 49 shows a schematic of the ECS evaluated in this project.

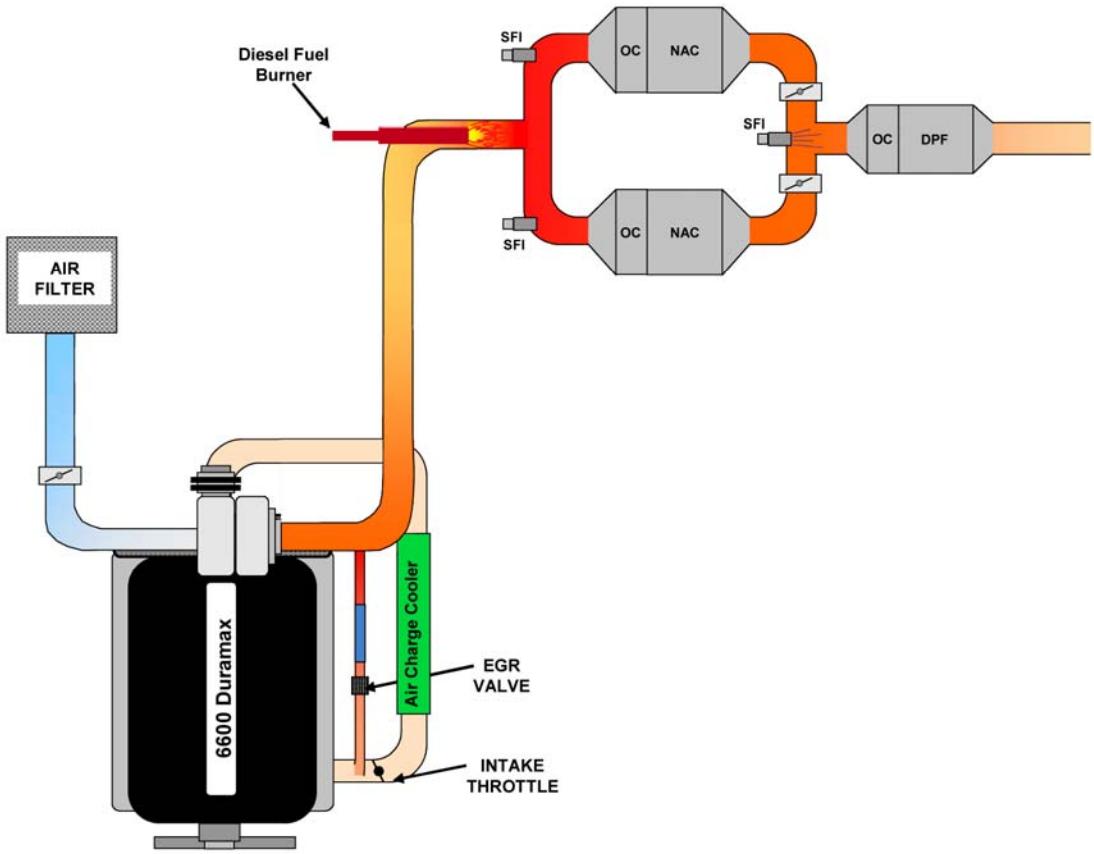

Figure 49. Schematic of an ECS

Control Strategy Overview

The controller strategy developed to manage the ECS consisted of three main software "controllers" or elements. Each controller was a piece of software that was developed to monitor and control the hardware associated with a specific subsystem. All software controllers interacted and exchanged information with each other to create an integrated solution. In the SwRI approach, there were three main controllers: the EGR controller, the ECS controller, and the burner controller. A schematic overview of the emissions controller is shown in Figure 50.

The EGR controller was responsible for the proportional control of the EGR valve and intake throttle. EGR control was modified to reduce flow during cold starting and acceleration conditions. The EGR controller communicated information about EGR flow to the ECS controller. EGR calibration was described earlier in Section 3.1.

The ECS controller was responsible for estimating engine-out NO_x mass, running the NO_x mass model for each NAC, determining the NAC regeneration state of the system, tracking engine load to determine if additional heat from the burner was needed, and calculating the amount of reductant needed for each regeneration. The ECS controller

communicated information about pre-burn needs and regeneration state to the burner controller.

The burner controller was responsible for tracking when the engine started, controlling engine-start ECS warm-up schedules, and for monitoring data from the ECS controller to determine when burner pre-heating would be required prior to NAC regeneration.

The full transient control strategy can be broken down into three areas:

1. NO_x regeneration management
2. General thermal management
3. Cold-start thermal management.

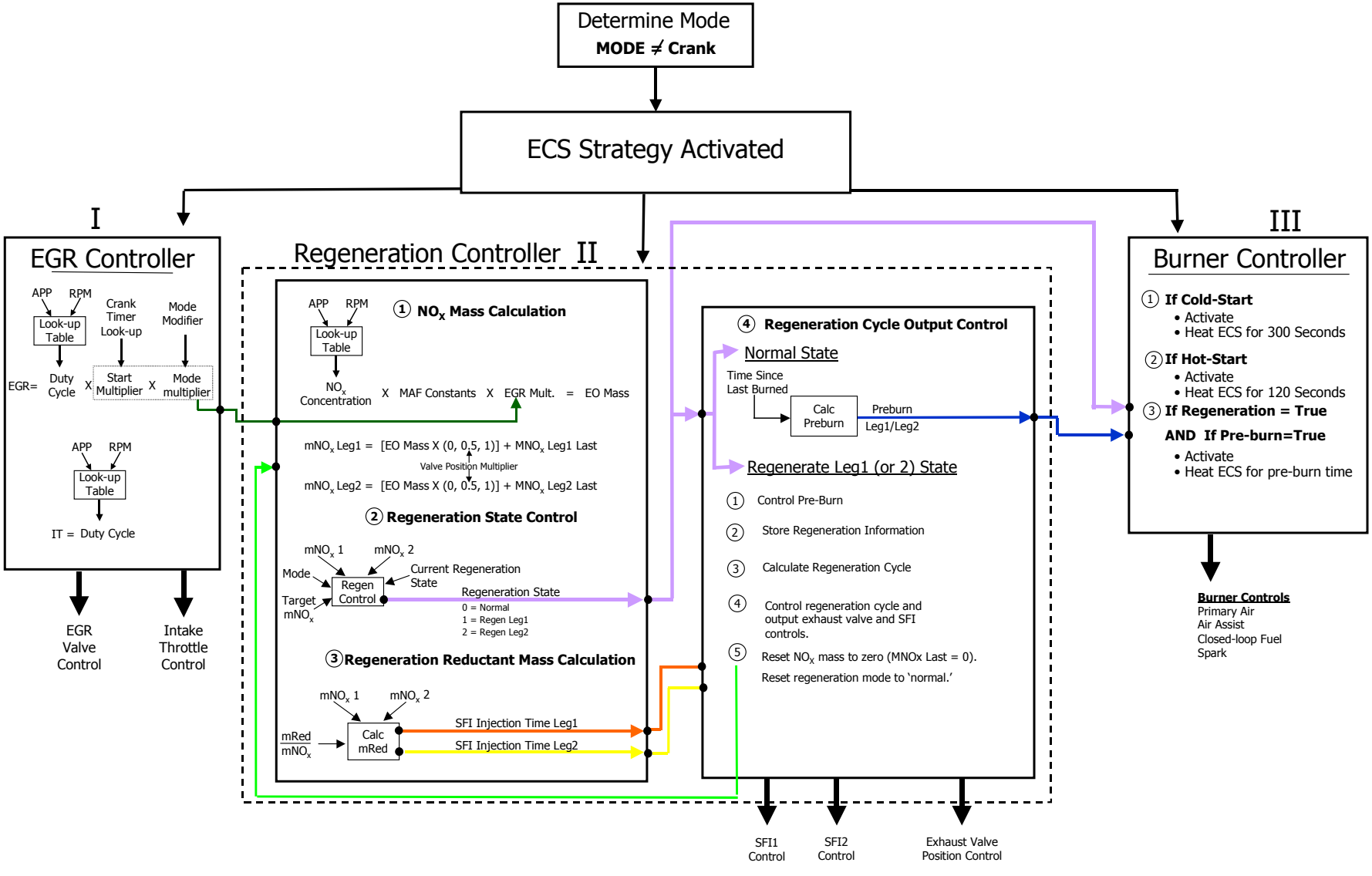

Figure 50. Schematic overview of software controller designed for ECS management

NO_x Regeneration Management

The following section describes how regeneration was carried out in this system and the catalysts' interaction. During normal operation (adsorbing mode), both exhaust flow control valves were open, and the exhaust was free to flow down both legs (refer to Figure 49 for the ECS schematic). The NO_x mass model continually estimated the mass of NO_x trapped in each NAC. Once a predetermined mass of NO_x was reached, a regeneration event was triggered. The NAC controller first determined if the burner needed to be operated to increase the ECS temperature. If necessary, the burner was operated for a fixed period of time prior to continuing with the regeneration sequence. The exhaust flow control valve in the leg to be regenerated then closed, directing all of the exhaust flow through the opposite leg. After a short period of time, the supplemental, in-exhaust fuel injection was activated in the leg to be regenerated. The exhaust flow control valve in the regenerating leg remained closed for a period of time after the supplemental fuel was injected. Following this time period, the exhaust flow control valve opened, and the exhaust flowed down both legs. This sequence repeated, alternating legs for regeneration as controlled by the NO_x mass model. Using this approach to regeneration allowed at least one leg of the system to always be adsorbing.

During regeneration, the overall rich mixture first entered the oxidation catalyst, where the fuel was partially oxidized to form lighter hydrocarbons and CO while simultaneously removing excess O_2 in the feed stream. The other function of the oxidation catalyst was to absorb the very high exotherm resulting from the oxidation of the injected fuel and O_2 remaining in the exhaust stream. This catalyst was more thermally stable than the NAC, and by absorbing this release of heat, it provided some thermal protection for the NAC.

A NO_x mass model was created to predict the level of NO_x stored in the adsorber system and predict when each adsorber was in need of regeneration. The NO_x mass model estimated the amount of NO_x stored in the adsorbers in real-time, integrating the instantaneous NO_x mass entering each adsorber and assumed 100% adsorption. The model also assumed that during regeneration, 100% of the stored NO_x was removed from the adsorber. The concept of this model is shown in Figure 51.

The NO_x concentration used in this model was based on a look-up table of measured NO_x concentration as a function of engine speed and load. The NO_x map was generated under steady-state conditions, and as such there was some error associated with transient operation. An alternative to using a NO_x mass look-up table would be to use an exhaust NO_x sensor to measure engine-out NO_x directly. This method would provide a more direct and perhaps more accurate result. However, in production, if a sensor would be used, it would most likely need a NO_x concentration look-up table as a back-up alternative in the event of sensor failure.

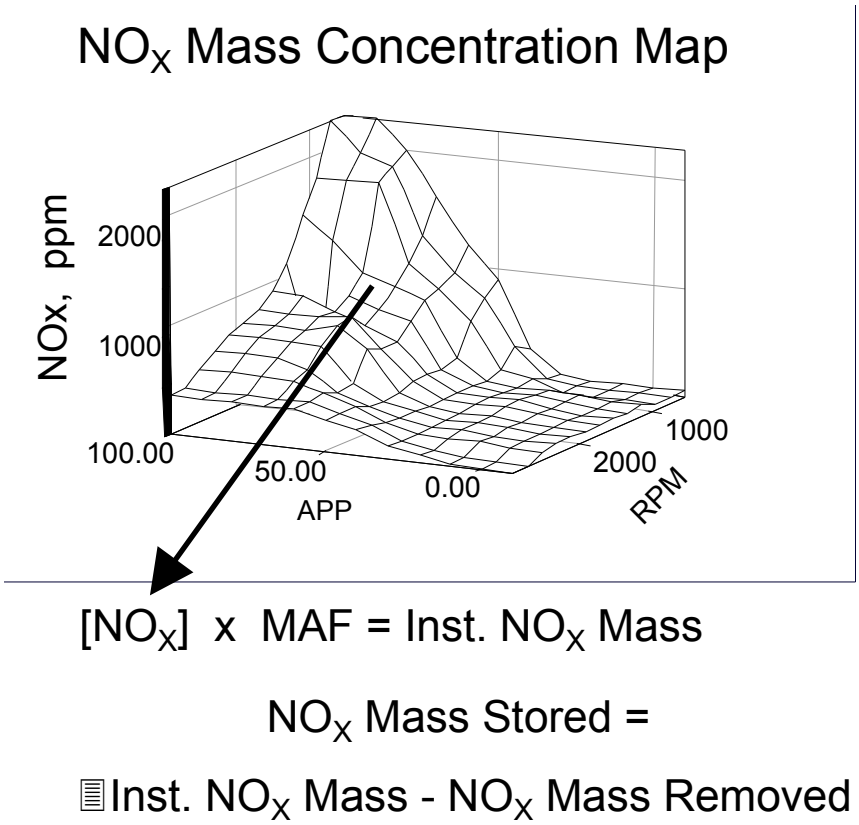

Figure 51. NO_x mass model concept

General Thermal Management.

Examination of the baseline temperature data across the FTP test cycle showed that the measured exhaust gas temperature at the catalyst inlet location averaged only 165°C, well below the 275°C to 400°C temperature range recommended by the catalyst supplier for efficient NAC operation. Examination of the data revealed three main areas of engine operation that presented special thermal management needs:

1. Cold-start - to create rapid warm-up for ensuring that the emission systems are active within 10 to 20 seconds after engine start
2. Deceleration and idle – to prevent rapid cooling during deceleration and increasing low idle temperatures
3. Cruise – to increase the average exhaust gas temperature under steady-state, lightly loaded operation.

Due to the large difference between the normal operating temperature of the engine and the required temperature for high-efficiency catalyst performance, it became obvious that a large amount of supplemental heat would need to be added to the system to achieve the desired performance. The large amount of supplemental heat required indicated that a large fuel penalty would be incurred in creating the necessary heat, and the most fuel efficient solution for the application was sought to minimize the fuel economy penalty. The results of a heat loss analysis led to the conclusion that for the engine operating over lightly loaded conditions (i.e., the FTP-

75), the temperature requirements may be extremely difficult and costly to meet using an engine-based approach alone (an exhaustive study of several options showed that up to 75% of the supplemental heat generated at the engine could be lost before the catalyst inlet). It was decided that the source of heat necessary to achieve the temperature window should come from an external source (e.g., electric heater or fuel burner) installed in close proximity to the catalysts.

Due to the energy requirements needed to raise the exhaust gas temperature during general operation and particularly during a cold start, a decision was made to use a fuel burner. It was also felt that the fuel for the burner should come from the same source as the engine (diesel) to maintain fuel singularity in the application.

A fuel burner was created for this application and installed in the exhaust of the Duramax (as was shown in Figure 49). The burner control was designed to monitor engine and exhaust conditions, detect cold-start or temperature balancing needs, and self activate when conditions indicated a need to increase the exhaust gas temperature. Figure 52 shows the temperature at the oxidation catalyst inlet location for the Cold-Start UDDS (Bags 1 and 2 of the FTP-75), the stock, no-EGR configuration, and for using the burner in combination with HP-EGR and intake throttling (all other temperature management controls were eliminated). The additional fuel consumed by the burner was used to calculate the efficiency of the conversion of fuel to heat energy and the transfer of that heat to the catalyst. This burner-based approach was found to be 90% efficient.

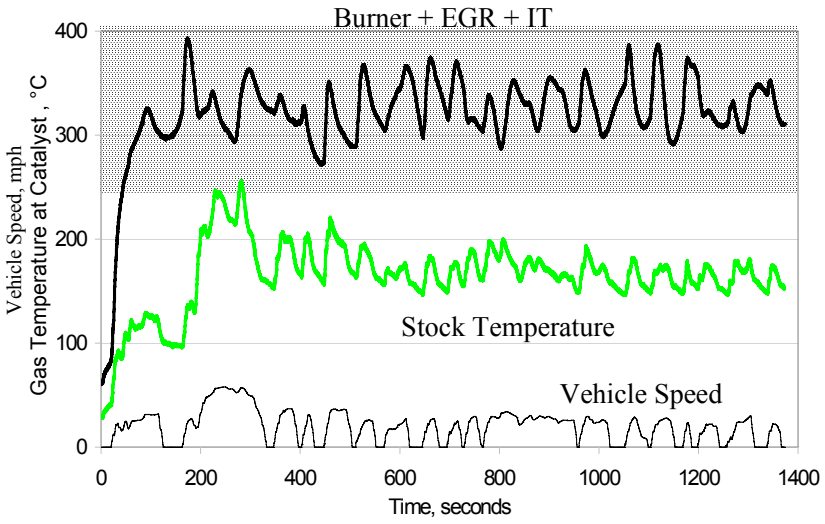

Figure 52. Exhaust gas temperature at catalyst inlet location for burner + oxidation catalyst and stock, no-EGR configuration

Cold-Start Thermal Management

In the absence of any cold-start strategy, the temperature in the front of the first catalyst (oxidation catalyst) would not exceed 200°C for well over 200 seconds over the Cold-Start UDDS cycle and never exceeded 300°C. In order to achieve high conversion efficiencies, the front oxidation and NACs needed to be at operating temperature (275°C - 405°C) as soon as

possible (preferably in under 20 seconds) after engine start. During this work, several cold-start strategies were developed.

Cold-start strategy 1 (S1) involved activating the burner and running it in thermal balancing mode for 120 seconds. Using this strategy, the front of the NACs (2.5-cm deep on the centerline of the NAC substrate) did not reach over 300°C until 75 seconds after cold start, and the back of the adsorber, NAC5 (12.7-cm deep on the centerline), did not exceed 300°C until 180 seconds into the cycle. Figure 53 shows the NAC bed temperatures for the base system, S1.

To further improve cold-start emissions performance, it was necessary to accelerate the heat up of the NAC to operating temperature. The cold-start strategy was modified to improve burner output and to add additional energy to the NAC. Cold-start strategy 2 (S2) increased burner airflow from 226 l/min to 263 l/min, and added short bursts of SFI to add chemical energy to the NACs. The increased burner airflow improved burner temperature output and resulted in increased temperature at the inlet to the oxidation catalysts. Once the oxidation catalysts had reached sufficient temperature, the SFI (in-exhaust injection) was activated, supplying short bursts of fuel to each leg under full-flow conditions.

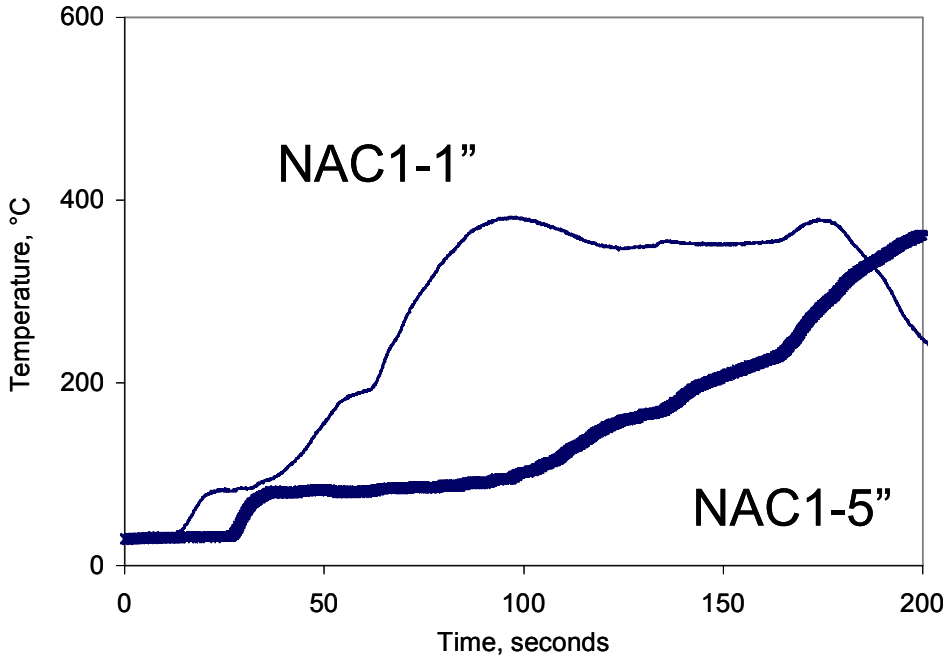

Figure 53. NAC1 bed temperature for S1

When examining the results of S2, it can be seen that supplemental heat was getting into the front of the NAC, but was not being transferred throughout the NAC. In order to raise the temperature at the back of the NAC, more exhaust flow was required to push the energy through the catalyst. Cold-start strategy 3 (S3) was developed to target transferring heat through the NAC. Under S3, EGR was eliminated for the first 120 seconds after cold-start. EGR originally was reduced under cold-start for driveability reasons, but was maintained at a low level for NO_x control. Figure 54 shows that strategy S3 worked well to accelerate the heat-up of the entire NAC, and that NAC5 achieved 300°C in 120 seconds (compared to 180 seconds with S1). S3 also achieved substantially accelerated warm-up of the DPF (see Figure 55).

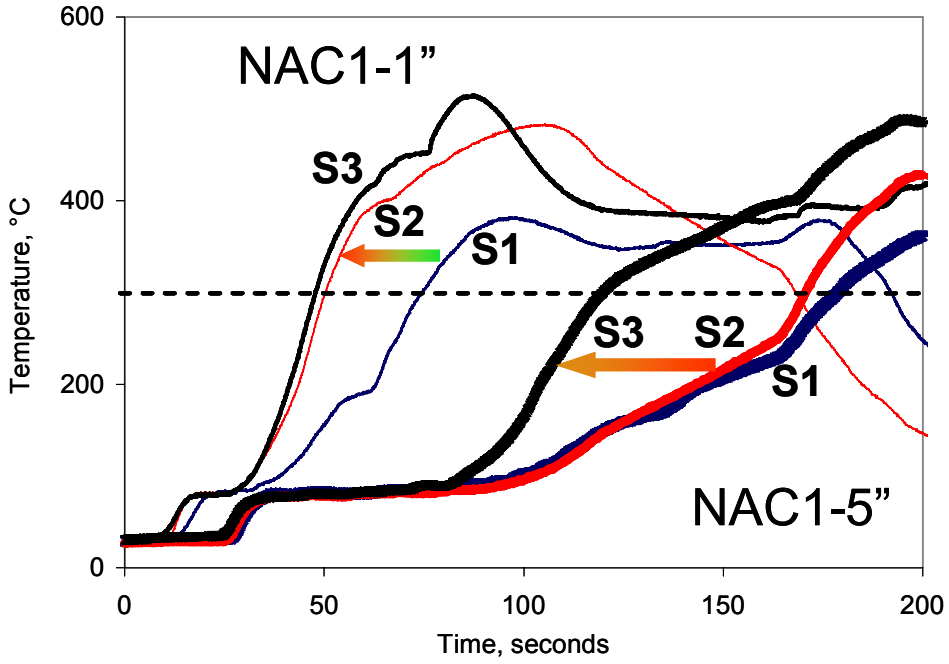

Figure 54. Effect of cold-start strategy on NAC1 bed temperatures

Using a burner to rapidly add heat energy to the exhaust emission components accelerated catalyst light-off to less than 20 seconds for the oxidation pre-catalysts and to 50 seconds for the front of the NAC. In operating situations in which supplemental heat is required, the burner system provides an efficient means for maintaining the temperature window for efficient operation of the ECS.

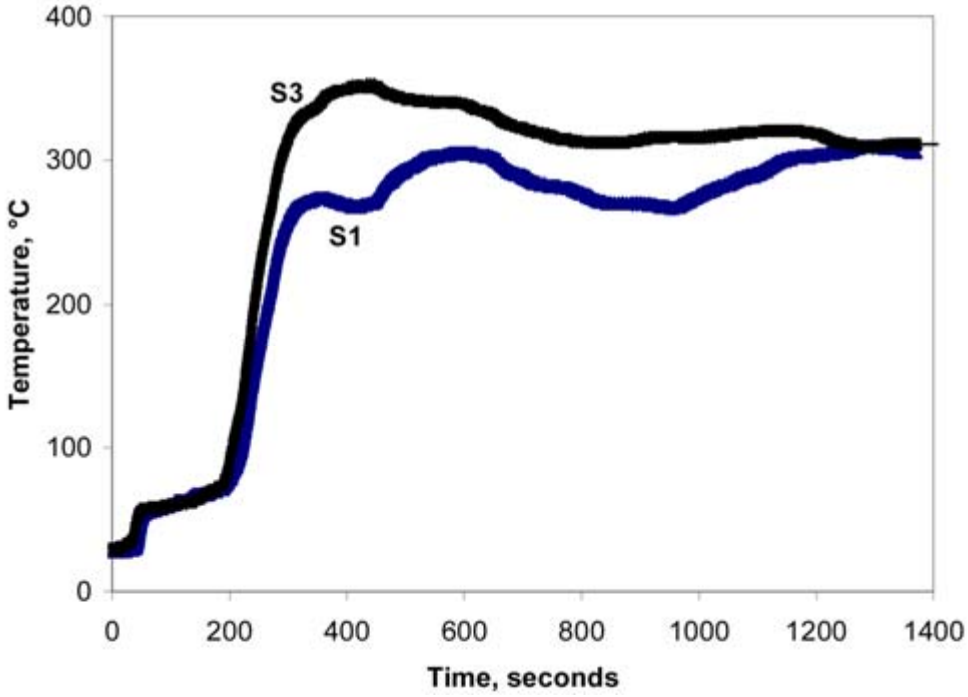

Figure 55. Impact of accelerated NAC S4 on DPF warm up

3.2.3 Fuel Economy Penalty Associated with Emission Control System Operation

A fuel penalty is incurred whenever energy is put into the system beyond that which is necessary to power the engine/vehicle over the desired operating cycle. In this project, the magnitude of fuel economy penalty was a function of the thermal penalty (energy added to increase the ECS temperature sufficiently) and the regeneration penalty (fuel used for removing NO_x from the NAC). The total thermal penalty was a function of the engine-out exhaust temperature, the exhaust mass flow rate, and the efficiency of converting fuel chemical energy to heat at the ECS. The regeneration fuel penalty was a function of the engine-out NO_x mass, NAC volume, the reductant type, and the level of NO_x reduction required from the ECS (the emissions goal).

The thermal fuel economy penalty was the energy input to the system in order to raise the temperature of the ECS system into its operating window and is summarized in Equation 1.

$$Energy = \dot{m} \times c_p \times \Delta T \qquad \text{(Eq. 1)}$$

$\dot{m}$ = exhaust mass flow rate
c_p = specific heat of exhaust gas
ΔT = desired temperature – engine provided temperature
λ = efficiency in converting fuel energy to heat at the ECS

As discussed in Section 3.1, the average exhaust gas temperature was less than 165°C across the Cold-Start UDDS, significantly below the NAC operating window of 275-400°C necessary to achieve the high levels of NO_x reduction required to meet the project goals, as shown in Figure 56. EGR was used to reduce the exhaust mass flow ($\dot{m}$) to lessen the energy required. The average exhaust flow rate over the Cold-Start UDDS was reduced by 33% through the use of EGR, as shown in Figure 57. A diesel-fueled burner was used to supply the necessary heat directly to the exhaust gas upstream of the NACs (ΔT). The burner was found to be the most efficient method for increasing the exhaust temperature as compared to other strategies such as intake throttling and turbo-charger by pass systems. The entire fuel economy penalty associated with the thermal requirements only brought the ECS into its operating window; it did not directly contribute to NO_x reduction.

The fuel economy penalty associated with actually reducing the NO_x with the ECS was referred to as the regeneration fuel economy penalty. The regeneration fuel economy penalty was a function of:

- Engine-out NO_x mass
- Reductant type
- NAC volume
- NAC efficiency
- Exhaust environment at regeneration initiation
- Emissions goal.

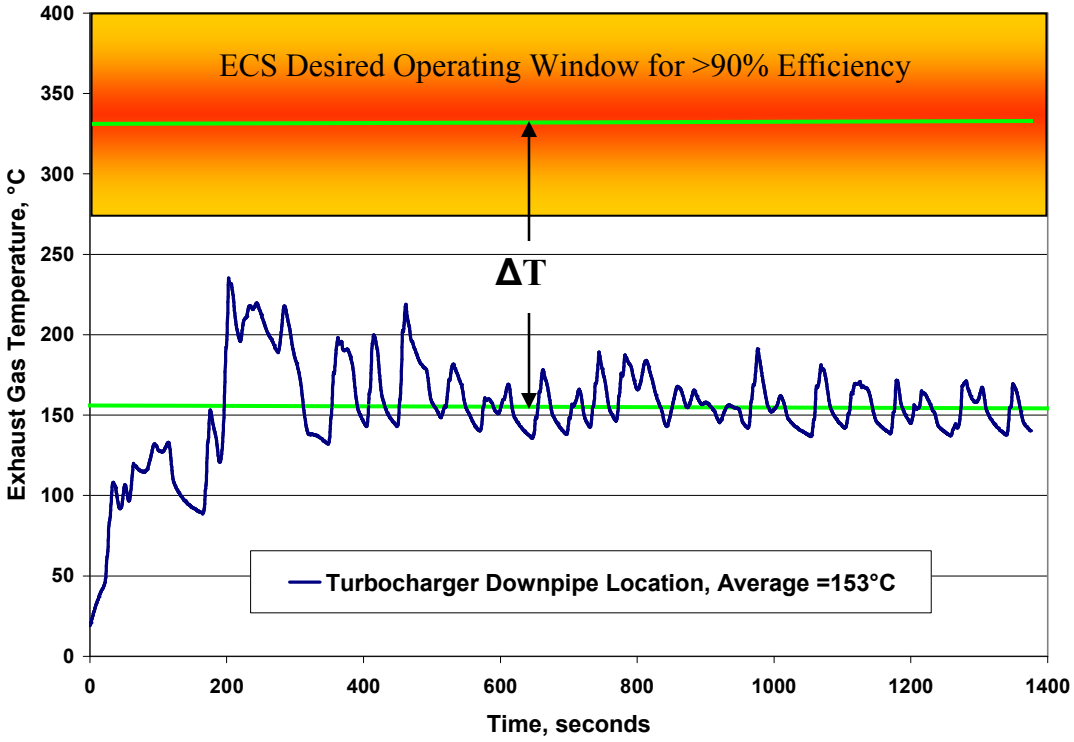

Figure 56. Exhaust gas temperature over the Cold-Start UDDS and desired operating window for ECS

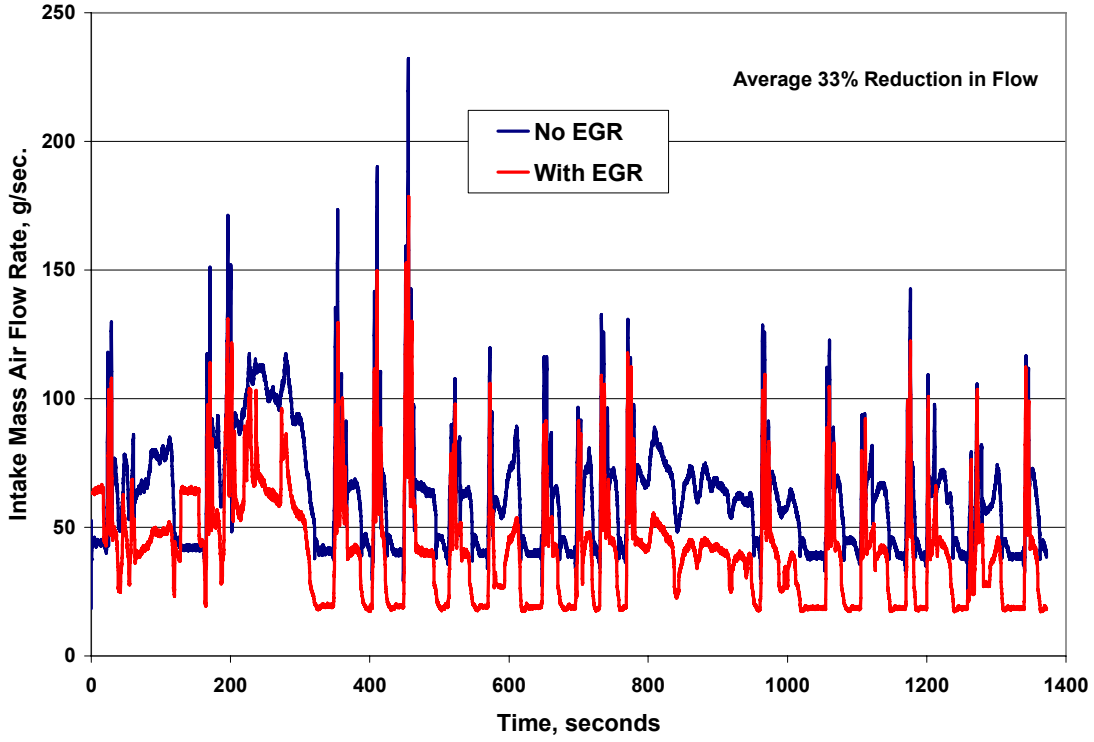

Figure 57. Exhaust mass flow rate over the Cold-Start UDDS with and without EGR

Higher levels of NO_x mass emitted from the engine, requires more frequent regenerations for a given level of NO_x reduction efficiency. Figure 58 shows an example of the NO_x reduction efficiency (at steady-state) for different levels of NO_x concentration at constant NAC temperature. Certain reductants are more efficient at regenerating the NAC (i.e., hydrogen, CO) while others are less efficient (diesel fuel, larger hydrocarbons). Thus, the type of reductant will have a direct impact on the efficiency of the ECS, and subsequently, on the amount of reductant required for a given level of NO_x reduction. As diesel fuel was used as the reductant in this program, the regeneration frequency had a direct impact on the fuel economy penalty. The NACs ability to store NO_x is reduced as NO_x is stored on the NAC, thus, the volume of the NAC directly affects the frequency of regeneration for a given level of NO_x reduction. This ability to store NO_x is also a function of the NAC formulation and operating temperature as shown in Figure 59. Thus, the efficiency of the NAC to store NO_x also directly affects the frequency of regeneration. When a regeneration is initiated, it is necessary to achieve overall reducing conditions in the NAC. Therefore, the exhaust environment will have a direct impact on the amount of reductant required to achieve overall reducing conditions (exhaust oxygen concentration and mass flow). Ultimately, the most important factor affecting the regeneration fuel economy penalty is the desired emissions goal. Achieving a tailpipe NO_x emissions level that requires a 95% reduction over the engine-out emissions will result in a fuel economy penalty substantially larger than one associated with achieving a NO_x reduction of 75% over the engine-out emissions.

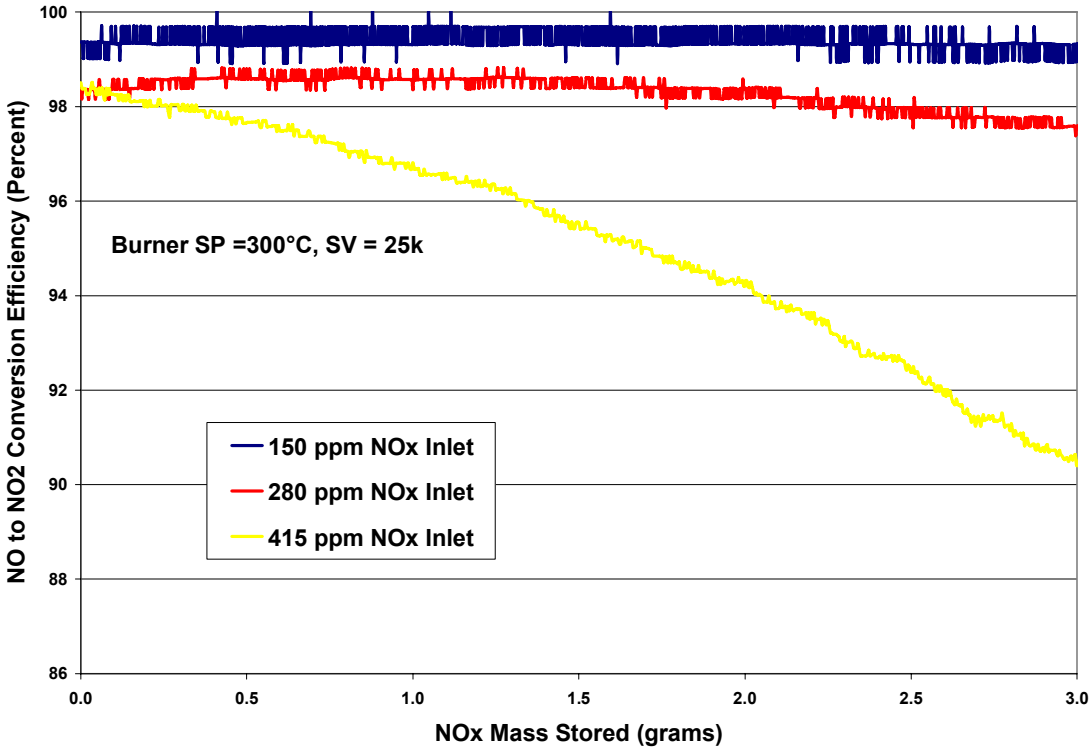

Figure 58. NO_x reduction for various NO_x inlet concentrations at constant inlet temperature

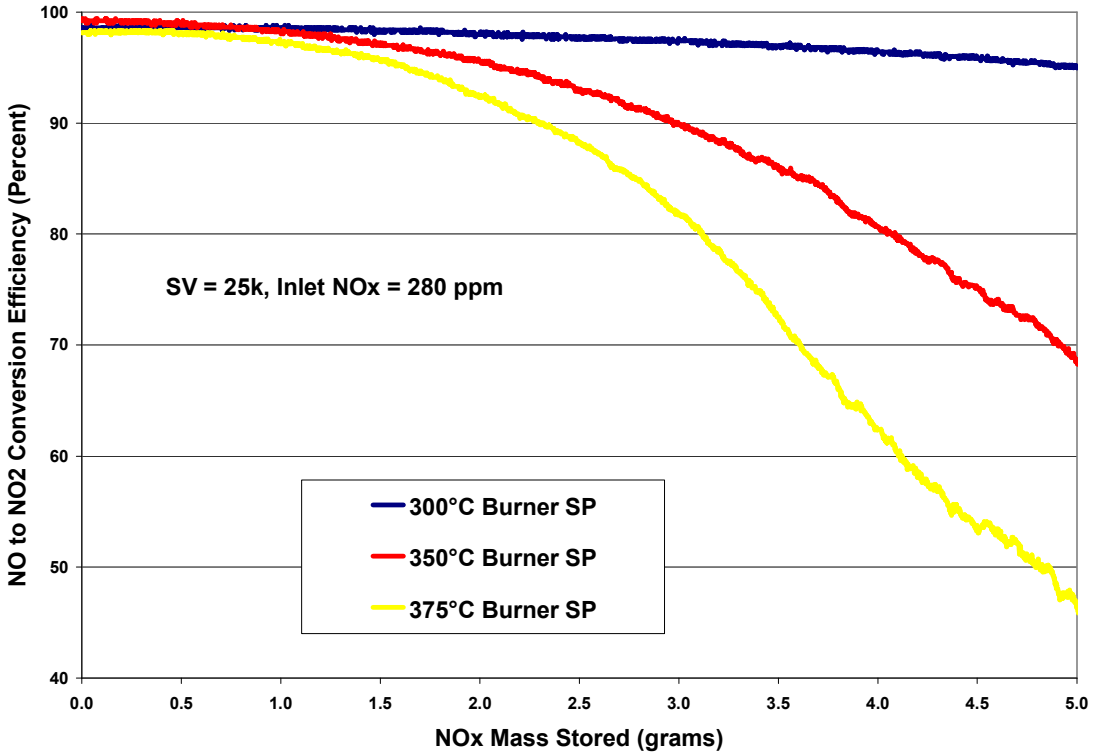

Figure 59. NO_x reduction for various NO_x inlet concentrations at constant inlet temperature

Figure 60 summarizes the fuel economy penalty due to EGR, regeneration, and thermal management for the Hot-Start UDDS, HFET, and US06 cycles. This figure shows that the total fuel economy penalty for the Hot-Start UDDS cycle is high (18%) due to the level of NO_x reduction required (>98%), and the low average exhaust gas temperature (thermal penalty contributes over half the total fuel economy penalty). As the cycle work increases (UDDS < HFET < US06), the total fuel economy penalty decreased (as does the overall NO_x reduction efficiency). Figure 61 summarizes the fuel penalty attributable to regeneration and the overall NO_x reduction (after 300 hours of aging) for the Hot-Start UDDS, HFET, and US06. Figure 60 and 61 both show that high levels of NO_x reduction can be achieved with a relatively small total fuel economy penalty (90% reduction over the US06 for a 4% fuel economy penalty) when minimal additional thermal energy is required by the ECS. However, when the engine-out exhaust gas temperature is far below the necessary operating window and extremely high levels of NO_x reduction are required (such as the Hot-Start UDDS), the fuel economy penalty can be quite high. These results imply that a more appropriately sized engine/vehicle combination has potential for reasonable fuel economy penalties over certification cycles and real-world driving.

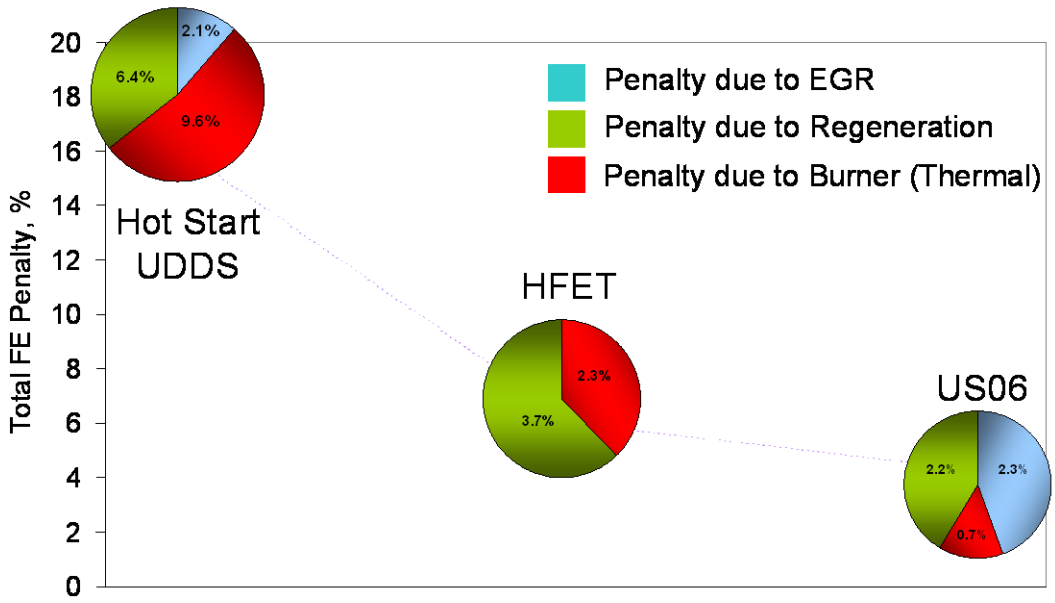

Figure 60. Fuel economy penalty and source over Hot-Start UDDS, HFET, and US06

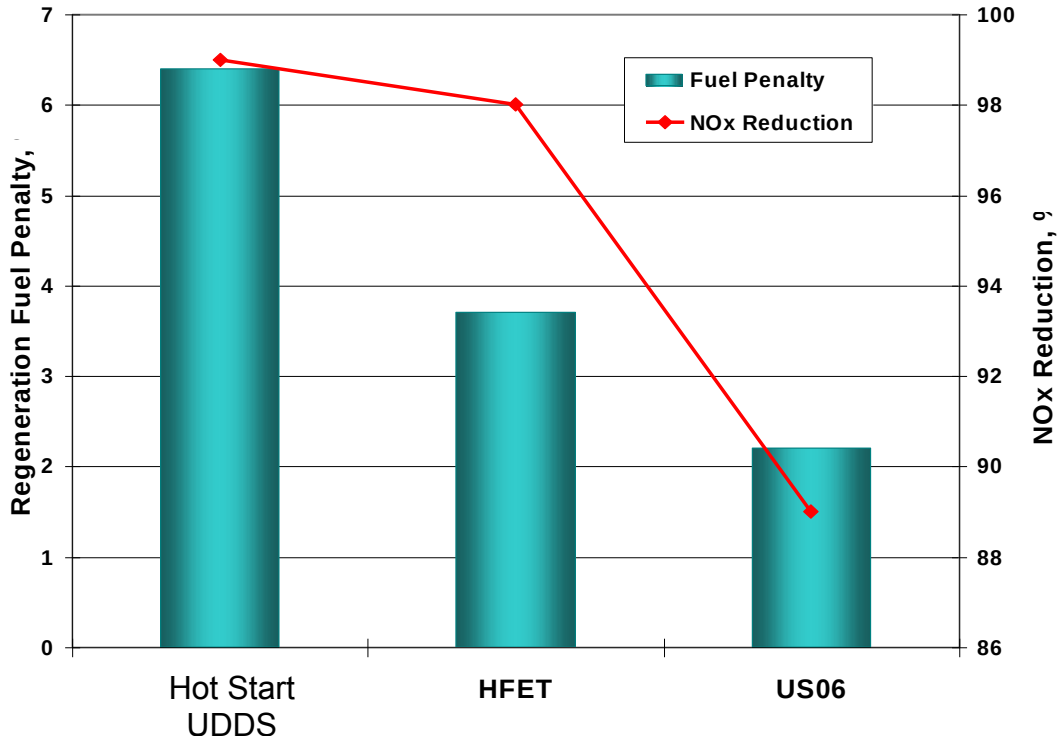

Figure 61. Regeneration penalty and associated NO_x reduction for the Hot-Start UDDS, HFET, and US06

3.3 Development of Desulfurization Process

One of the drawbacks to a NAC-based aftertreatment system is the requirement to intermittently "desulfate" the adsorber due to its high affinity for adsorbing sulfur oxides. The accumulation of sulfur on the available adsorption sites inhibits the NAC's ability to reduce NO_x by reducing its NO to NO_2 conversion performance and blocking NO_2 adsorption sites. In order to maintain a high level of NO_x reduction, the NAC must be intermittently cleansed of this sulfur accumulation.

For this program, after every 100 hours of aging, approximately 660 kilograms of fuel were consumed upstream of the NACs (engine, burner, and SFI). Given a fuel sulfur level of 15 ppm, there was a total fuel sulfur mass exposure of approximately 9.9 grams total over 100 hours. This mass of sulfur is assumed to be split evenly between the two exhaust legs, resulting in a fuel sulfur mass exposure for each NAC of approximately 4.95 grams. The engine oil consumption rate was approximately 0.35 liters (315g) every 100 hours. An oil sulfur level of 6,400 ppm results in a total oil sulfur mass exposure of approximately 2 grams for 100 hours of aging (1g for each leg). Therefore, the total sulfur mass exposure for each NAC over 100 hours of aging was approximately 6 grams (assuming an equal split of exhaust between the two exhaust legs).

In general, desulfurization of most NACs requires elevated bed temperatures (>650°C) and overall reducing conditions (lambda < 1). Four different on-engine desulfurization strategies were developed during this program. Each strategy attempted to create specific conditions within the catalyst in order to remove the stored sulfur, while minimizing thermal damage to the catalyst or engine. All desulfurization strategy development was conducted on the first generation NACs.

Ultimately, based on input from the ECS supplier, an off-line desulfurization process was developed on a gasoline engine. This option was accepted due to the limited availability of NACs, the potential for thermally damaging aged NACs during desulfurization, delays in receiving the second generation components, and the necessity to achieve extremely high levels of NO_x reduction. This cycle used a rich/lean pertubated approach and desulfated one NAC at a time. The gasoline SI engine was run at a constant speed and load with an exhaust flow rate of approximately 52 g/s. The fuel sulfur content was less than 30 ppm. The engine was run under rich conditions (lambda = 0.9) during the warm-up phase until the three NAC bed temperatures (1", 3", and 5" in) reached 600°C. At this point the engine air-fuel ratio was then pertubated between lambda of 0.9 and 1.05 (five seconds at each air-fuel ratio). The measured NAC bed temperatures typically reached 650°C (the desired desulfurization temperature) approximately 2 minutes after beginning the perturbation. The air-fuel perturbation was continued for an additional 5 minutes, after which it was ceased and the engine held at lambda of 0.9 for approximately 90 seconds. At this point in time the engine was brought to idle conditions (still at lambda of 0.9) and allowed to idle until the NAC bed temperatures dropped below 520°C (the typical peak temperature observed during transient emission evaluations). This idle period typically lasted 800-900 seconds. The entire process was then repeated on the second DOC/NAC combination.

The DOC/NACs were first subjected to desulfurization after 200 hours of aging. After this point, a desulfurization was conducted every 100 hours of aging after the pre-desulfurization emission evaluations had been completed. A "dummy" DOC/NAC was always run prior to the actual test parts to warm-up the engine and ensure the operating conditions were repeatable. An

example of the engine-out lambda and NAC system temperatures during a desulfurization is shown in Figure 62.

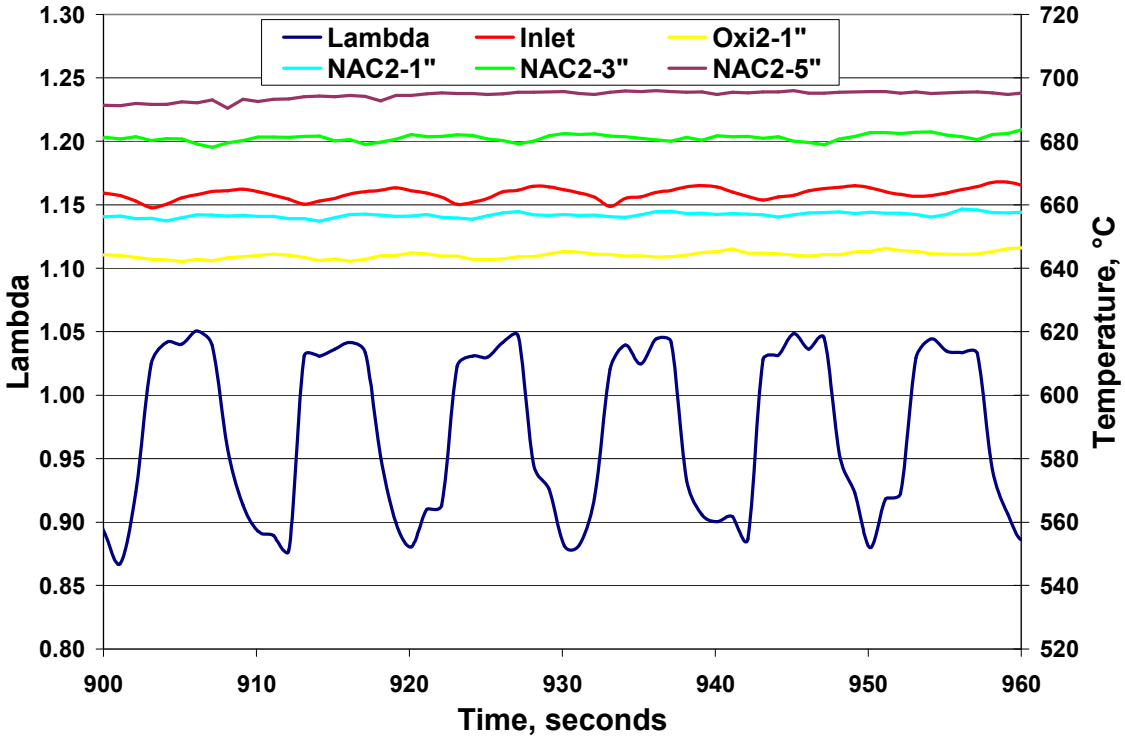

Figure 62. Example of engine-out lambda and NAC system temperatures during desulfurization

During the course of the program, an attempt was made to quantify the amount of sulfur (in the form of SO_2 and H_2S) released from the NAC system during a typical desulfurization or during each desulfurization. For the 1,300- and 1,400-hour desulfurizations, raw exhaust after the NAC system was pulled through impingers using the same sampling procedures as detailed in Section 2.2.3 for SO_2 and H_2S. Sampling began when the NAC bed temperatures reached 600°C (immediately before beginning the rich/lean cycling) and continued for approximately 2 minutes after cycling ceased (total sample time of 540 seconds). Table 21 summarizes the sulfur mass measured (in the form of H_2S and SO_2) during the 1,300- and 1,400-hr desulfurizations. Also this table provides an estimate of the total sulfur mass consumed in the engine, burner, and SFI for both the fuel and oil (theoretically the largest mass of sulfur that could be deposited on the NAC). After completing the 1,400-hour desulfurization and bringing the engine to idle conditions, a strong H_2S smell was observed in the test cell long after sampling had ceased, indicating that sulfur was still being removed from the NAC. In addition, condensed water was observed in the sample line immediately before the impinge. As H_2S is highly soluble in water, it is likely that a significant portion of the H_2S emitted was not collected. Modifications were made to the sample cart in an effort to increase the sample volume to maintain the sample temperature above the water condensation temperature.

The H_2S sampling period was subsequently increased and broken into four distinct periods. The first sampling period began during the warm-up phase, approximately 420 seconds prior to the NAC bed temperatures reaching 600°C. All sampling periods were 420 seconds in duration. The second sampling period began when the air-fuel perturbation was initiated. The third sampling period followed immediately thereafter when the air-fuel perturbation ceased, and the engine was brought to idle conditions. The fourth sampling period covered the last portion of the idle period. The 420-second sample duration was chosen in an effort to eliminate sample saturation and minimize lost periods of sampling due to bubbler changeover. However, for the third sampling period (first idle period at rich conditions), the primary and secondary samples were both found to be saturated, indicating a probable loss of sample. Due to the extremely high levels of H_2S emitted during the idle period, the established sampling and analytical procedures were not adequate to accurately quantify the mass of H_2S being emitted. Table 2 summarizes the H_2S mass measured at the 1,600-hour desulfurization point using the modified sampling procedures (a problem was encountered during the analysis for the first sample for NAC2 and no quantification of H_2S mass was possible). After this aging point, no further attempts to quantify the sulfur removal were made as the 1,600-hour results indicated a substantial portion of the maximum theoretical mass of sulfur deposited on the NACs was being removed during the desulfurization procedure. Substantial modifications to the sampling and analysis system would have been required to accurately quantify the H_2S mass emitted during desulfurization and was beyond the scope of this program.

Table 21. Sulfur Mass Summary for 1,300- and 1,400-Hour Desulfurizations

	NAC1 1,300 Hours	NAC1 1,400 Hours	NAC2 1,300 Hours	NAC2 1,400 Hours
SO_2 Mass, g	0.829	0.610	1.047	0.524
H_2S Mass, g	2.696	2.649	2.618	2.629
Total S Mass, g	2.952	2.797	2.987	2.747
Estimated Fuel + Oil Sulfur Mass For 100 Hours of Aging, g	5.95		5.95	
Sulfur Removal	50%	47%	50%	46%

Table 22. H_2S Mass Measured during 1,600-Hour Desulfurization

	Sample Period 1 H_2S Mass, g	Sample Period 2 H_2S Mass, g	Sample Period 3 H_2S Mass, g	Sample Period 4 H_2S Mass, g	Total Sulfur Mass Contribution from H_2S, g
NAC1	1.503	2.456	0.826	0.219	5.005
NAC2	No Data	3.134	1.378	0.525	5.037

Section 4: Results

Study results of the demonstration phase are organized around four sets of study questions. Section 4.1 addresses the initial performance of the ECS through the first 300 hours of testing, and Section 4.2 describes the performance of the desulfurization process as well as the long-term aging performance of the ECS. The interaction of sulfur with ECS performance and the potential impacts of fuel properties on tailpipe emissions are presented in Sections 4.3 and 4.4, respectively. Finally, Section 4.5 discusses some technical problems that were encountered and the remedial actions that were taken. Unregulated emissions results are presented in a separate report that incorporates findings from other APBF-DEC studies.

4.1 Initial Performance

This section describes the performance of the ECS during the initial 300 hours of aging, focusing on the initial impact of the ECS on regulated emissions and fuel economy and the impact of sulfur on a fresh ECS. The following study questions are addressed:

Q1.1 Can the system meet the 2007-2010 regulated emissions levels for NO_x, NMHC, and PM?

Q1.2 What is the impact on other regulated emissions (THC and CO) and fuel economy?

Q1.3 How does system performance change during the early life (under 300 hours) of the system?

Q1.4 Are there similar patterns for various transient duty cycles (Cold- and Hot-Start UDDS, US06, HFET)?

At the start of the demonstration phase, three pairs of engine-out emissions tests were performed, one with each of the three test fuels (i.e., D8, D15, and BP15). Each series consisted of a Cold-Start UDDS test cycle followed by a Hot-Start UDDS, USO6, and HFET. These baseline tests were performed without EGR. In addition, a single series of baseline engine-out tests was performed with EGR activated. Following the installation of a fresh ECS, a triplicate series of tests was performed using the D15 fuel. After 50 hours of aging, the system was re-evaluated. This evaluation process was repeated every 50 hours using either a duplicate or triplicate series of tests until the first desulfurization event at 200 hours. All tests with the ECS were performed with EGR activated. These tailpipe results are compared to both sets of baseline engine-out emissions in order to characterize the NO_x reduction performance of the total system (ECS + EGR) as well as the NO_x reduction efficiency of the ECS relative to engine-out emissions with comparable EGR. During each test with the ECS, the total amount of engine-out accumulated NO_x was recorded along with the total tailpipe NO_x. It was confirmed that the engine-out results were consistent with the single series of engine-out measurements taken prior to the installation of a fresh ECS at the start of the study.

Table 23 shows the average composite FTP emissions from the seven engine-out tests (six without EGR and one with EGR) and the 18 tailpipe tests conducted prior to the first desulfurization, along with 95% confidence intervals. Emission reductions are calculated

relative to engine-out with and without EGR. Note that emission reduction does not necessarily equate to NO_x conversion efficiency because the back pressure caused by the ECS affects engine-out emissions by changing the amount of EGR in use.

The reductions in NO_x, NMHC, CO, and PM emissions due to the ECS were all statistically significant, as was the reduction in fuel economy (18.7% relative to engine-out without EGR and 16.7% relative to engine-out with EGR). Tailpipe emissions for THC were significantly greater than engine-out THC emissions due to the fuel used as a reductant and use of a burner to increase the temperature of the exhaust.

Table 23. Average Engine-Out and Initial Tailpipe Composite FTP Regulated Emissions and Fuel Economy—with 95% Confidence Intervals

Emission Parameter	Unit	Engine Out			Tailpipe (0-200 Hours) w/ EGR			Regulated Emission Standard[3]
		EGR	Average[1]	95% Confidence Interval	Average[2]	95% Confidence Interval	Percent Reduction	
NO_x	g/mi	Without	4.38	(4.34, 4.42)	0.095	(0.069, 0.12)	97.8%	0.07
		With	2.12	-[4]			95.5%	
NMHC	g/mi	Without	0.198	(0.19, 0.207)	0.165	(0.145, 0.186)	16.7%	0.09
		With	no data	-			-	
THC	g/mi	Without	0.204	(0.194, 0.213)	0.463	(0.434, 0.491)	-126.9%	N/A
		With	0.264	-			-75.1%	
CO	g/mi	Without	2.02	(1.85, 2.18)	0.258	(0.215, 0.301)	87.2%	4.2
		With	4.43	-			94.2%	
PM	g/mi	Without	0.065	(0.056, 0.074)	0.005	(0.004, 0.007)	91.6%	0.01
		With	0.145	-			96.2%	
Fuel Economy	mi/gal	Without	18.4	(18.2, 18.6)	15.0	(14.8, 15.1)	18.7%	N/A
		With	18.0	-			16.7%	

[1] Engine-out average without EGR is based on 6 tests; engine-out average with EGR is based on one test.

[2] Average of 18 tests performed prior to first desulfurization at 200 hours

[3] Tier 2 Bin 5 full useful life

[4] Confidence intervals cannot be determined based on a single test; however, the values are generally consistent with the average engine-out results obtained during testing with the ECS.

N/A = Not applicable

Although the average tailpipe NO_x emissions of 0.095 g/mi were higher than the regulated emissions standard of 0.07 g/mi, the difference was not statistically significant. Nevertheless, the reduction efficiency of 97.8% relative to engine-out without EGR was encouraging. That is, even though the NO_x emissions target was not reached, the high-efficiency performance of the ECS showed promise for this technology. With more control over the engine controls and combustion process engine out emissions levels could be reduced to a level where these NOx conversion efficiencies would lead to a system that would meet the project goals. Average NMHC emissions of 0.165 g/mi were 83% higher than the applicable standard, again due to the

use of the diesel fuel burner. It is anticipated that a production system with finer thermal management control and lower engine-out NO_x will not experience this problem. Average PM emissions were 50% lower than the applicable standard, well within the project's emissions target.

Figure 63 shows the average FTP composite NO_x emissions and reduction efficiency relative to engine-out emissions without EGR during the first 300 hours of aging. The error bars on the emissions plot indicate the range of values observed among the duplicate or triplicate measurements. Prior to the first desulfurization there was no particular trend in tailpipe emissions; however, a trend is evident between 200 hours and 300 hours. Performance improved significantly following the desulfurization at 300 hours. This is discussed more fully in Section 4.2.

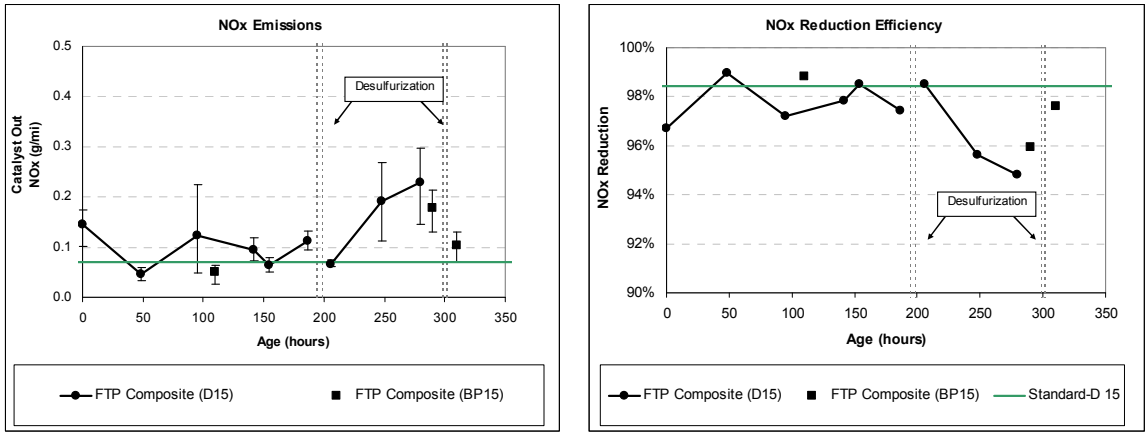

Figure 63. NO_x Composite FTP emissions and reduction efficiency during the first 300 hours of aging

Figure 64 displays the average NO_x emissions and reduction efficiency relative to engine-out without EGR for each of the four test cycles. Generally there are similar patterns among the four test cycles; however, the US06 emissions are consistently higher. Strong evidence that NO_x emissions from the US06 and HFET tests were increasing prior to the first desulfurization event at 200 hours was also observed. This is likely due to the fact that the catalyst used during the aging portion of the testing were not de-greened, and their performance had not stabilized at this early point in the aging process.

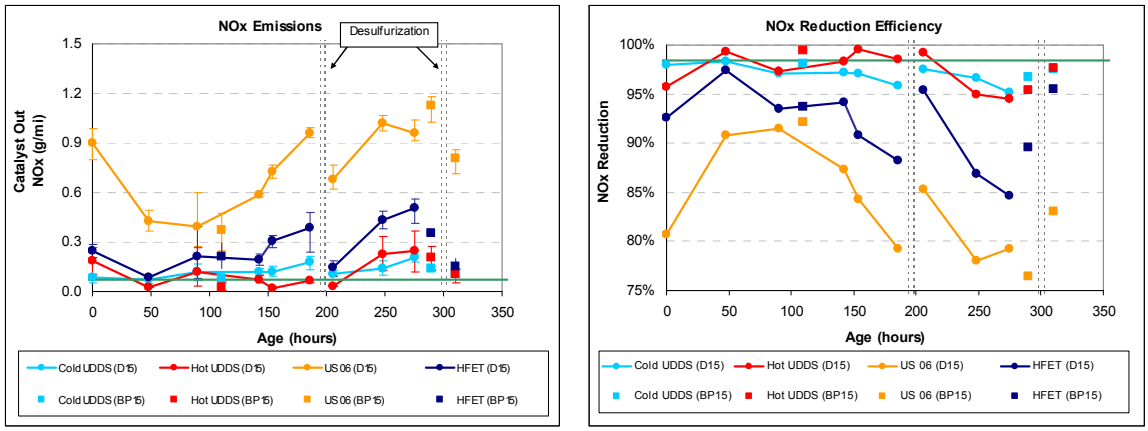

Figure 64. NO_x emissions and NO_x reduction efficiency during the Cold-Start UDDS, Hot-Start UDDS, US06, and HFET test cycles over the first 300 hours of aging

Figure 65 shows the average FTP composite emissions of NMHC, CO, and PM, and fuel economy during the first 300 hours of aging. Except for a slight increase in CO after 100 hours, there were no significant trends. Also, the desulfurization events at 200 and 300 hours had no impact on these emissions or fuel economy.

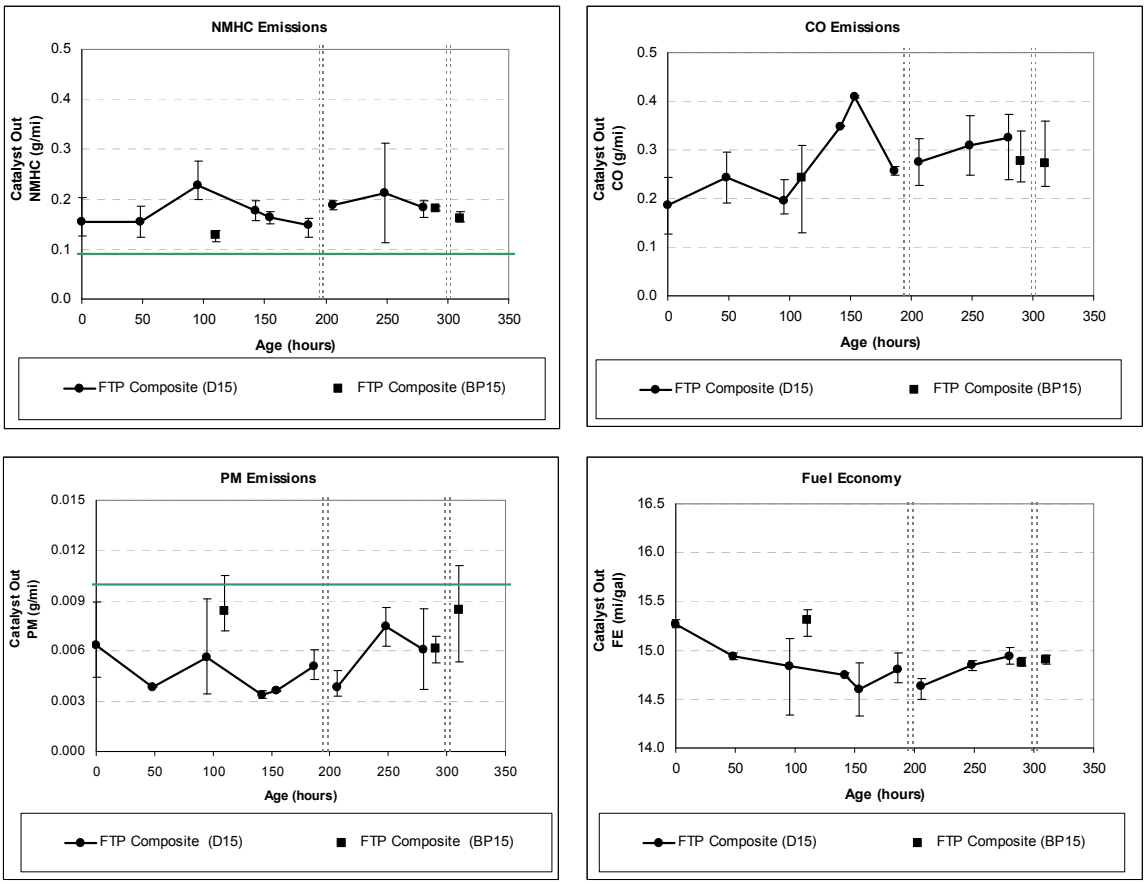

Figure 65. Composite FTP emissions of NMHC, CO, and PM and fuel economy during the first 300 hours of aging

4.2 Aging and Desulfurization (300 to 2,000-hours)

This section addresses the impact of 2,000-hours of aging and sulfur accumulation on ECS performance and the effectiveness of periodic desulfurizations for restoring NO_x reduction performance. The long-term impact on regulated emissions and fuel economy are also described. The following study questions are addressed:

Q2.1 How do NO_x emissions change as the system ages? Specifically, how do the maximum (pre-desulfurization), minimum (post-desulfurization), and average NO_x levels change?

Q2.2 Is the increase in NO_x emissions between consecutive desulfurizations constant over time?

Q2.3 How effective is desulfurization at restoring the initial NO_x reduction performance of the system (initially and over time)?

Q2.4 Does the performance of the system stabilize within the first 2,000-hours? If so, at what point does this occur?

Q2.5 Are there temporal trends with respect to other regulated emissions or fuel economy?

The durability portion of the study was conducted using the D15 fuel during aging, as well as for the evaluations performed immediately before and after the desulfurization events. These events were scheduled every 100 hours. Each evaluation consisted of a duplicate or triplicate series of motoring dynamometer engine tests, each emulating a Cold-Start UDDS followed by Hot-Start UDDS, US06, and HFET duty cycles.

4.2.1 Average NO_x Emissions and Reduction Efficiency over 2,000-hours

The results are summarized in Figure 66. The upper graph shows the average NO_x FTP composite emissions for each evaluation. The vertical lines identify the desulfurization events, and the error bars denote the minimum and maximum measurements within each evaluation period. The lower graph displays the same results in terms of NO_x reduction efficiency relative to engine-out emissions both with and without EGR. The Tier 2 Bin 5 NO_x emissions standard of 0.07 g/mi corresponds to a target NO_x reduction efficiency of 98.4% relative to engine-out without EGR and 96.7% relative to engine-out with EGR.

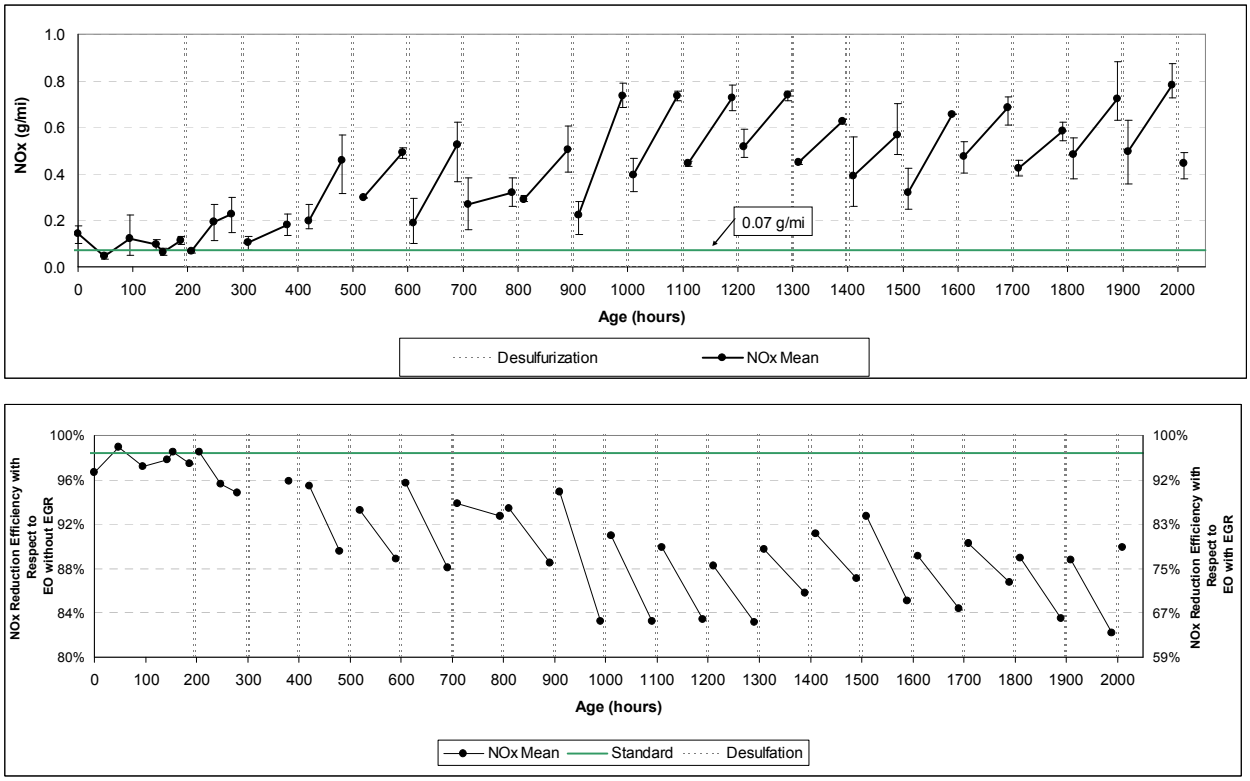

Figure 66. NO_x emissions (FTP composite) and NO_x reduction efficiency versus ECS age (vertical lines identify desulfurization events)

These plots show that NO_x reduction efficiency decreases during the first 1,000 hours of aging. Initially the reduction efficiency relative to engine-out without EGR is relatively steady at 98%; however, by 1,000 hours the efficiency ranges from 84% immediately before the desulfurization event to about 90% immediately after the event.

4.2.2 Performance Degradation and Desulfurization Effectiveness

Figure 67 illustrates the degradation in catalyst performance between desulfurizations and the effectiveness of the desulfurization process at restoring performance. The upper graph demonstrates that the loss in NO_x reduction efficiency (FTP composite) between desulfurizations is generally about 6% of the engine-out without EGR emissions, with a slight trend ranging between 4% and 6%. The lower graph demonstrates that there is also a 6% improvement in NO_x reduction efficiency at each desulfurization event, with a slight trend ranging between 3% and 6%. Although these trend lines, based on log-linear models, show slight changes in NO_x reduction efficiency, the slopes of the regression lines were not statistically different from zero. Combined, these graphs indicate that the desulfurization process generally compensates for the increased degradation in catalyst performance between desulfurizations throughout the 2,000-hour test. Nevertheless, the cumulative effect of the initial 1% change between desulfurizations was found to be significant as is shown in the following analysis.

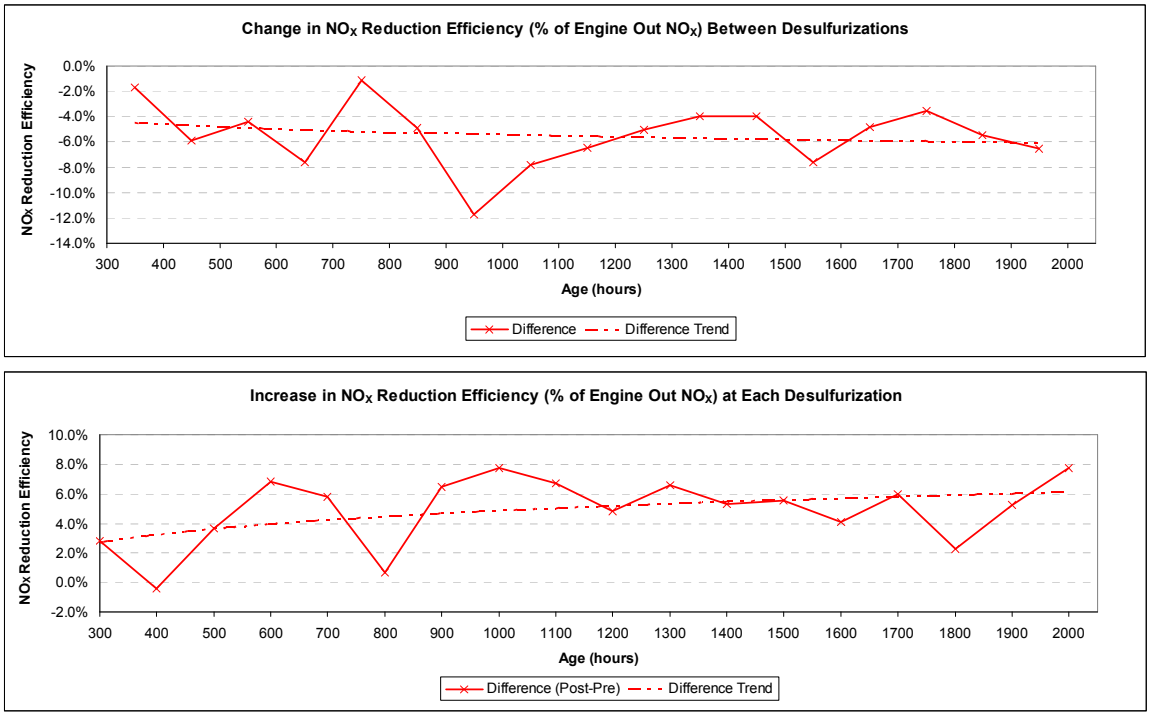

Figure 67. Effectiveness at desulfurization and deterioration of the catalyst between desulfurizations for FTP composite NO_x emissions compared to aging hours (Trends for these were not statistically significant.)

The overall trends in FTP composite NO_x emissions between 300 and 2,000 hours of aging were also modeled using a log-linear model, as shown in the upper graph in Figure 68. To account for

the effects of the desulfurization process, separate models were fit to three sets of NO_x emissions data: (1) measurements made before a desulfurization event, (2) measurements made after a desulfurization event, and (3) the average of measurements made at the beginning (post-desulfurization) and end (pre-desulfurization) of each 100-hour aging period. The latter results, plotted at the midpoint of the aging period, represent the best estimate of the average emissions over time; however, we could not verify that the increase in NO_x emissions within an aging period is linear. The lower graph in Figure 68 shows the same trends in terms of NO_x reduction efficiency relative to engine-out with and without EGR. All three of the regression lines shown in Figure 68 were found to have statistically significant trends at the 95% confidence level.

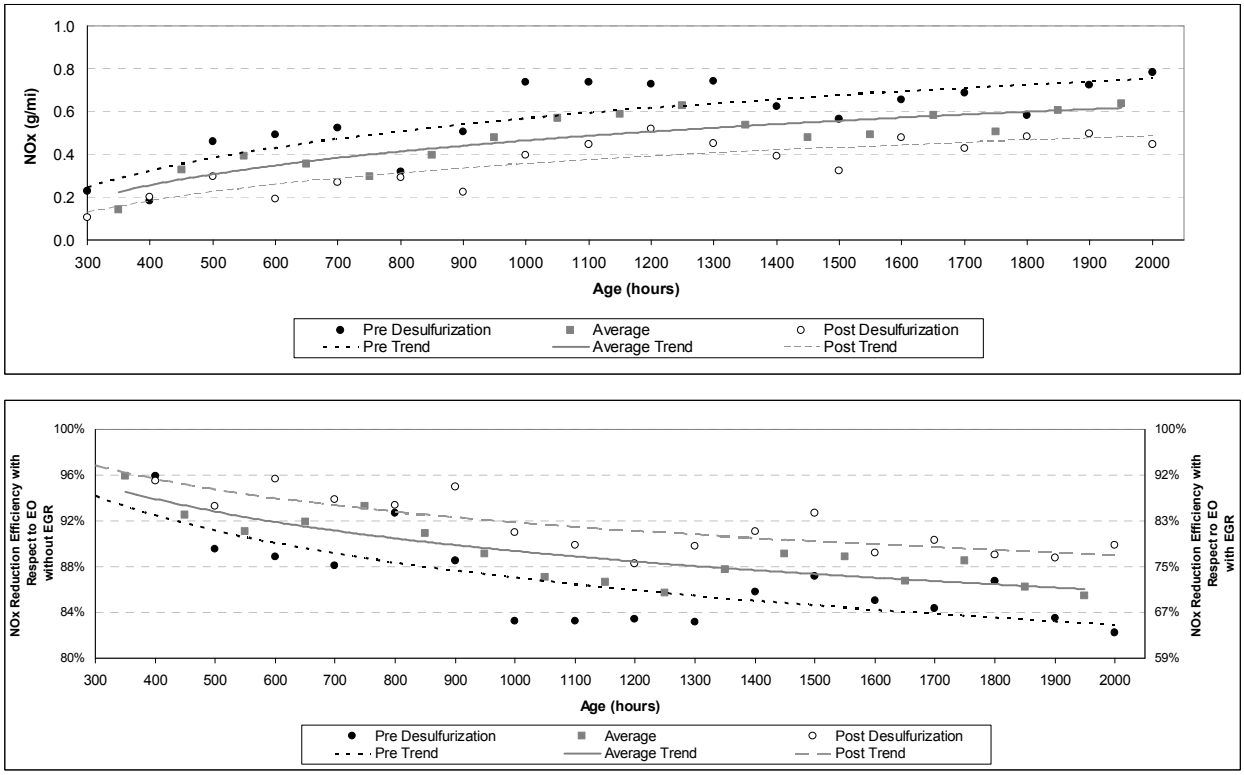

Figure 68. NO_x emissions (FTP composite) and NO_x reduction efficiency (FTP composite) versus ECS age with statistical trend lines: pre-desulfurization, post-desulfurization, and average results

4.2.3 Determination of System Stabilization

Additional analyses were performed to determine if there were persistent trends in emissions results over time. As illustrated in Figure 69, this analysis was accomplished by iteratively truncating the left-most data from each of the three data sets, refitting the regression model, and evaluating the significance of the regression slope parameter. This analysis determined that the trends are not statistically significant after 800 to 900 hours of aging.

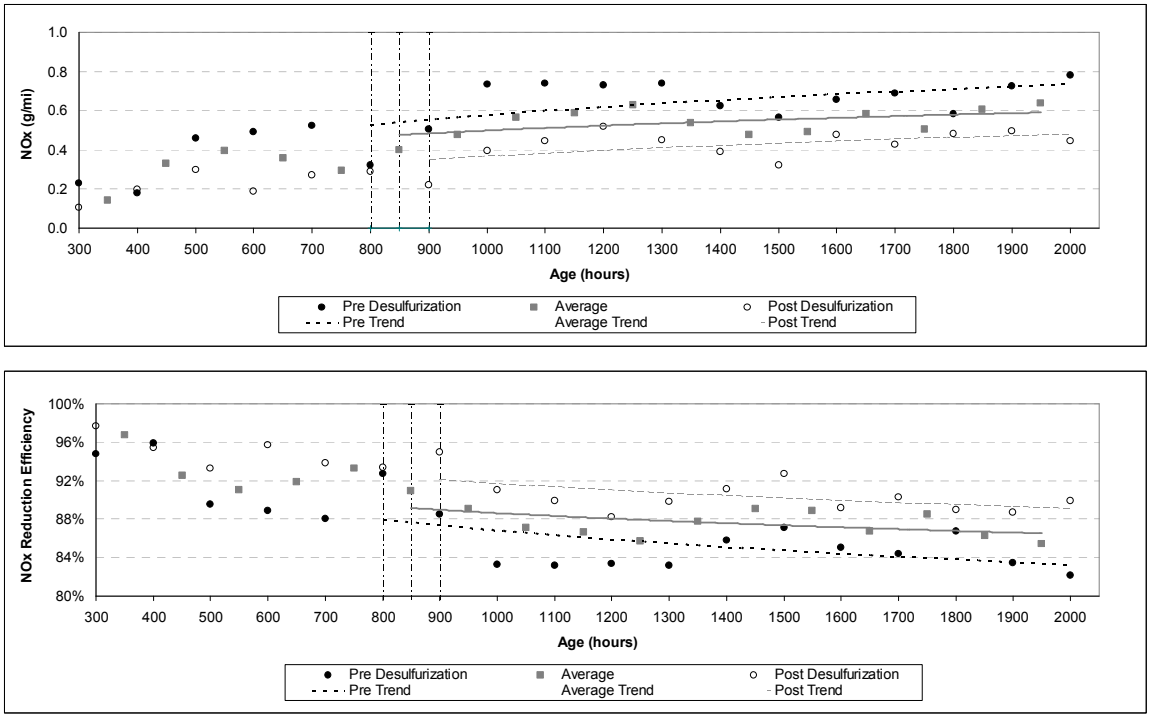

Figure 69. Statistical trends in FTP composite NO_x emissions and NO_x conversion at pre-desulfurization, post-desulfurization, and midpoint between desulfurizations are not statistically significant after 800, 900, and 850 hours, respectively

4.2.4 Trends in Other Regulated Emissions and Fuel Economy

Figures 70 to 74 display the trends in the other average FTP composite regulated emissions of NMHC; percent NMHC in THC, CO, and PM; and fuel economy for each data set versus time. There were some anomalies in the data. For example, at 700 hours, there was a spike in NMHC pre- and post-desulfurization measurements; between 700 and 800 hours, CO was relatively elevated and FE was relatively low; and between 1,100 and 1,200 hours, CO was relatively low. Despite these anomalies, the fitted curves representing average emissions or fuel economy at the beginning, midpoint, and end of each 100-hour aging period are virtually identical, indicating that sulfur accumulation on the catalyst has no effect on these emissions. Using the same iterative approach described above, we found that there are statistically significant trends in NMHC and CO emissions through 1,400 hours; but there are no trends in PM emissions. Percent NMHC and fuel economy increase steadily through about 1,100 hours.

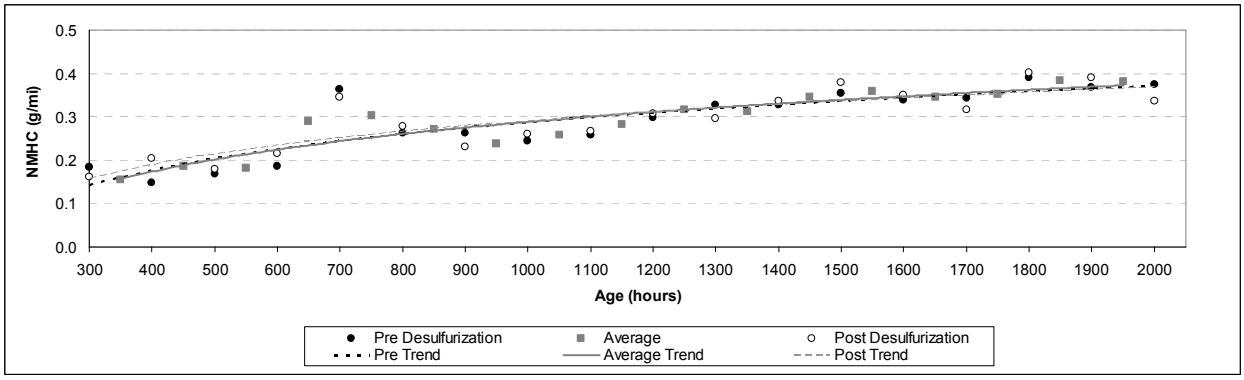

Figure 70. FTP composite NMHC emissions compared to aging hours: pre-Desulfurization, post-desulfurization, and average results (Trend is statistically significant through 1,400 Hours.)

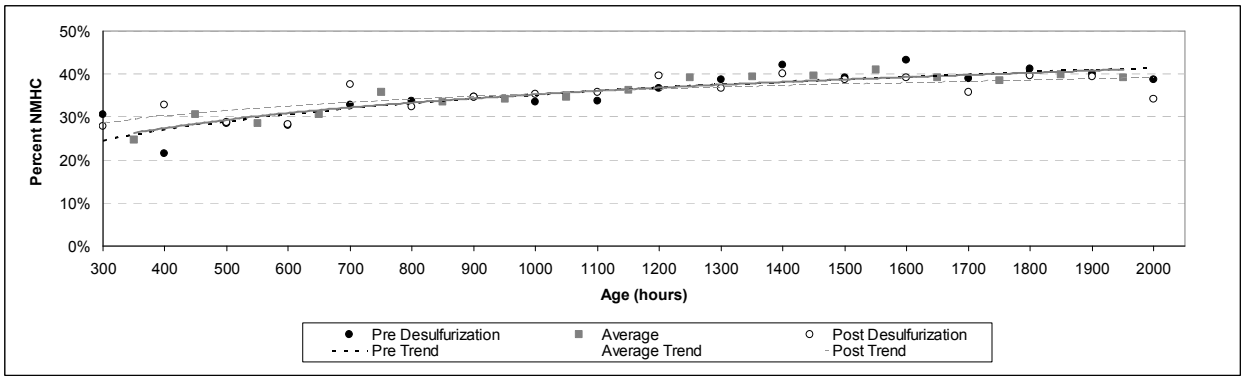

Figure 71. FTP composite percent NMHC emissions compared to aging hours: pre-desulfurization, post-desulfurization, and average results (Trend is not statistically significant after 1,100 hours.)

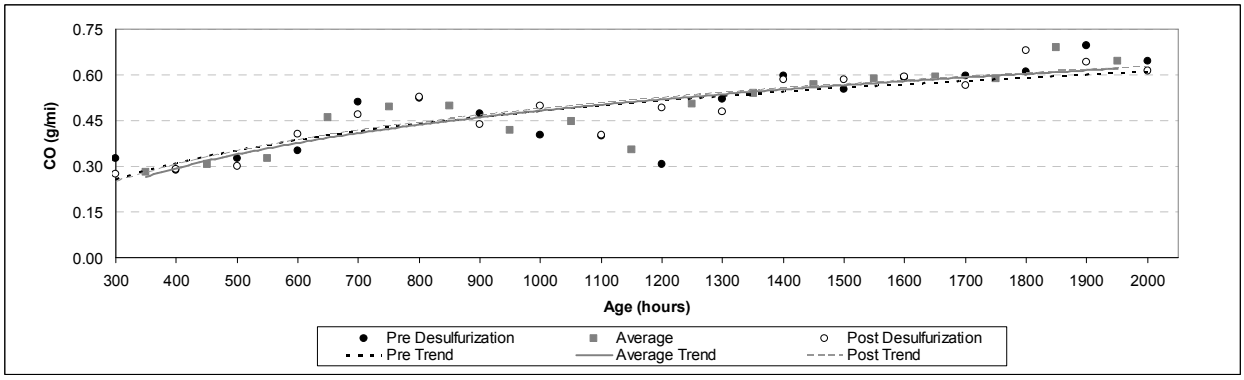

Figure 72. FTP composite CO emissions compared to aging hours: pre-desulfurization, post-desulfurization, and average results (Trend is statistically significant through 1400 hours.)

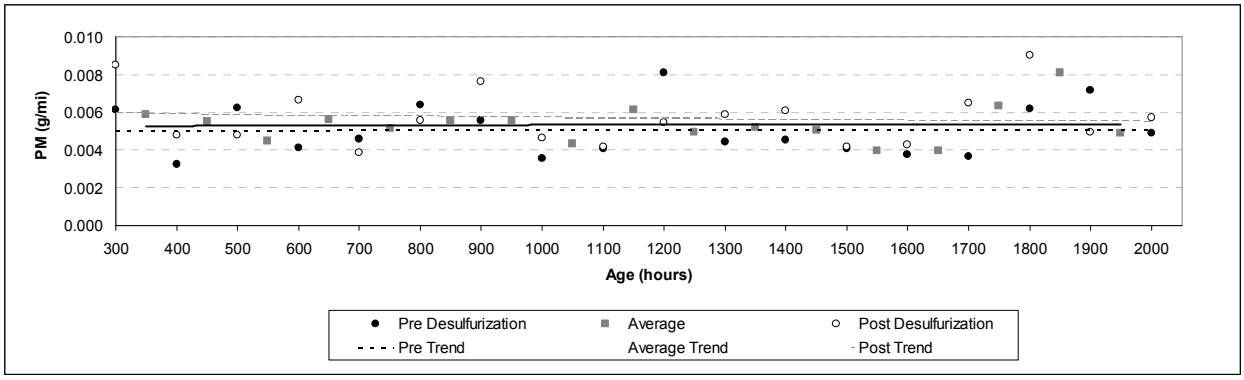

Figure 73. FTP composite PM emissions compared to aging hours: pre-desulfurization, post-desulfurization, and average results (Trend is not statistically significant.)

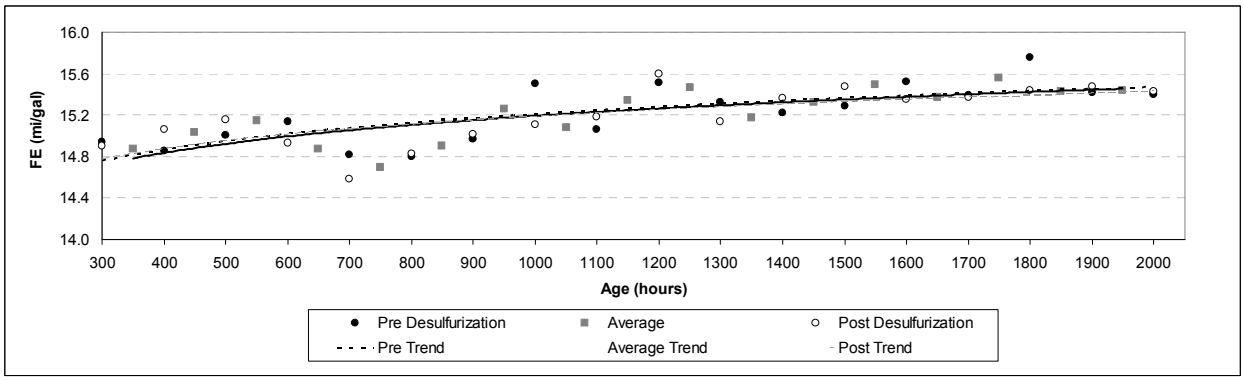

Figure 74. FTP composite FE compared to aging hours: pre-desulfurization, post-desulfurization, and average results (Trend is statistically significant through 1100 hours.)

Table 24 compares the average composite FTP emissions from the seven engine-out tests (six without EGR and one with EGR) with the estimated FTP composite emissions measured at 1950 hours. The 1,950-hour estimates were based on the regression model derived from the measurements taken between 350 and 1,950 hours. For each estimate, 95% confidence intervals are provided. As before, emission reductions were calculated relative to engine-out with and without EGR. The reductions in NO_x, CO, and PM emissions due to the ECS were all statistically significant, as was the reduction in fuel economy (16.0% relative to engine-out without EGR and 13.9% relative to engine-out with EGR).

Table 24. Average Engine-Out and Estimated 1,950-Hour Average Tailpipe Composite FTP Regulated Emissions and Fuel Economy—with 95% Confidence Intervals

Emission Parameter	Unit	Engine Out			Tailpipe Average (1950 Hours) w/ EGR			Regulated Emission Standard[3]
		EGR	Average[1]	95% Confidence Interval	Average[2]	95% Confidence Interval	Percent Reduction	
NO_X	g/mi	Without	4.38	(4.34, 4.42)	0.616	(0.558, 0.675)	85.9%	0.07
		With	2.12	-[4]			70.9%	
NMHC	g/mi	Without	0.20	(0.19, 0.207)	0.372	(0.349, 0.395)	-87.6%	0.09
		With	no data	-			-	
THC	g/mi	Without	0.20	(0.194, 0.213)	0.730	(0.695, 0.764)	-257.8%	N/A
		With	0.26	-			-176.2%	
CO	g/mi	Without	2.02	(1.85, 2.18)	0.620	(0.571, 0.669)	69.3%	4.2
		With	4.43	-			86.0%	
PM	g/mi	Without	0.07	(0.056, 0.074)	0.005	(0.005, 0.006)	91.8%	0.01
		With	0.15	-			96.3%	
Fuel Economy	mi/gal	Without	18.40	(18.2, 18.6)	15.453	(15.312, 15.594)	16.0%	N/A
		With	17.95	-			13.9%	

1 Engine-out average without EGR is based on 6 tests; engine-out average with EGR is based on 1 test.

2 Estimates based on the regression model derived from measurements taken between 350 and 1,950 hours.

3 Tier 2 Bin 5 full useful life

4 Confidence intervals cannot be determined based on a single test; however, the values are generally consistent with the average engine-out results obtained during testing with the ECS.

N/A = Not applicable

4.2.5 Soluble Organic Fraction and Sulfate Emissions

Figure 75 displays the average emissions of sulfate measured in PM samples collected at the beginning and end of alternate 100-hour aging cycles. Results are presented for each of the four test cycles (Cold-Start UDDS, Hot-Start UDDS, US06, and HFET) as well as the calculated FTP composite. The average emissions of sulfate are fairly consistent across the four transient cycles; however, there appears to be an increasing trend in Composite FTP sulfate emissions starting at approximately 1,400 hours. The apparent decrease in sulfate measurements between 400 and 900 hours is due to measurements at or below the detection limits due to high background levels during this period. Over the whole program, the sulfate emissions only account for about 1% of the total PM mass, which were all below 0.10 g/mi. The apparent upward trend in sulfate emissions in the 1,500- to 2,000-hour range, while not significant, may be due to the release of a small amount stored sulfur in the catalysts.

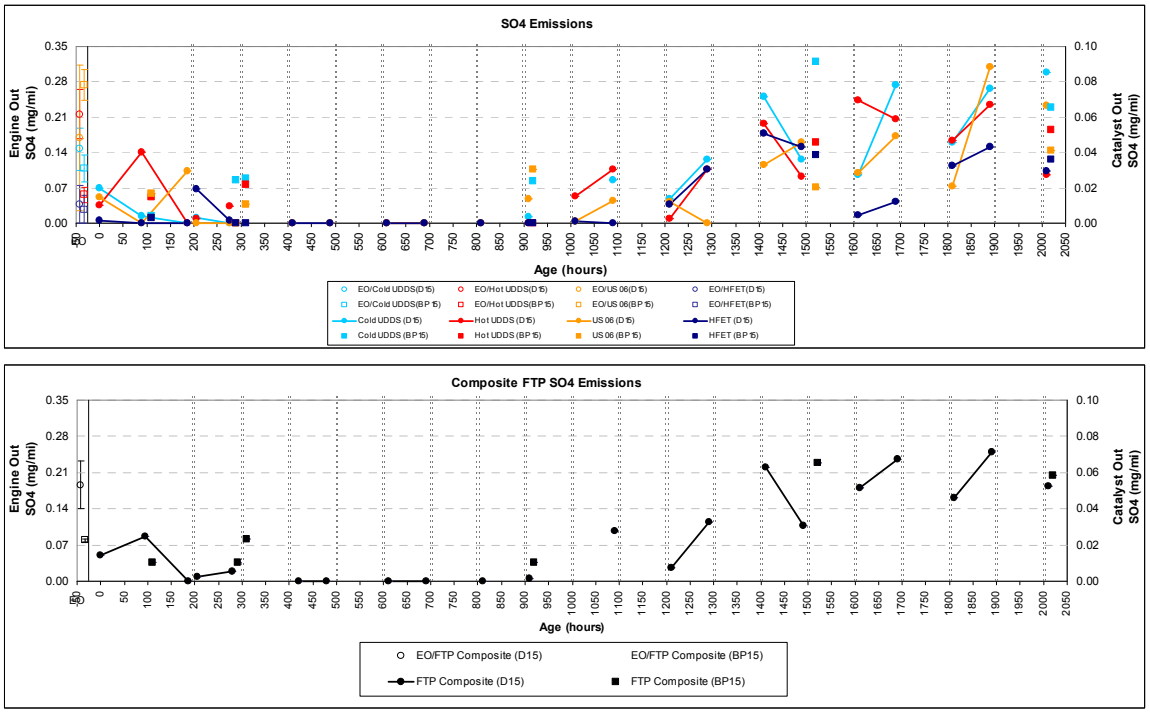

Figure 75. Sulfate emissions (Cold-Start UDDS, Hot-Start UDDS, US06, HFET, and FTP composite) versus ECS age (vertical lines identify desulfurization events)

Figure 76 displays the average percentage of SOF emissions measured in PM samples collected at the beginning and end of alternate 100-hour aging cycles. Results are presented for each of the four test cycles (Cold-Start UDDS, Hot-Start UDDS, US06, and HFET) as well as the calculated FTP composite mode. Average emissions of SOF are fairly consistent across the four transient cycles, and the average emissions of Composite FTP SOF are fairly consistent at approximately 80% after the desulfurization at 400 hours.

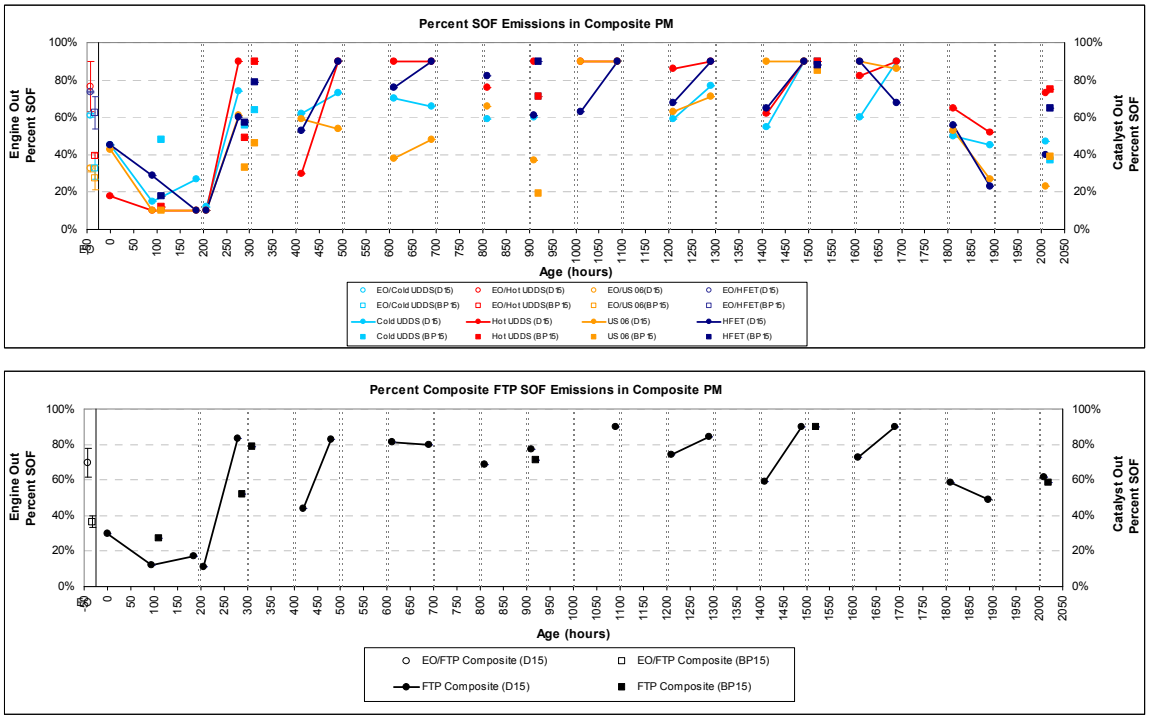

Figure 76. Percent SOF emissions (Cold-Start UDDS, Hot-Start UDDS, US06, HFET, and FTP composite) versus ECS age (Vertical lines identify desulfurization events.)

4.3 Sulfur Mass Balance

Understanding the mechanisms by which sulfur from the fuel and lubricants interacts with the ECS is important for designing an effective and durable system. This section presents a mass balance approach to gain insight on the disposition of sulfur in the system. The following study questions are addressed:

Q3.1 How much sulfur is emitted during the desulfurization process?

Q3.2 How does the amount of sulfur emitted during the aging cycle compare to the amount emitted during the desulfurization process? Do these rates change over time?

Q3.3 What happens to the differences between these amounts?

Although there were no plans to routinely monitor sulfur emissions during aging or desulfurization events, special tests were performed periodically to measure the mass of SO_2 and H_2S emitted during desulfurization events. These results were used to estimate total sulfur accumulation on the catalysts for comparison with estimated engine-out emissions based on measured fuel and oil consumption.

As described in Section 3.3, measurements of SO_2 and H_2S were made during the desulfurization events at 1,300 and 1,400 hours. The SO_2 measurements are believed to be accurate; however, it was suspected that a significant portion of the H_2S emissions was not captured. Therefore, the

sampling method for H_2S was modified before it was used again during the 1,600-hour desulfurization event.

The calculations summarized in Table 25 demonstrate that nearly all of the sulfur emitted during the 100-hour aging cycle, as estimated by measured fuel and oil properties and consumption rates, is accounted for by the measured emissions of SO_2 and H_2S.

Table 25. Sulfur Mass Balance between Engine-Out and Desulfurization Emissions

	Measured Sulfur Mass from Desulfurization Events (g)			Estimated Sulfur Mass from Engine-Out Emissions (g/100 hrs)			
Catalyst	Average SO_2 (note 1)	Average H_2S (note 2)	Total Sulfur	Sulfur from Oil[3]	Sulfur from Fuel[4]	Total Sulfur	Percent Recovery
NAC1	0.720	5.004	5.068	1.008	5.025	6.033	84%
NAC2	0.786	7.199	7.167	1.008	5.025	6.033	119%
Total	1.506	12.203	12.235	2.016	10.05	12.066	101%

1 Average SO_2 measured during 1,300- and 1,400-hour desulfurizations using measurement methods described in Section 2.2.3

2 Average H_2S measured during 1,600-hour desulfurization using modified methods (See Section 3.3.)

3 Oil consumption = 0.0035 liter/hr. Oil density = 0/9kg/liter. Sulfur concentration = 6,400 ppm. Assumes equal exposure to the two catalysts.

4 Fuel consumption = 6.7 kg/hr. Sulfur concentration = 15 ppm. Assumes equal exposure to the two catalysts.

Tailpipe emissions of SO_2 and H_2S were not routinely measured, except as part of the unregulated emissions tests performed at 100, 300, 900, 1,500, and 2,000-hours. H_2S levels were consistently below the detection limits of the analytical method. SO_2 levels were measured at less than 0.5 mg/mi, which corresponds to less than 0.025 grams of sulfur per 100 miles. This is consistent with achieving an estimated 100% recovery of sulfur from the desulfurization events.

4.4 Fuel Effects on Regulated Emissions (D15 vs. BP15)

Two different ultra-low-sulfur diesel fuels, ranging from 3 ppm to 30 ppm, were tested. This section investigates whether the fuels or fuel sulfur levels have direct impacts on regulated emissions or fuel economy. The following study questions are addressed:

Q4.1 Are there differences in emissions from DECSE and BP fuels?

Q4.2 If such differences exist, are they consistent over time?

Analysis of variance models were used to compare the two test fuels in terms of the average emissions of NO_x, hydrocarbon, PM, and fuel economy. The model was used to calculate average emissions for each combination of fuel type, aging time, and test cycle (Cold-Start UDDS, Hot-Start UDDS, US06, and HFET). A 95% confidence interval was computed for each estimate in order to assess the differences between the fuels.

Figure 77 displays the average NO_x emissions with BP15 and D15 fuels at 100, 300, 900, 1,500, and 2,000 hours of testing under the FTP composite, Cold-Start UDDS, Hot-Start UDDS, US06, and HFET test cycles. The error bars represent 95% confidence bounds on the estimated average emissions. Statistical tests were performed to determine if the differences in average emissions at various combinations of test cycles and aging times were statistically significant. While there were a few instances in which the differences were statistically significant, there was no consistent pattern over time. Similar comparisons were performed on the PM and NMHC emissions and fuel economy. Again, there were no consistent patterns in the differences in emissions or fuel economy between tests run on the two fuels.

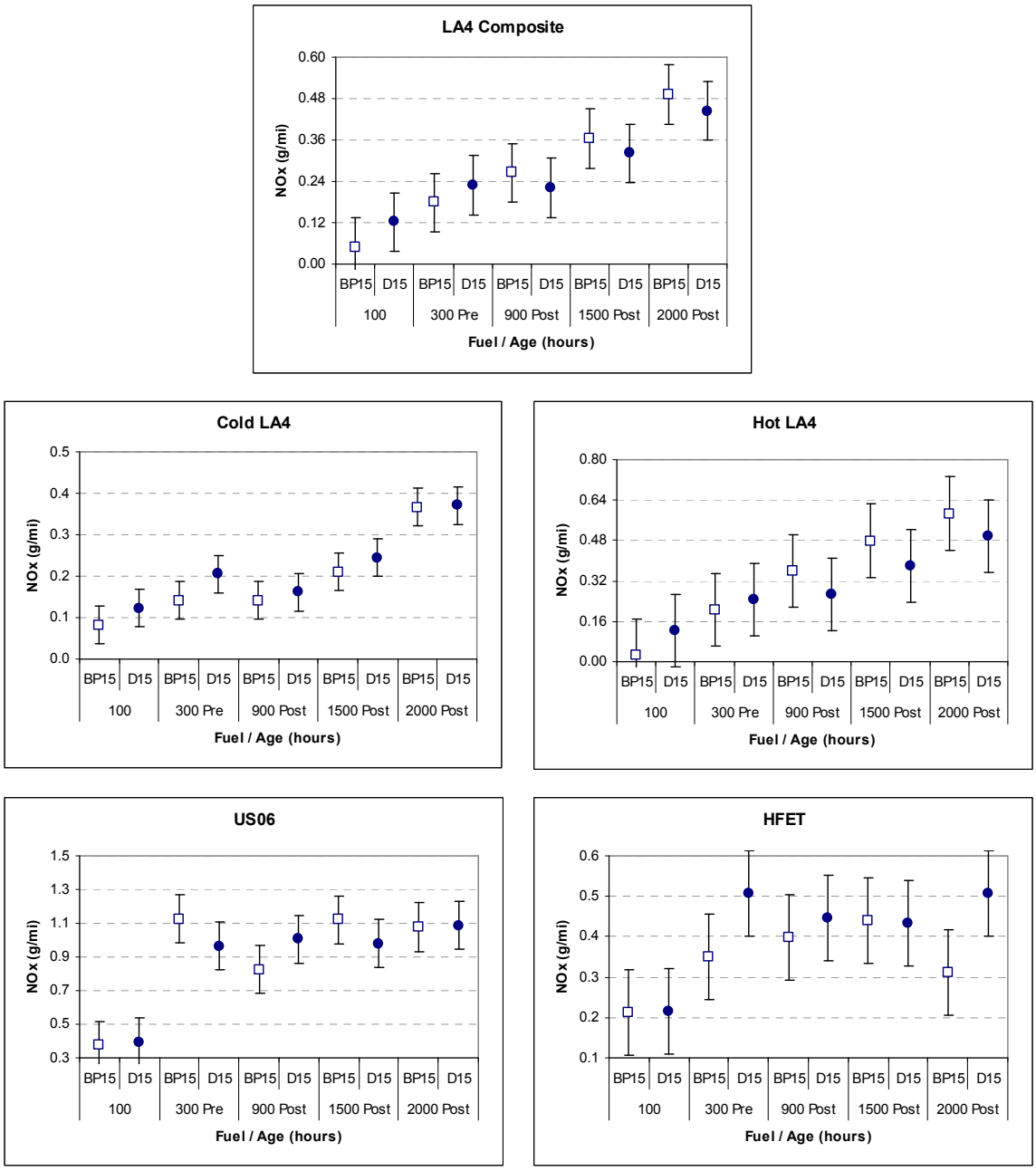

Figure 77. Average NO_x emissions with 95% confidence intervals by fuel type and ECS age

4.5 Discussion of Technical Problems and Remedial Actions

A number of different problems arose during the course of the program. Some of the main problems encountered and the solutions devised are discussed below. In addition, some proposed modifications for improved performance of the design/strategy utilized are also discussed.

4.5.1 Second-Generation Emission Control System Components

The initial system evaluated (first-generation System B shown in Figure 78) utilized relatively small-diameter (14.4-cm diameter, 7.6-cm length), high precious metal content oxidation catalysts mounted upstream of each NAC and upstream of the DPF (15.2-cm length). The intent for these catalysts was to break down the diesel fuel used as a reductant into smaller (more NAC friendly) hydrocarbons and CO. The oxidation catalyst upstream of the DPF was intended to minimize any hydrocarbon slip resulting from "overfueling" during regeneration.

Due to the high level of NO_x reduction required to meet the program goal, it was anticipated that overfueling would be needed to ensure maximum NO_x reduction under all possible regeneration conditions. While the small diameter (14.4-cm) pre-NAC oxidation catalysts produced high levels of CO upon in-exhaust injection (greater than 3% into the NAC), they caused unacceptably high engine exhaust back pressure during high-load conditions due to their small frontal area. As a result, the designated ECS supplier provided new oxidation catalysts (identical loading, but 24.1-cm in diameter and 7.6-cm length) which were delivered in late June 2003. Figure 79 shows the second-generation System B utilizing the new components.

The new oxidation catalysts resulted in a significant volume increase (3.8 times), adding additional thermal mass upstream of the NACs. As all strategy development/optimization had been performed on the first-generation system, the additional volume and mass of the second-generation, pre-NAC oxidation catalysts introduced a number of issues related to the ECS performance.

Due to the increased pre-NAC oxidation catalyst mass, substantially more heat was required from the burner to quickly bring the ECS to operating temperature following a cold start. This requirement led to increased THC emissions from the burner as it was being operated at its upper-functional limit. The EGR calibration was also modified at idle conditions in an effort to transfer more heat to the pre-NAC oxidation catalysts through increased exhaust mass flow.

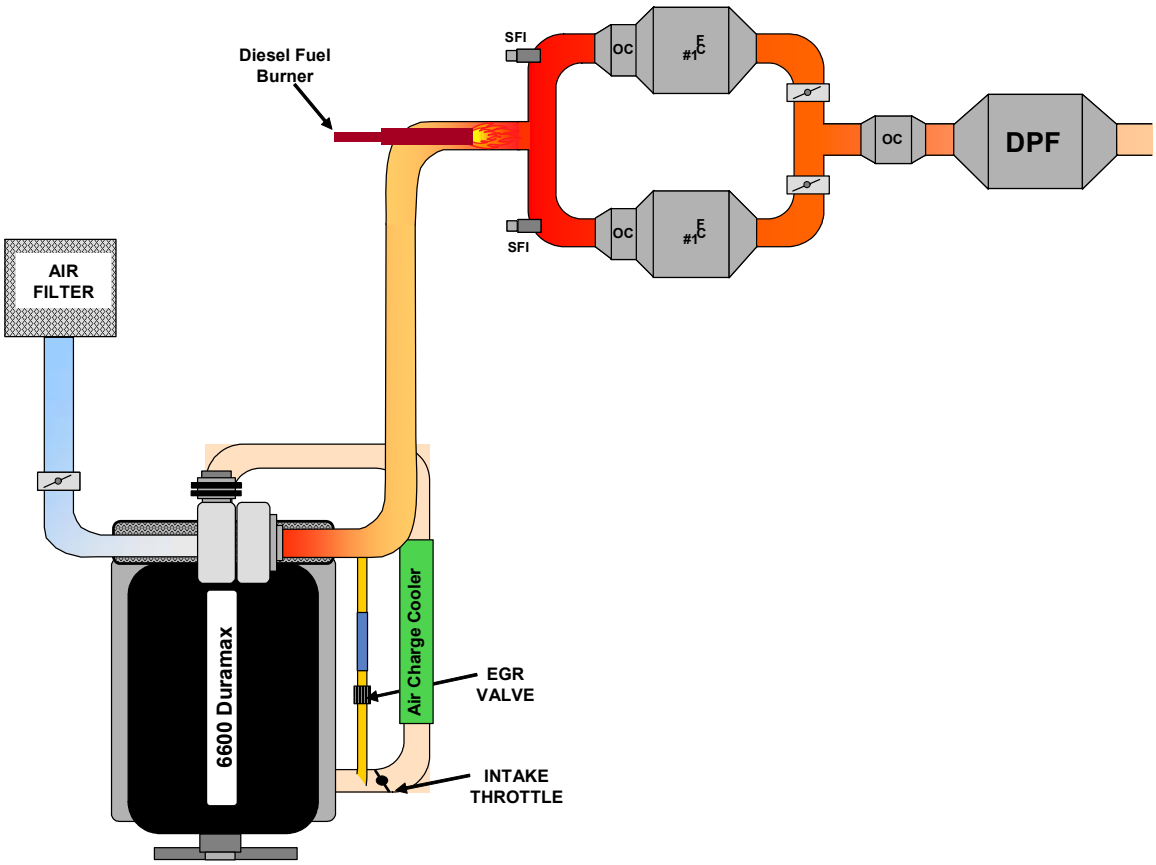

Figure 78. First-generation System B

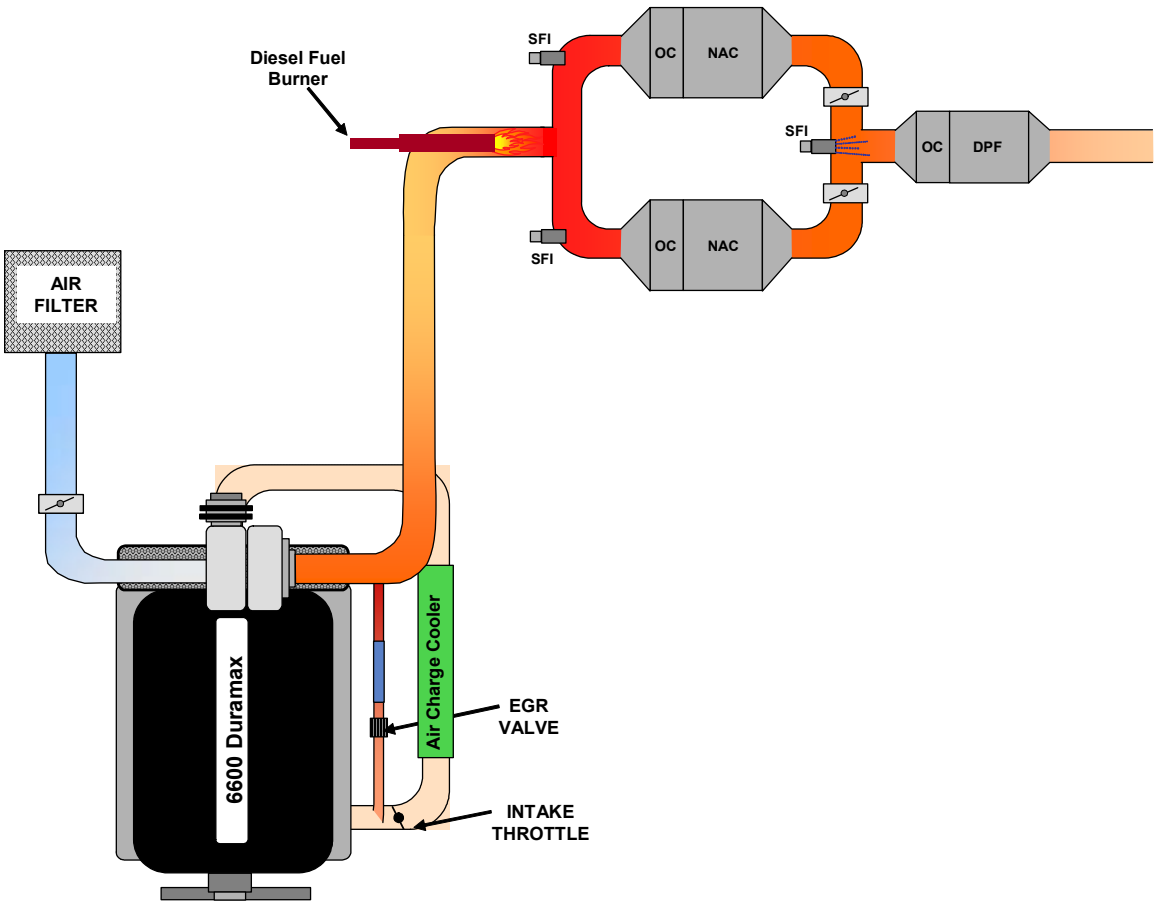

Figure 79. Second-generation System B

During warmed-up, transient operation, the second-generation system exhibited higher levels of NO_x reduction than the first-generation system; however, during the aging portion of the cycle, plugging of the oxidation catalysts was observed, as shown in Figure 80. As this phenomenon was not observed with the first-generation system, it appeared that the combination of increased thermal mass and reduced space velocity due to the larger pre-NAC oxidation catalysts had an undesirable effect.

The cause for the plugging was theorized to result from low temperatures at the edge of the catalyst when fuel was injected during regeneration. At low-load, low-temperature exhaust conditions (i.e., idle), if a regeneration was initiated (preceded by burner preheating), insufficient heat was transferred to the periphery of the pre-NAC oxidation catalyst, resulting in an interaction between the raw fuel and PM present in the exhaust, causing a carbonaceous buildup on the face of the catalyst. After this buildup or face plugging began, it continued growing inward, even if the catalyst was brought to temperatures in excess of 600°C during the aging cycle.

In an attempt to minimize or eliminate the face plugging, the order of the aging cycle modes was modified prior to the 500-hour aging block to eliminate extended periods at low exhaust temperature (i.e., idle followed by low-load, low-speed conditions). In addition, the burner

preheating time was slightly increased in an attempt to raise the pre-NAC bed temperature. Using a combination of these approaches, the face plugging was reduced, but not completely eliminated. Face plugging of the pre-NAC oxidation catalyst continued to be a problem throughout the program, specifically in Leg 2, which required cleaning approximately every 50 hours. The pre-NAC oxidation catalyst in Leg 1 was cleaned as a precautionary measure every 100 hours, even though it typically showed minimal plugging/edge discoloration after this duration.

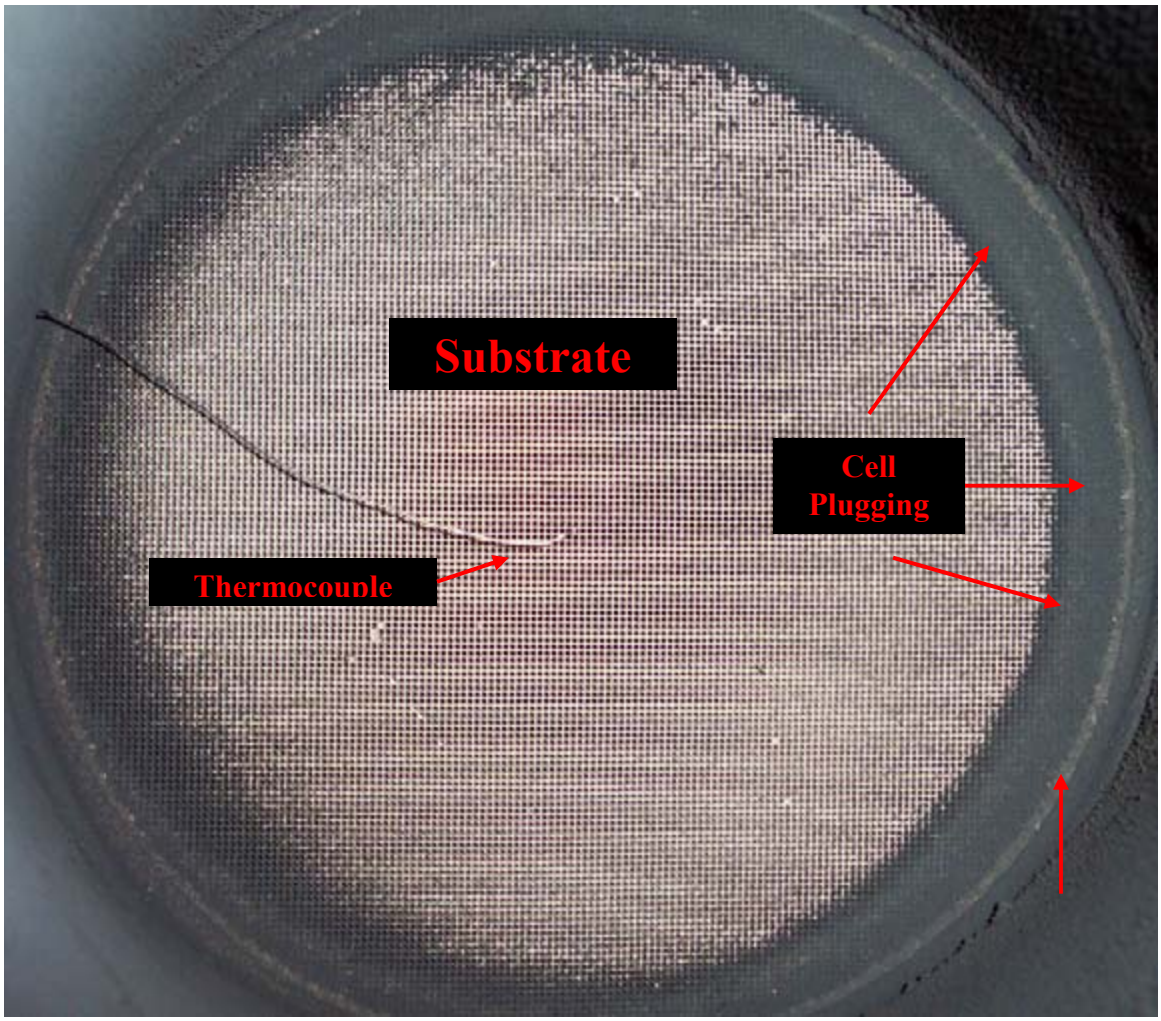

Figure 80. Face plugging of pre-NAC oxidation catalyst

In addition to the pre-NAC oxidation catalyst face plugging observed with the second-generation components, the DPF was no longer passively regenerating during the aging cycle. The exact cause of this problem was unknown; however, the increased efficiency of the second-generation, pre-NAC oxidation catalysts and NACs may have contributed to this problem, significantly reducing the amount of NO/NO_2 available for PM oxidation in the DPF. A third in-exhaust

injector was added to the system to ensure continuous regeneration of the DPF by raising its operating temperature. As this problem arose fairly late in the program, no optimization of the DPF regeneration fuel usage was performed. Sufficient fuel was provided to ensure that the DPF reached at least 625°C during the steady-state portion of the aging cycle. This third, in-exhaust injector was utilized only during the aging cycle and increased fuel consumption by approximately 8% (the fuel used by this injector was not included when calculating the total fuel sulfur exposure of the NACs during aging). This injector was activated for approximately 1 second out of every 7 seconds during the aging cycle (14% duty cycle).

The new, larger pre-NAC oxidation catalysts also required increased burner run time prior to a burner-assisted regeneration in order to raise the temperature of the larger thermal mass. This change led to occasional high-temperature spikes (850°C) in the pre-NAC oxidation catalysts when the exhaust flow rate was suddenly lowered during a regeneration preheating cycle (e.g., deceleration to an idle period). Upon the next increase in exhaust flow (i.e., acceleration), the temperature "wave" within the pre-NAC oxidation catalyst was passed on to the NAC (albeit with a reduced peak temperature typically no greater than 550°C), often resulting in thermal desorption of NO_2 from the NAC.

4.5.2 Diesel-Fueled Burner

The diesel-fueled burner described earlier was a laboratory-built unit fabricated within the limited time frame of this program. As a laboratory prototype the unit experienced multiple failures during the 2,000-hour aging portion of the program. A maintenance schedule was developed in order to minimize burner system component failure and its subsequent effect on the system performance.

The electrodes were found to be the weakest component of the burner and were replaced after every 100-hour aging block, regardless of whether or not they exhibited cracking. Cracked electrodes led to burner misfires, which, if they occurred during an emission test, invalidated the test (and required repeating the entire prep sequence). Thus, the electrodes were replaced prior to beginning a sequence of emission tests after aging.

The silicon carbide foam used as a flame holder also exhibited poor durability related to the mounting system. As a result, the foam was only used during the emission tests and removed for aging. The fuel injector in the burner also required periodic cleaning (approximately every 500 hours of operation) to maintain its spray pattern.

The fuel pumps used to supply the necessary 470kPa of pressure to the burner and in-exhaust injectors suffered failures after 1,000 to 1,200 hours of total run time. These failures led to no fuel being injected during regeneration, in the case of the in-exhaust injectors, or complete misfires of the burner, resulting in no additional heat being added to the system.

The current-to-pressure regulator used for controlling the airflow to the burner failed due to the presence of water in the air system between the 1,000-hour, pre- and post-desulfurization evaluations. This failure led to intermittently reduced burner airflow that resulted in "dirty" burner operation and intermittent misfires.

4.5.3 In-Exhaust Injectors

The water-cooled, in-exhaust injectors also exhibited durability problems during the aging portion of the program. PM would collect on the tip of the injector, resulting in poor fuel distribution. The tips of the injectors were cleaned after every 100-hour aging block as part of routine maintenance.

There appeared to be some cross talk between the two exhaust legs during a regeneration (i.e., fuel injected into the regenerating leg would also be observed in the opposite leg). Placing the exhaust flow control valves upstream of the in-exhaust injection probably would have eliminated this problem. However, the durability of the valves in this position would have been questionable.

4.5.4 Exhaust System and Flow Maldistribution

The prototype, hand-fabricated, air-gap exhaust manifolds failed after 800 hours of aging, causing damage to the turbocharger, necessitating a replacement. As no air-gap manifold replacements were readily available, the stock, cast iron exhaust manifolds were reinstalled. As the diesel-fueled burner supplied the majority of temperature to the ECS for the configuration utilized, no significant change in ECS performance was observed due to this change.

The dual-leg exhaust configuration had an inherent flow distribution problem. As the exhaust from the engine encountered the burner flow stream orthogonally, the exhaust mass flow rate affected the burner distribution to the two exhaust legs. At low engine exhaust flow rates, the burner output was relatively well distributed to the two exhaust legs. However, at higher engine exhaust flow rates, the burner flow stream would be "converted" towards Leg 1, affecting the temperature and oxygen concentration in each leg prior to a burner-assisted regeneration. A total redesign and fabrication of the exhaust system would have been required to eliminate this issue. In order to minimize the effect of this maldistribution, the DOC/NAC combination was switched from one leg to the other every 100 hours of aging.

The wiring for the exhaust valve position switch (used as feedback to the control system) was broken during one of the many NAC system position swaps (affecting the 148-hour emission evaluations). In an attempt to minimize fuel penalty during regeneration, this system was used to time the in-exhaust injection to avoid injecting fuel into the regenerating leg prior to the exhaust valve closing. A timer safety had been incorporated in the regeneration controller, so that if no valve closure signal was received 2 seconds after the valve closure command was issued, fuel was injected into the leg to be regenerated. No significant change in ECS performance was observed for the tests in which the valve position switch was inoperable.

4.5.5 Particle Sampling

Due to the extremely low levels of PM measured after the DPF, it was decided to sample multiple runs (two or three, depending on test matrix) of a particular test cycle (i.e., Cold-Start UDDS, Hot-Start UDDS, etc.) on a single 90-mm filter. While this approach doubled or tripled the mass collected on a single filter, it also introduced sample handling errors resulting from installing and removing the filter itself from the holder assembly multiple times.

4.5.6 Engine-Related Components

The stock EGR valve failed after 700 hours, most likely due to excessive temperatures found after the EGR cooler caused by the high levels of EGR demanded by the new calibration. The EGR cooler was cleaned when the EGR valve was replaced as a precautionary measure. A larger EGR cooler probably would have prevented the EGR valve failure. However, due to packaging constraints, a larger cooler was not installed.

4.5.7 Test Cell Equipment

The direct-current electric dynamometer used for simulating the vehicle load in the testing suffered an armature failure, necessitating replacement prior to the 248-hour emission evaluations. The replacement dynamometer was unable to perform at the same level, requiring modification to the control cycle and resulting in engine speeds higher than commanded during the high-load transient portion of the US06 cycle.

4.5.8 Emission Control System Components/Regeneration Control System Performance

As the ECS aged, the pre-NAC oxidation catalysts appeared to require higher operating temperatures to effectively break down the injected fuel needed for regeneration and to maintain their NO to NO_2 reduction efficiency. However, at the same time, the NACs appeared to become more sensitive to higher temperatures after aging, thermally desorbing NO_2 at temperatures above 450°C.

Throughout the emission evaluations performed in this program, a large variation in test-to-test repeatability was observed. This variation became more pronounced as the aging progressed. . An analysis of the second-by-second data revealed that a large portion of this variability was attributable to differences in the timing of regenerations for a particular test cycle. As the NO_x mass model target for regeneration is a "floating" variable (based on accumulated NO_x mass upper and lower limits and operating mode), regeneration can occur at different times during a particular test cycle due to small differences in accelerator pedal position. In addition, the regeneration controller has a floating NO_x mass target for regeneration, which is affected by mode type.

As an example, the lower NO_x mass limit for regeneration initiation is increased by 0.3 grams if the mode is identified as hard acceleration. The purpose of this strategy was to delay regeneration during less favorable modes (e.g., hard acceleration) and encourage it during more desirable modes (e.g., cruise). If the NO_x mass model accumulation passed the 1.5-gram lower limit threshold, and the mode was "cruise," regeneration would be initiated. However, if the mode was designated as "acceleration" or "hard acceleration" during this transition past 1.5 grams of accumulated NO_x, the regeneration would be delayed until the upper limit of the NO_x mass window was reached, or the operating mode changed to one more favorable for regeneration (e.g., cruise).

If a regeneration typically occurred immediately before a deceleration/idle period, a small change in engine operation could result in this particular regeneration being delayed until the next acceleration event. This change in timing could then affect the timing of subsequent regenerations. The efficiency of a particular regeneration is linked to the engine operating condition at the time the regeneration event is initiated. A change in the timing of a particular regeneration event could result in different exhaust flow rates, temperatures, and exhaust composition at the initiation of regeneration. All of these factors affect the efficiency of the regeneration event. In addition, a single incomplete regeneration could impact all subsequent regenerations as the NAC would not necessarily be at the same condition (level of loading) when the next regeneration was initiated. These factors all affected the test-to-test repeatability.

An example of a difference in regeneration timing is shown for three repeat Hot-Start UDDS tests conducted after 1,500 hours of aging. In this case, Runs 1 and 2 had the first regeneration of the cycle occur for Leg 2 while the third test had its first regeneration occur on Leg 1. This resulted in significantly different regeneration timing for the three repeat tests with a subsequent impact in system NO_x reduction efficiency. Figure 81 shows the NO_x mass model accumulation for Leg 1 for the three repeat tests. In this figure, it can be seen that the "reset" of accumulated NO_x mass (corresponding to a regeneration) for the third run occurred approximately 75 seconds into the cycle, while for Runs 1 and 2 the first regeneration for Leg 1 occurred approximately 115 seconds after engine-start. This difference resulted in the Leg 1 regenerations for Run 3 being "out of phase" with the regenerations for Runs 1 and 2, as shown in Figure 81. The resultant accumulated tailpipe NO_x for the three "repeat" tests is shown in Figure 82. From this figure it can be seen that this difference in regeneration timing had a significant impact on the NO_x reduction efficiency of the system. The timing of regenerations for Run 3 was obviously less favorable and resulted in higher tailpipe NO_x mass.

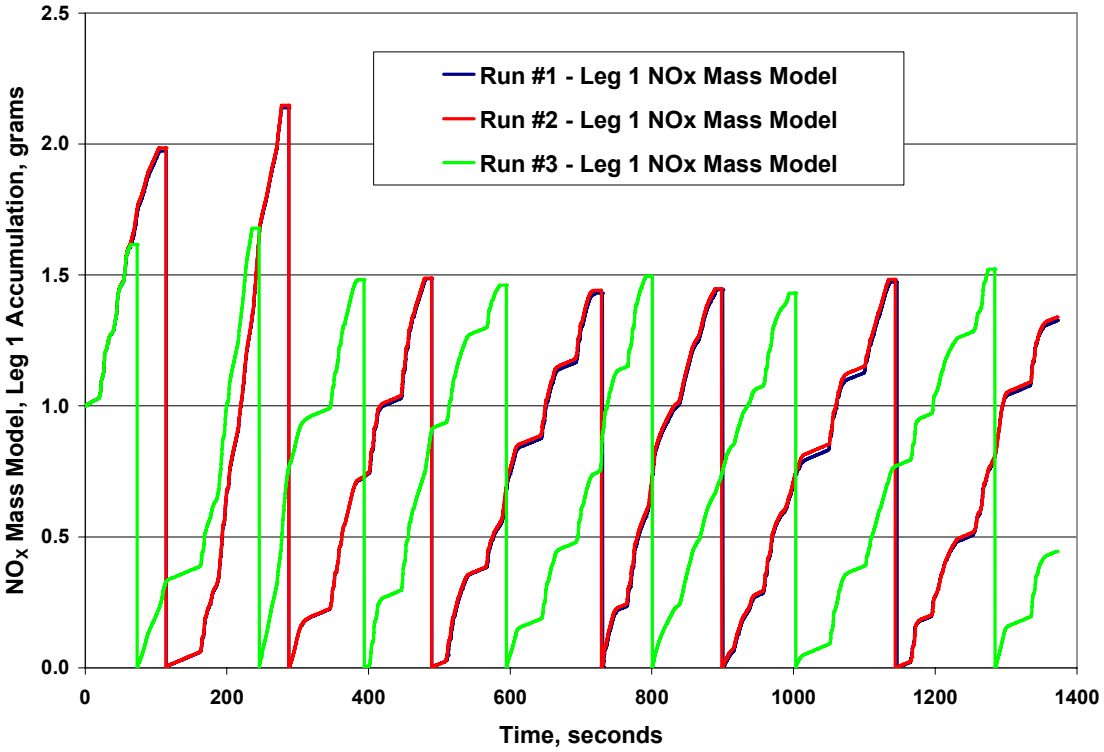

Figure 81. NO_x mass model accumulation for Leg 1 over Hot-Start UDDS

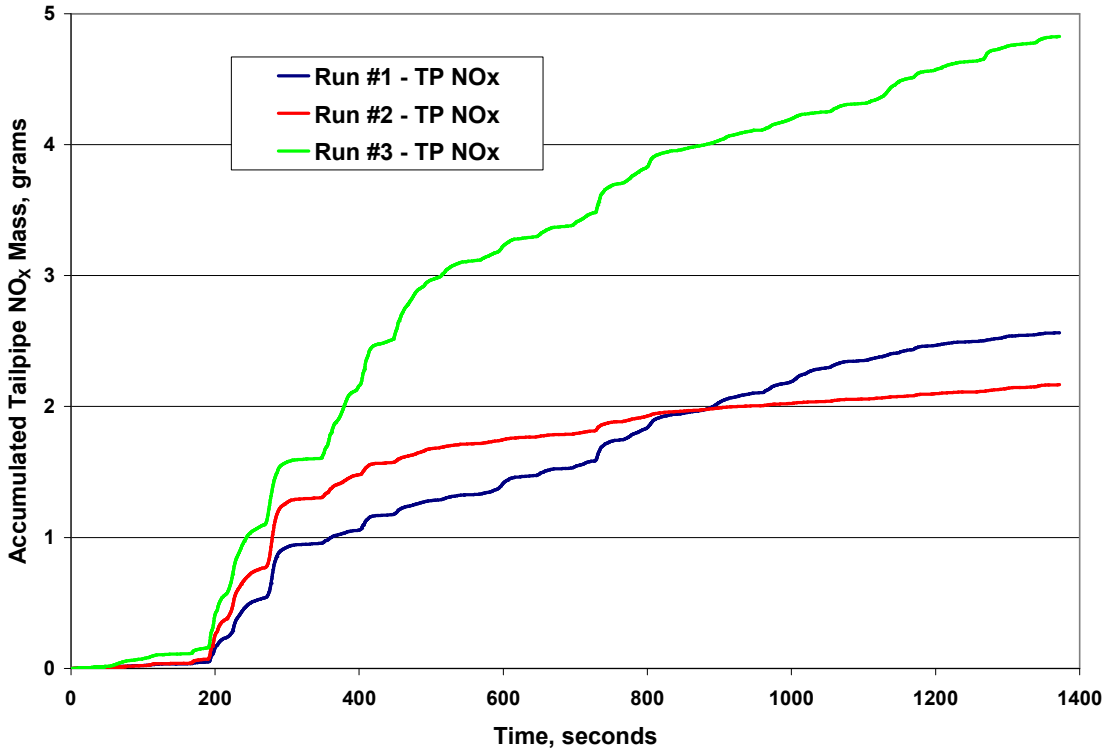

Figure 82. Accumulated tailpipe NO_x mass for three repeat runs after 1,500 hours of aging (post-desulfurization) for Hot-Start UDDS

4.5.9 Possible Improvements to Emission Control System/Exhaust Configuration

The extremely high levels of NO_x reduction required to meet the program goals (99% over the FTP), and the low exhaust temperature (average of less than 165°C at the catalyst inlet location over the FTP), resulted in many system design constraints and requirements. The need for a fully functional ECS within seconds after engine-start required an auxiliary heating device (diesel-fueled burner) and the placement of this device immediately upstream of the NACs. In order to make use of the heat generated by the diesel-fueled burner, it was decided to place the DPF after the NACs. However, in this configuration the DPF did not assist in NO to NO_2 conversion, placing this burden on the pre-NAC oxidation catalysts and the NACs themselves. In addition, there was minimal NO_2 available to the DPF for passive PM reduction due to the high level of NO_x reduction required by the upstream NACs.

An improved system design may have been to move the DPF upstream of the NACs and burner (as shown in Figure 83), utilizing in-cylinder post injection to provide heat to the DPF when needed for regeneration. This placement would allow the DPF to assist in NO to NO_2 conversion, allow passive regeneration at a lower temperature due to the increased NO_2/PM ratio, and perhaps most importantly, act as a thermal capacitor. In the System B configuration, the pre-NAC oxidation catalysts and NACs themselves were subjected to large swings in exhaust temperature. This required activating the burner more frequently in order to ensure that the

oxidation catalysts would be sufficiently active to break down the fuel injected during a regeneration. Placing the large DPF upstream of these components would significantly dampen these temperature fluctuations, helping maintain the oxidation catalysts and NACs at a more uniform temperature; however, the burner would still be required to rapidly heat the NACs to operating temperature after a cold start.

For the test cell evaluations, the NOx mass model introduced significant variability from test to test due to its real-time determination of the need for regeneration. A fixed regeneration strategy versus time may have produced more repeatable results; however, this approach would essentially lock in the regeneration strategy for a given test cycle, being unrepresentative of actual in-use need. While the "cycle-beater" approach was advocated by some due to its more research-oriented perspective, the more production-like approach described was favored by the bulk of the steering committee.

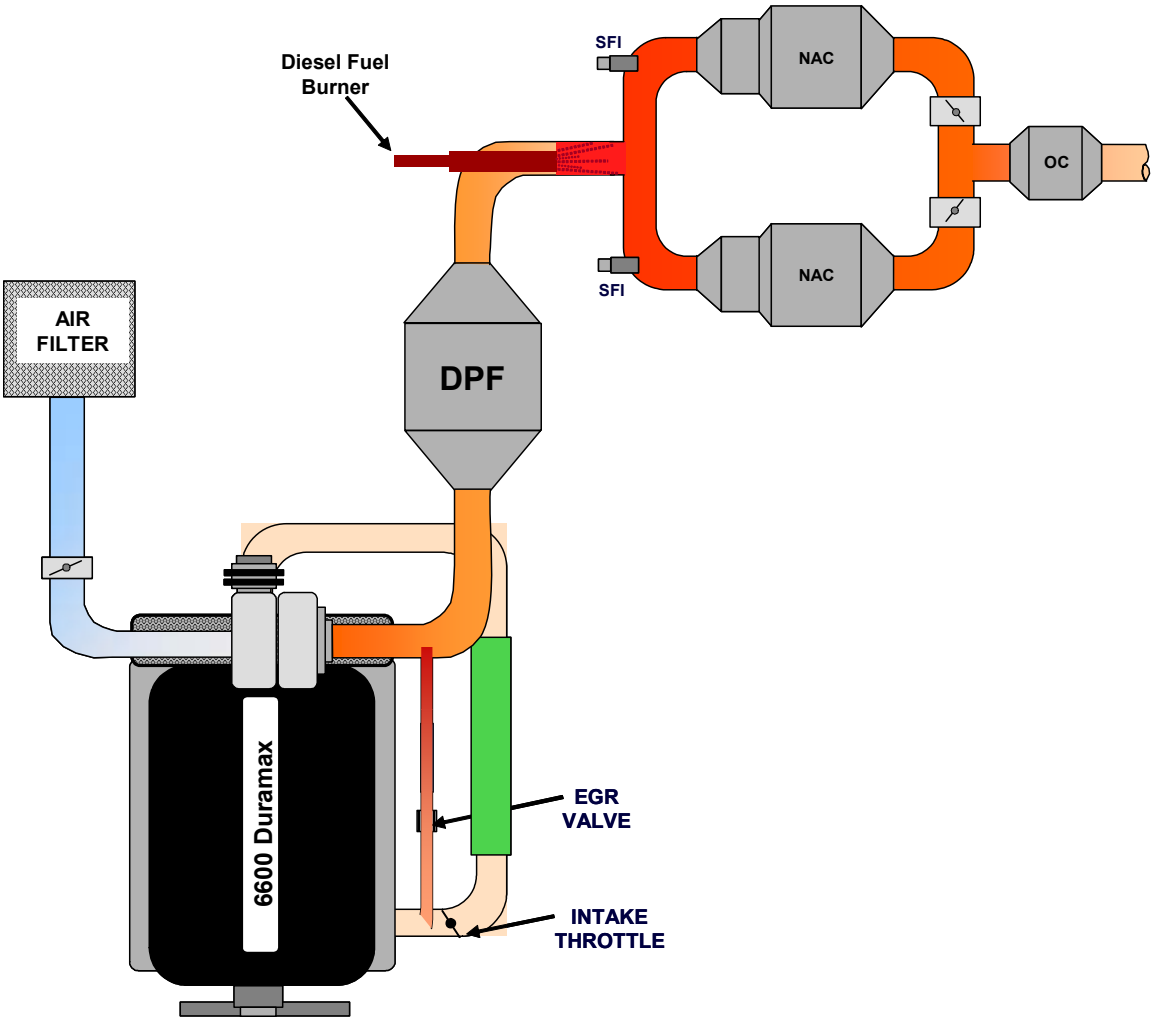

Figure 83. Possible improved system design configuration

Section 5: Conclusions

The goal of this project was to demonstrate the ability of an NAC/DPF ECS to meet Tier 2–Bin 5 standards with FTP transient test limits of 0.07 g/mi NO_x and 0.01 g/mi PM in an SUV/pick-up truck vehicle platform without producing unreasonably high emissions during other modes of operation. Additionally, hydrocarbon and CO emissions standards had to be met while minimizing impacts on fuel economy.

The test was performed for 2,000-hours with evaluations performed before and after desulfurizations that were performed every 100 hours. The majority of the testing was performed with 15-ppm sulfur fuel developed for the DECSE program. Additionally, an 8-ppm sulfur fuel was evaluated. Unregulated emissions tests were performed; however, these results are to be presented in a separate report that incorporates findings from other APBF-DEC projects.

Objectives

The objectives of this project are to

1. Demonstrate the emissions potential of advanced fuels, engines, and ECSs for meeting federal Tier 2–Bin 5 emissions standards
2. Evaluate the effect of fuel sulfur level on emissions and fuel economy, ECS performance, and catalyst degradation.

The federal standards, being implemented between 2004 and 2009, are as follows: PM of 0.01 g/mi, NO_x of 0.07 g/mi, and NMHC of 0.09 g/mi. These standards are to be met when testing over the FTP-75 test cycle at a full useful life of 120,000 miles.

The following is a summary of the significant conclusions from the study. Further details are provided in Section 4 of the report.

Initial Performance

- During the first 200 hours of testing, tailpipe emissions of NO_x averaged 0.095 g/mi (+/- 0.026 g/mi with 95% confidence) using the FTP composite test cycle. Although higher than the regulated emissions limit of 0.07 g/mi, the estimated NO_x emissions were 97.8% lower than engine-out emissions without EGR and 95.5% lower than engine-out emissions with EGR. Figure 63 presents the NO_x emissions and reduction efficiency results during the first 300 hours of testing.
- The ECS reductions in NO_x (97.8%), CO (87.2%), and PM (91.6%) emissions were statistically significant, as was the reduction in fuel economy (18.7%). The 16.7% decrease in NMHC emissions (from 0.198 to 0.165 g/mi) was also statistically significant. Initial tailpipe emissions of CO and PM were below the regulated limits; however, the engine-out and tailpipe emissions of NMHC were above the Tier 2–Bin 5 limit of 0.09 g/mi. These test results are shown in Figure 65.

Aging and Desulfurization

- The loss in NO_x reduction efficiency of the catalysts between consecutive desulfurization events increased slightly from 4% to 6% throughout the 2,000-hour test. However, the desulfurization process was effective at restoring catalyst performance. The desulfurization process produced an improvement in NO_x reduction efficiency that changed from 3% at the beginning of the test to 6% at end of the 2,000-hour test.
- Although there was a decrease in NO_x reduction efficiency during the early aging periods, Figure 69 illustrates that the increase in NO_x emissions—or decrease in NO_x reduction efficiency—was not statistically significant after approximately 850 hours of testing.
- There were statistically significant increases in NMHC and CO emissions, and fuel consumption during the 2,000-hour test; but there was no significant change in PM emissions. Table 24 compares the initial estimated engine-out regulated emissions and fuel economy (with and without EGR) with the estimated tailpipe emissions at 1,950 hours—midway between the last two desulfurization events. The system achieved emissions reduction efficiencies of 85.9% for NO_x, 69.3% for CO, and 91.8% for PM. Fuel economy decreased by 16%, and NMHC emissions increased by 87.6% partially due to the use of the diesel fuel burner and the diesel fuel used as a reductant for catalyst regeneration.
- A comparison of measured sulfur emissions with the amount of sulfur contained in the fuel and lubricant demonstrated that nearly all of the sulfur accumulated on the catalysts was effectively removed during the desulfurization process.

Fuel Effects on Regulated Emissions

- There were no consistent significant differences in the emissions from tests conducted with the DECSE and BP fuels.

Unregulated Emissions

- Unregulated emissions results are presented in a separate report.

Future Work

The results of this work have identified a number of areas worthy of additional study. These include further evaluation of the NAC desulfurization process analyzing both deterioration mechanisms and the composition of the liberated sulfur compounds, and the evaluation of other fuel formulations on the performance of emission control devices (e.g., the impact of biodiesel blends on NACs and DPFs). One specific area of research is related to the impact of biodiesel blends on DPF regeneration temperature.

References

Dzubay, T.G.; Nelson, R.O. (1975) "Self Absorption Corrections for X-Ray Fluorescence Analysis of Aerosols." Pickles, W.L. et al. ed. *Advances in X-Ray Analysis*. New York, NY: Plenum Publishing Corp. Vol. 18. p. 619.

Diesel Emissions Control – Sulfur Effects Project (DECSE) Summary of Reports (February 2002). U.S. Department of Energy. NREL/TP-540-31600. Golden, CO: National Renewable Energy Laboratory. Available at: http://www.nrel.gov/docs/fy02osti/31600.pdf

Siegl, W.O.; Richert, J.F.O.; Jensen, T.E.; Schuetzle, D.; Swarin, S.J.; Loo, J.F.; Prostak, A.; Nagy, D.; Schlenker, A.N. (1993) "Improved Emissions Speciation Methodology for Phase II of the Auto/Oil Air Quality Improvement Research Program – Hydrocarbon and Oxygenates." Society of Automotive Engineers. SAE Paper 930142.

U.S. Patent No. 6,742,328, System B3, (June 2004).

U.S. Patent No. 5,771,68, Active Porous Media Aftertreatment Control System, (June 1998).

A Strong Energy Portfolio for a Strong America

Energy efficiency and clean, renewable energy will mean a stronger econ omy, a cleaner environment, and greater energy independence for America. Working with a wide array of state, community, industry, and university partners, the U.S. Department of Energy's Office of Energy Efficiency and Renewable Energy invests in a diverse portfolio of energy technologies.

Produced for the U.S. Department of Energy by the National Renewable Energy Laboratory

For more information contact:
EERE Information Center
1-877-EERE-INF (1-877-337-3463)
www.eere.energy.gov

DOE/GO-102007-2377
March 2007